CHALMERS
UNIVERSITY OF TECHNOLOGY

Chemically active bed material in fluidized-bed combustion and related processes for CO_2 mitigation

Master's thesis in Sustainable Energy Systems

CATRIN LINDBERG

DEPARTMENT OF SPACE, EARTH AND ENVIRONMENT, ENERGY TECHNOLOGY

CHALMERS UNIVERSITY OF TECHNOLOGY
Gothenburg, Sweden 2022
www.chalmers.se

Master's thesis 2022

Chemically active bed material in fluidized-bed combustion and related processes for CO_2 mitigation

CATRIN LINDBERG

CHALMERS
UNIVERSITY OF TECHNOLOGY

Department of space, earth and environment, energy technology
Division of energy technology
Chalmers University of Technology
Gothenburg, Sweden 2022

Chemically active bed material in fluidiced-bed combustion and related processes for CO_2 mitigation
CATRIN LINDBERG

© CATRIN LINDBERG, 2022.

Supervisor: Felicia Eliasson Störner, Department of space, earth and environment, energy technology
Examiner: Magnus Rydén, Department of space, earth and environment, energy technology

Master's Thesis 2022
Department of space, earth and environment, energy technology
Division of energy technology
Chalmers University of Technology
SE-412 96 Gothenburg
Telephone +46 31 772 1000

Typeset in LaTeX
Printed by Chalmers Reproservice
Gothenburg, Sweden 2022

Chemically active bed material in fluidized-bed combustion and related processes for CO_2 mitigation.

CATRIN LINDBERG
Department of energy technology
Chalmers University of Technology

Abstract

There are two technologies of fluidized bed combustion that recently have been developed with attempt to increase the fuel conversion and enable more efficient CO_2 mitigation. These methods are called Oxygen carrier aided combustion (OCAC) and Chemical looping combustion (CLC), which both uses oxygen carrying bed material. Research have been done on both synthetic and naturally occurring oxygen carriers.Expensive synthetic materials might not be suitable when operating wilt solid fuels. These expensive materials are not attractive when operating with solid fuel, since the process implies formation of ashes and the material have to be replaced with fresh material. Researcher are currently looking for alternative materials that can be used in OCAC and CLC, which have to be cheap, accessible at large quantities and available at close distance. attention have been payed to material streams from the metallurgical industries.

This study has investigated two potential materials as oxygen carriers which both are available in large quantities in the metallurgical industries in north Europe to a lower price than synthetic materials. Magnetite fines is an industrial slag product from LKAB and copper smelter slag is a by-product from Boliden AB. Experiments have been done in a lab- scale fluidized bed reactor to investigate the materials reactivity with oxygen as well as fuel conversion of syngas and methane fuel for CLC configuration. Experiments were also done for OCAC configuration to investigate the materials potential to move the combustion reactions down in the bed. Furthermore, the physical properties of each material were investigated visually to identify any significant changes during operation.

Results from this study shows that magnetite fines and copper smelter slag are reactive with syngas and moderate reactive with methane in CLC configuration. Magnetite fines shows no tendency for agglomeration and sintering which was expected due to the high content of FeO and low concentration of other components commonly causing this affects. However, copper smelter slag showed tendency for agglomeration after visual inspection of the material. Further research is however necessary to fully understand how the physical properties of the materials are affected when operating as oxygen carriers in CLC and OCAC. Lab-scale experiments with longer operational time and investigation of the physical properties and changes in chemical composition are interesting for further research.

Keywords: Chemical looping combustion, Oxygen carrier aided combustion, oxygen carrier, magnetite fines, copper smelter slag.

Acknowledgements

This thesis would not been accomplished without the help and support that I have received throughout the process. Firstly, I like to thank my supervisor Felicia Eliasson Störner who have been my support though the entire project. She has helped me to see both the large picture of my project as well as the details. When I have felt a need of someone to discuss my thought and ideas with has Felicia been available and helpful.
Secondly, I like to thank Magnus Rydén who also been a good support for me to ask questions to and helping me to understand the details. I also like to thank Magnus for introducing me to the research group for energy technology at Chalmers University of Technology. It has been inspiring to get an insight to your interesting research.
Thirdly I want to give my thank to Nasrin Nemati, Viktor Stenberg, Johannes Öhlin, Jessica Bohwalli och Rustan Hwitt. Thay have supervised and helped me in different ways to make the experiments possible. You all made it possible for me to start the experiments early in the morning and running til late, make adjustments and solved problems that came up during the experiments.
I also want to send a final thank you to my family and friends that have supported and encouraged me during the project and my time at Chalmers University of Technology. It would not have been the same experience without all the people I met on this journey.

Catrin Lindberg, Gothenburg, September 2022

Contents

List of Figures **xi**

List of Tables **xv**

1 Introduction **1**
1.1 Introduction . . . 1
1.2 Aim project . . . 2
1.3 Goal and scope . . . 2

2 Theory **3**
2.1 Fluidized bed combustion . . . 3
2.2 Chemical Looping Combustion . . . 4
2.3 Oxygen Carrier Aided Combustion . . . 5
2.4 Chemically active bed materials . . . 6
2.5 Mechanical stability . . . 7

3 Methods **9**
3.1 Lab scale fluidized bed boiler . . . 9
3.2 Bed material . . . 10
3.2.1 Calculations of properties for bed material . . . 12
3.2.2 Chemical reactions . . . 13
3.3 Experimental setup for CLC operation . . . 14
3.4 Experimental setup for OCAC operation . . . 16
3.5 Evaluation of fuel gas conversion . . . 17

4 Results **19**
4.1 Chemical activity in CLC . . . 19
4.1.1 Chemical activity of magnetite fines . . . 19
4.1.1.1 Reactivity with syngas . . . 19
4.1.1.2 Reactivity with methane . . . 22
4.1.2 Chemical activity of copper smelter slag . . . 25
4.1.2.1 Reactivity with syngas . . . 25
4.1.2.2 Reactivity with methane . . . 28
4.1.3 Discussion CLC operation . . . 32
4.2 Chemical activity in OCAC . . . 33
4.2.1 Magnetite fines for OCAC . . . 33
4.2.2 Copper smelter slag in OCAC . . . 35

4.3 General observations 37
4.4 Future work on this topic 39

5 Conclusion **41**

Bibliography **43**

A Appendix A **I**
A.1 Results for CLC operation I
A.1.1 Results for magnetite fines with syngas I
A.1.2 Results for magnetite fines with methane X
A.1.3 Results for copper smelter slag with syngas XVIII
A.1.4 Results for copper smelter slag with methane XXIII
A.2 Results for OCAC operation XXX
A.2.1 Results for magnetite fines XXX
A.2.2 Results for copper smelter slag XXXI

List of Figures

1 Particle size distribution for magnetite fines and copper smelter slag after crushing and sieving. 12

2 Dry gas concentration over time during reduction stages in CLC cycle for magnetite fines at 840°C. 20

3 Mean dry gas concentration for CLC cycles with magnetite fines as bed material and syngas as fuel, for bed temperatures 840°C, 890°C and 940°C. 21

4 CO_2 yield as function of the mass based oxygen carrier conversion of magnetite fines for combustion with syngas, at different bed temperatures. 22

5 Mean dry gas concentration for CLC cycles with magnetite fines as bed material and methane as fuel, for bed temperatures 840°C and 940°C. 23

6 CO_2 yield as function of the mass based oxygen carrier conversion of magnetite fines for combustion with methane, at different bed temperatures. 24

7 Dry gas concentration over time during reduction with syngas in CLC cycle for copper smelter slag at 840°C. 26

8 Mean dry gas concentration for CLC cycles with copper smelter slag as bed material and syngas as fuel, for bed temperature s 840°C, 890°C and 940°C 27

9 CO_2 yield as function of the mass based oxygen carrier conversion of copper smelter slag for combustion with syngas, at different bed temperatures. 28

10 Dry gas concentration over time during reduction with methane in CLC cycle for copper smelter slag at 840°C. 29

10 Dry gas concentration over time during reduction with methane in CLC cycle for copper smelter slag at 840°C. 30

11 Mean dry gas concentration for CLC cycles with copper smelter slag as bed material and methane as fuel, for bed temperature s 840°C, 890°C and 940°C 31

12 CO_2 yield as function of the mass based oxygen carrier conversion of copper smelter slag for combustion with methane, at different bed temperatures. 32

13 Dry gas concentration of CH_4 measured at different height over the distribution plate at bed temperatures 600°C, 700°C, 750°C, 800°C, 850°C and 900°C for magnetite fines in OCAC. 34
14 Dry gas concentration of CO measured at different height over the distribution plate at bed temperature 600°C, 750°C and 850°C for magnetite fines in OCAC. 35
15 Dry gas concentration of CH_4 measured at different height over the distribution plate at bed temperature 600°C, 750°C and 850°C for copper smelter slag in OCAC. 36
16 Dry gas concentration of CO measured at different height over the distribution plate at bed temperature 600°C, 750°C and 850°C for copper smelter slag in OCAC. 37

A.1 CO_2 concentration over time during reduction with syngas in CLC cycle for magnetite fines at 840°C I
A.2 CO concentration over time during reduction with syngas in CLC cycle for magnetite fines at 840°C II
A.3 CO_2 concentration over time during reduction with syngas in CLC cycle for magnetite fines at 890°C III
A.4 CO concentration over time during reduction with syngas in CLC cycle for magnetite fines at 890°C IV
A.5 CO_2 concentration over time during reduction with syngas in CLC cycle for magnetite fines at 940°C. V
A.6 CO concentration over time during reduction with syngas in CLC cycle for magnetite fines at 940°C. VI
A.7 Mean dry gas concentration for CLC cycles with magnetite fines as bed material and syngas as fuel, for bed temperature s 840°C, 890°C and 940°C VII
A.7 Mean dry gas concentration for CLC cycles with magnetite fines as bed material and syngas as fuel, for bed temperature s 840°C, 890°C and 940°C VIII
A.8 CO_2 yield as function of the mass based oxygen carrier conversion of magnetite fines for combustion with syngas, at different bed temperatures. IX
A.9 CH_4 concentration over time during reduction with methane in CLC cycle for magnetite fines at 840°C. X
A.10 CO2 concentration over time during reduction with methane in CLC cycle for magnetite fines at 840°C. XI
A.11 CO concentration over time during reduction with methane in CLC cycle for magnetite fines at 840°C. XII
A.12 CH_4 concentration over time during reduction with methane in CLC cycle for magnetite fines at 940°C. XIII
A.13 CO2 concentration over time during reduction with methane in CLC cycle for magnetite fines at 940°C. XIV
A.14 CO concentration over time during reduction with methane in CLC cycle for magnetite fines at 940°C. XV

A.15 Mean dry gas concentration for CLC cycles with magnetite fines as bed material and syngas as fuel, for bed temperature s 840°C and 940°C XVI
A.16 CO_2 yield as function of the mass based oxygen carrier conversion of magnetite fines for combustion with methane, at different bed temperatures. XVII
A.17 CO_2 concentration over time during reduction with syngas in CLC cycle for copper smelter slag at 840°C XVIII
A.18 CO concentration over time during reduction with syngas in CLC cycle for copper smelter slag at 840°C XVIII
A.19 CO_2 concentration over time during reduction with syngas in CLC cycle for copper smelter slag at 890°C XIX
A.20 CO concentration over time during reduction with syngas in CLC cycle for copper smelter slag at 890°C XIX
A.21 CO_2 concentration over time during reduction with syngas in CLC cycle for copper smelter slag at 940°C XX
A.22 CO concentration over time during reduction with syngas in CLC cycle for copper smelter slag at 940°C XX
A.23 Mean dry gas concentration for CLC cycles with copper smelter slag as bed material and syngas as fuel, for bed temperature s 840°C, 890°C and 940°C XXI
A.23 Mean dry gas concentration for CLC cycles with copper smelter slag as bed material and syngas as fuel, for bed temperature s 840°C, 890°C and 940°C XXII
A.24 CO_2 yield as function of the mass based oxygen carrier conversion of copper smelter slag for combustion with syngas, at different bed temperatures. XXII
A.25 CO_2 concentration over time during reduction with methane in CLC cycle for copper smelter slag at 840°C XXIII
A.26 CH_4 concentration over time during reduction with syngas in CLC cycle for copper smelter slag at 840°C XXIII
A.27 CO concentration over time during reduction with syngas in CLC cycle for copper smelter slag at 840°C XXIV
A.28 CO_2 concentration over time during reduction with syngas in CLC cycle for copper smelter slag at 890°C XXIV
A.29 CH_4 concentration over time during reduction with syngas in CLC cycle for copper smelter slag at 890°C XXV
A.30 CO concentration over time during reduction with syngas in CLC cycle for copper smelter slag at 890°C XXV
A.31 CO_2 concentration over time during reduction with syngas in CLC cycle for copper smelter slag at 940°C XXVI
A.32 CH_4 concentration over time during reduction with syngas in CLC cycle for copper smelter slag at 890°C XXVI
A.33 CO concentration over time during reduction with syngas in CLC cycle for copper smelter slag at 940°C XXVII

A.34 Mean dry gas concentration for CLC cycles with copper smelter slag as bed material and syngas as fuel, for bed temperature s 840°C, 890°C and 940°C XXVII
A.34 Mean dry gas concentration for CLC cycles with copper smelter slag as bed material and syngas as fuel, for bed temperature s 840°C, 890°C and 940°C XXVIII
A.35 CO_2 yield as function of the mass based oxygen carrier conversion of copper smelter slag for combustion with methane, at different bed temperatures. XXIX
A.36 Dry gas concentration of CH_4 measured at different height over the distribution plate at bed temperatures 600°C, 700°C, 750°C, 800°C, 850°C and 900°C for magnetite fines in OCAC. XXX
A.37 Dry gas concentration of CO measured at different height over the distribution plate at bed temperature 600°C, 750°C and 850°C for magnetite fines in OCAC. XXXI
A.38 Dry gas concentration of CH_4 measured at different height over the distribution plate at bed temperatures 600°C, 700°C, 750°C, 800°C, 850°C and 900°C for copper smelter slag in OCAC. XXXI
A.39 Dry gas concentration of CO measured at different height over the distribution plate at bed temperature 600°C, 750°C and 850°C for copper smelter slag in OCAC. XXXII

List of Tables

1 Height for measurement points in relation to the distribution plate in reactor. 10

2 Elementary composition of magnetite fines and copper smelter slag measured on the original material by LKAB and Boliden. Concentration of iron and manganese is reported as oxide, otherwise indicated as (Fe) and (Mn) for pure element. 11

3 Accumulated material weight fraction for different particle sizes for magnetite fines and copper smelter slag, as received from LKAB and Boliden. 12

4 Parameter values for magnetite fines and copper smelter slag after preparations. Calculations are based on the particle size distribution and physical properties at 800°C. 13

5 Gas flow and operational time for CLC cycle steps with syngas, CO/H_2 at the bed temperature of 840°C, 890°C and 940°C. 15

6 Gas flow and operational time for CLC cycle steps with methane at the bed temperature of 840°C, 890°C and 940°C. 16

7 Parameters for OCAC experiments. The gas flows for each bed temperature calculated for an air to fuel ratio at 1,05. 16

8 interior material mass and bulk density before and after conducted experiments for magnetite fines and copper smelter slag. 38

1
Introduction

1.1 Introduction

Today's society stands in front of a challenge to meet a growing demand of energy supply from energy sources with low greenhouse gas emissions for an increasing part of the world´s population. Solutions to this problem must be done with care of the environment and minimum climate impact from the adaptation process itself.

One technology used for energy generation is fluidized bed combustion where a bed of sand is fluidized with a gas flow and enables conversion of gaseous and solid fuels to carbon dioxide and water [1].

Development of the technology of fluidized bed combustion have been made to make fuel conversion more efficient and enable inherent carbon capture from such energy processes. *Chemical Looping Combustion* (CLC) is a new concept where the flue gas flow from the fuel conversion process is separated from the air flow with support from an oxygen carrier. The separated outlet gas flows enables inherent capture of CO_2 to low cost [2]. *Oxygen Carrier Aided Combustion* (OCAC) is a development of fluidized-bed combustion where sand is replaced with an oxygen carrier which improves the oxygen distribution in the reactor volume which decreases the need of excess air and improves the combustion rate.

Many materials have been investigated for their potential as oxygen carriers for these applications. Manufacture oxygen carriers generally have high reactivity which make them suitable for operation with gaseous fuel. However, these expensive materials might not be economically viable when operating with solid fuels, as municipal solid waste and biomass, since the process implies formation of ashes which can hinder chemical reaction between oxygen carriers and oxygen or fuel components. For this application research have paid attention to materials of natural ore and waste material containing metal oxides, which are accessible to a significant lower cost. One material that is commonly used today is ilmenite, a natural metal ore that is cheap, available in large quantities and shows properties suitable for improved fuel conversion. However, more research have to be done to find additional materials like ilmenite.

In order to find additional materials suitable as oxygen carrier interest have been payed to other material streams from the metallurgical industries. In particular of materials containing different metal oxides. With a growing request for circular economy and resource efficiency in mind, it is of interest to investigate the possibilities to use materials that already are available in large quantities and ideally are by-products from these industries. Such material is expected to be economical

beneficial and more resource efficient. This study have looked at two materials, one large-quantity product from LKAB and one industrial slag from Boliden AB.

1.2 Aim project

This study aims to find new low cost and available oxygen carriers to be used in CLC and OCAC for which two materials are investigated; magnetite fines and copper smelter slag. The study aim to evaluate if magnetite fines and copper smelter slag are reactive with oxygen and fuel when operating in a bubbling fluidized bed, with gaseous fuel. It also aims to evaluate if the bed material have potential to convert less reactive fuels present in biomass and solid waste fuel for CLC and OCAC configurations.

1.3 Goal and scope

Fuel conversion properties of the materials is evaluated from experiments in a lab-scale fluidized bed reactor for CLC batch configuration with syngas at different bed temperatures. Similar experiments are done with a less reactive gaseous fuel, methane. Furthermore, experiments are done in OCAC configuration at different bed temperatures to identify if the bed materials contribute to increase fuel conversion in the bed. Evaluation of sintering and agglomeration is also made by visual inspection.
Due to limitation in time frame of this project, material properties like sintering and agglomeration are evaluated qualitatively. No visual evaluations are made in microscope nor are quantitative measurements of attrition done.

2
Theory

2.1 Fluidized bed combustion

Fluidization is a phenomena where solid particles behaves physically as a fluid [3]. It occur when a bed of particles are exposed for a upward-lifting drag force from a gas or liquid which is larger than the downward force of gravity. At the stage where the drag force on the particle equals the weight of the particle the bed of particles becomes fluidized. The required fluid velocity to obtain fluidization is referred to the minimum fluidization velocity, u_{mf} and depends on the size and shape of the particle as well as the fluid used [1]. For application in combustion processes the fluid is gas, flowing through a bed of solid particles inside a vessel.
At the minimum fluidization velocity the bed is slightly expanded due to the up-lifting force, forming a homogeneous bed where the particles are scattered in the surrounding gas. For higher gas flow rate the homogeneous bed will be disrupted and gas bubbles will start to form. The bed is then no longer homogeneous and is in this stage called a *heterogeneous fluidized bed* or *bubbling fluidized bed* [1]. The total volume of the bed is not significantly increased compared to the homogeneous fluidized bed. In the two-phase system the gas can flow through the bed of particles either as bubbles or as part of the emulsion phase where particles are mixed with gas [3]. The total volumetric flowrate of gas through the system is then the sum of the volumetric flow in the bubbles and in the emulsion phase according to equation 1

$$Q_{bed} = Q_{emulsion} + Q_{bubbles} = A_{bed}u_{mf} + A_{bed}(u_o - u_{mf}) \tag{1}$$

where Q_{bed} is the total volumetric flow rate, $Q_{emulsion}$ is the gas flow rate in the emulsion phase and $Q_{bubbles}$ is the flow rate of gas passing through the bed as bubbles. A_{bed} is the cross-section area of the bed and u_o is the superficial gas velocity through the system [3]. The flow rate in the emulsion phase is the dominant part in equation 1 for a system with a gas velocity close to the minimum fluidization velocity. Higher gas velocity will increase the share of gas in bubbles, $Q_{bubbles}$, in the two-phase system. Furthermore, bubbles in a bubbling fluidized bed are small at the bottom of the bed and will coalesce to fewer and larger bubbles higher up in the bed. If the velocity is high enough will the bed expand due to large bubbles. This phenomena with large bubbles are called *slugging* and can occur both in axial direction along the reactor and horizontally across the reactor [1], [3]. Slugging causes less contact between the gas phase and the solid phase, which is unfavourable in terms of chemical reaction and heat transfer. At even higher gas velocity the bed shows a turbulent

state where there is no longer a visible top surface of the bed and the bubbles are changed to turbulent voids. Therefore is this stage called *turbulent fluidized bed*. At this stage may particles be dragged upwards with the gas flow and leaving the reactor. A cyclone can be used in order to collect particles at the outlet and return them back to the bed in a cyclic path which is called *circulating fluidized bed boiler* [1].
Different states of fluidization is favourable depending on the industrial application. Bubbling and turbulent fluidized bed is a common performance for combustion processes due to efficient heat exchange [1]. Furthermore the fluidized bed boiler can handle a large particle size distribution as well as small particles, *fines*, which allows variation of bed material and solid fuel. Additional advantage for fluidized bed boilers is that the temperature is easily controlled and stabilised and can therefore operate in large-scale continuous operations [1]. Therefore fluidized bed boilers are common for combustion of fuels as solid coal or municipal solid waste to generate heat and electricity. However biomass is also used and is expected to increase as energy source in the future.
Two new technologies have been developed from the concept of fluidized bed combustion. One technology enables CO_2 separation and the other concepts improves the fuel conversion. *Chemical Looping Combustion* use chemically active bed material to inherently separate CO_2 from the other flue gases components and therefor reduces the cost for CO_2 mitigation. Similar bed material is used in *Oxygen Carrier Aided Combustion* to improve heat transfer and increase fuel conversion efficiency. Commercial fluidized bed combustion use silica sand as solid bed material, which contributes to good temperature distribution and circulation of fuel and oxygen in the boiler [4]. Silica sand is chemically inert and does not contribute to the combustion reaction itself. Instead of silica sand uses the knew technologies chemically active bed material.

2.2 Chemical Looping Combustion

Chemical looping combustion (CLC) is a technology with aim to ease carbon capture in flue gases from fluidized bed boilers. A material that can easily be oxidised and chemically reduced is used to transport oxygen between two parts of the system. These materials are therefore called oxygen carriers for which metal oxides have been found suitable by previous research [2]. One part of the system is the fuel reactor, where the metal oxide is reduced through reaction with gaseous fuel in a fluidized bed boiler. Equation 2 shows a general reduction reaction with a hydrocarbon in the fuel reactor, where M_yO_x denotes the oxidized for of a metal oxide and M_yO_{x-1} denotes the reduced form after reaction with a hydro carbon [2].

$$(2n+m)M_yO_x + C_nH_{2m} \rightarrow (2n+m)M_yO_{x-1} + mH_2O + nCO_2 \tag{2}$$

The outlet gases from the fuel reactor is only water H_2O and carbon dioxide CO_2. The reduced oxygen carrier is led to a second fluidized bed, the air reactor, where

it is oxidised again as shown in equation 3 ,[2].

$$M_yO_{x-1} + {}^1/_2O_2 \rightarrow M_yO_x \tag{3}$$

The flue gases from the air reactor contains nitrogen and unreacted oxygen. The large flow of nitrogen is in this way separated from the carbon dioxide in the fuel reactor outlet which makes it possible to avoid expensive and energy demanding gas separation steps to capture CO_2 [2]. The CO_2 can then be captured directly by condensing the steam.
A system with an air reactor and a fuel reactor is commonly designed with two interconnected fluidized beds as described above [5]. However a more simple design is possible to use for experimental lab-scale reactors, using one fluidized bed boiler without cyclone or a second reactor. Oxidation and reduction is operated in the same reactor in a cyclic process. First is the reactor operating with an air gas flow in which the bed material is oxidised. Secondly is the reactor operating with inert nitrogen gas N_2 followed by a third step for reduction operating with gaseous fuel. In a last step the reactor is flushed with N_2 again before step one with air is repeated for the next cycle. Experiments for CLC operation have been done in a batch reactor system at Chalmers University of Technology which is discussed further in section 3.3 [6].

2.3 Oxygen Carrier Aided Combustion

Oxygen Carrier Aided Combustion (OCAC) is another technology for fuel combustion developed from the concept of oxygen carrier in CLC. The technology is based on the commercial fluidized bed boiler, but instead of using sand as bed material one use oxygen carriers as part of the bed interior or totally replacing sand. Similar to oxygen carriers in CLC, the bed material is reactive with oxygen and can therefore transfer oxygen from one zone rich in oxygen to another where the concentration of oxygen is low but has a high fuel content. It enables improved interaction between oxygen and fuel in areas where gas mixing otherwise would be low and the combustion reaction would be unfavourable. The general chemical reaction is the same as for CLC, see reaction 2 and 3 The technology has shown potential to increase the fuel conversion in the boiler compared to commercial bubbling fluidized-bed combustion. Furthermore oxygen carrier has been presented as an alternative to operate for reduced bubble size in purpose to increase interaction between the gas bubbles and the emulsion phase in a fluidized-bed. This implies increased conversion ratio down in the bed, compared to operation with silica-sand at the same gas velocity, which has shown tendency to reduce incomplete fuel conversion and formation of NO [7].
Due to improvement of the combustion process OCAC is attractive for combustion of municipal solid waste and biomass fuels that usually emits large amounts of unconverted fuel components and products from incomplete combustion, as CO. The technology might also reduce the amount of NO_x formation. OCAC has successfully been tested in pilot projects and is today used in a number of operating plants in Sweden and several studies has been made on suitable bed materials, based on earlier findings of oxygen carriers for CLC [8].

2.4 Chemically active bed materials

Development of oxygen carriers has been a topic for research during the last two decades which has resulted in knowledge about the general good properties for an oxygen carrying material. Important criteria presented in earlier research are i) high reactivity with fuel and oxygen, with ability of full fuel conversion to CO_2 and H_2O ii) low tendency for fragmentation, attrition and agglomeration. iii) low production cost and minimum environmental impact [9].

Oxygen carriers consists of metal oxides, a chemical compound consisting of one or a few metal ions and a number of oxygen atoms. For simplicity they can all be written as MeO or Me_xO_y, where x and y denotes the number of metal ions and oxygen atoms respectively. Common components of interest within this research area are oxides of Fe, Mn, Cu and Ni, where Ni has shown the highest reactivity with fuel. The reactivity for Cu is also high while Fe and Mn are less reactive but still suitable as oxygen carriers [9]. However the cost is lower for the less reactive materials which have made them attractive for the application. Research have been made on natural materials, from different metal ores, waste materials and synthetic manufactured oxygen carrier material. Manufactured oxygen carriers have been of highest interest in research, both to investigate their reactivity and to evaluate the process in large scale for the materials that have shown good potential reactivity. However the high cost of manufactured oxygen carrier is a large drawback, especially when operating with solid fuels, as municipal solid waste and biomass, where reactive ashes accumulate in the bed. The accumulated ashes forms a layer on the oxygen carrier particles and could limit their reactivity and therefore need to be replaced with new bed material. If using synthetic oxygen carriers this would be expensive. Furthermore, manufactured oxygen carriers have high reactivity which is not as important when operating with solid fuel, as for gaseous fuel. For operation with solid fuels are instead chemically active materials from natural ore and waste materials more attractive since they are available in large quantities to a lower price [9].

One metal ore that has shown properties for an oxygen carrier is *ilmenite* [9],[10]. Ilmenite is a naturally available metal ore containing oxides of iron, *Fe*, and Titanium, *Ti*. The material is mined in large quantities at several places around the world and is available to a relatively low cost [10]. Ilmenite has shown ability to convert CO with good conversion rate in CLC and moderate conversion for CH_4. Initial studies on the materials showed an increased reactivity with number of CLC cycles and no reduction of reactivity have been seen when operating with gaseous fuel [10].

Ilmenite have also been tested in OCAC for biomass as fuel in a study by Thunman et al. [11]. This study showed that an increased share of ilmenite in the interior bed of silica-sand, reduced the concentration of CO and hydrocarbonHC in the furnace, which indicates an increased fuel conversion compared to when a interior bed of only inert silica-sand. Since biomass are discussed to become a larger share of the fuels for energy processes in the future, it is of interest for researchers to find additional oxygen carrying materials suitable for interaction with biomass.

In today's industry it is necessary to look at potentials for circular economy and

industrial symbiosis to make use of all material flows within the society. Therefore is it interesting to search for alternative oxygen carriers among large quantity products and by-products from the metal industries. The bulk products have potential to be cheap, especially the by-products which in many cases is not used for specific applications but instead used as additional material in construction work, landfill material or placed in deposit dams [12], [13]. Together with LKAB and Boliden three materials have been identified which may be of interest for OCAC and CLC operations; copper smelter slag, magnetite fines and enrichment sand.

2.5 Mechanical stability

Particle characteristics of the bed material are important parameters for the performance of an fluidized bed boiler. Operation at high temperature implies a risk for sintering, agglomeration, attrition and swelling of the bed particles. Sintering and agglomeration changes the particle size distribution and the fluidization properties. In turn it influence the chemical reactivity and performance of the boiler [1]. Sintering can also cause defluidization, in which case the boiler must be stopped. One other important aspect is the materials mechanical stability during long operational time. Particles in a fluidized bed boiler collide with each other at a high velocity, for which the material´s mechanical stability have impact on attrition of the material. Attrition of the particles results in changed particles size distribution, which effects the heat and mass transfer and the reaction rate. A changed particle size distribution also affect the fluidization of the bed and causes risk for elutrition of material [14]. If elutrition occur bed material is lost from the bed and must be replaces with new fresh feed [15]. Tendency for attrition varies for specific materials, the reactor geometry, the chemical reaction present and the operational conditions. It is therefor important to evaluate the mechanical stability in an early stage of investigation of new bed materials.

3
Methods

Experiments were performed in a lab-scale fluidized bed reactor designed and built at Chalmers University of Technology for previous investigations of OCAC made by Stenberg et al. [7]. The reactor has also been operated for batch CLC configuration in experiments by Tsuji [6]. Results from these studies show that the reactor can be used for lab-scale experiments for both OCAC and CLC and was therefore used for both processes in this study. This chapter first presents the design of the reactor together with the connected analysis equipment. The bed materials and calculations of bed material properties are described in section 3.2 followed by further description of the experimental setup for CLC and OCAC configurations in sections 3.3 and 3.4.

3.1 Lab scale fluidized bed boiler

The laboratory scale fluidized bed reactor is 1.28m high with inner diameter of 0.08m. It is made of steel and surrounded by an isolating furnace, which can be electrically heated in three separate sections. Inlet gases are mixed in a T-connection before entering the windbox at the bottom of the reactor, from which the gas is lead through 61 holes of 0.6mm in a 5mm thick bottom plate to the fluidized bed [7]. In order to hinder combustion of the fuel already in the windbox when mixing air and fuel, the temperature here is held below the auto-ignition temperatures of the fuels with a cooling coil. Cold air flows through the cooling coil which makes several passes through the windbox. The air flow rate can be regulated manually with a valve to control the cooling. The auto-ignition temperatures for methane is 537°C, [16]. The target is therefore to have a temperature in the windbox below 500°C for experiments where fuel and air are mixed in the windbox. Measurements of the reactor temperature and pressure is possible in the windbox (H0), just above the distribution plate (H1) and at additional seven heights above the distribution plate (H2-H8). The height where each measurement point is located is listed in table 1, for which the distribution plate is set to zero level.
The temperature is measured with type K thermocouples, of tolerance class 1, which are placed at the end of a tube ranging from the outside to the inside of the reactor wall. The temperature is measured at high-resolution mode with a NI 9213 measurement module which are connected to the thermocouples. The measurement module have an accuracy of <0.02°C. Pressure in the reactor is measured at the same locations as the thermocouples via pressure transducers which are in contact with the gas flow. The pressure is measured to identify if the bed is fluidized and to find if leakage or material loss occur.

Table 1: *Height for measurement points in relation to the distribution plate in reactor.*

Measurement point	**Height from distribution plate [cm]**
H8	79,65
H7	63,65
H6	47,65
H5	31,65
H4	15,65
H3	13,65
H2	8,88
H1	3,65
H0	-4,00

The gas composition can be measured at the same eight heights over the distribution plate (H1-H8) as for the temperature and pressure. The tubes for gas sampling is located at the opposite side of the reactor, relative the previous described measurement tubes. It has porous metal cups in the end, of nickel-chromium-iron-molybdenum alloy (316L), which hinders particles larger than 150µm from entering the sampling tube [17]. The sampling tubes for temperature and pressure measurement can be flushed with nitrogen to remove bed material. The gas sampling tubes can in a similar way be flushed with pressurised air to remove fines in the filter.

Gas samples are taken from the gas sampling tubes via a hose, which can be attached to the gas sampling tubes of interest. the hose is equipped with heating bands and kept at 190 degrees to reduce the risk of water condensing in the hose. The sampled gas is then passing two filter, one hot filter and one cold filter. The gas is dried in a condenser between the two filters. A gas analysis is then done in a SICK GMS810 gas analyser which sends data points to a computer every second. To make sure that the measurements are reliable was the gas analyser calibrated at the start of every experiment sequence.

3.2 Bed material

Two industrial metal oxides for use as bed materials have been studied experimentally in this report; magnetite fines and copper smelter slag. Magnetite fines and copper smelter slag are two material of small solid particles from metallurgical industries in Sweden. Magnetite fines are iron oxides of the form Fe_3O_4 where one iron ion is ferrous (II) and two are ferric (III). The material is produced by LKAB for use in steel production. Information about the elementary composition was provided by LKAB and is presented in table 2. Magnetite fines contains 70,96% Fe, given as Fe of the total mass, 0,65% SiO_2 and less than 1% other metal oxides. The second material investigated is copper smelter slag, a byproduct from the production process of copper at Boliden Rönnskär. Today copper smelter slag is used as construction material in buildings and roads [12]. It contains 42-45% iron oxide, given as FeO and

33-42% silica dioxid SiO_2. In comparison with magnetite fines, copper smelter slag contains less metal oxide and more inert silica.yet another material was investigated initially but discarded due to inappropriate physical properties.
Note that in table 2 components for iron Fe is given as the pure element for magnetite fines and as FeO for copper smelter slag. Weight percent for manganese is given as MnO for the latter two materials while given as Mn for copper smelter slag. It is only known how much iron Fe or iron oxide FeO the materials contains. However it is unknown which oxidation state the iron atoms have. Expected forms of iron oxides are further discussed in section 2.2.

Table 2: *Elementary composition of magnetite fines and copper smelter slag measured on the original material by LKAB and Boliden. Concentration of iron and manganese is reported as oxide, otherwise indicated as (Fe) and (Mn) for pure element.*

	Magnetite fines	**Copper smelter slag**
Component	**Weight percent (w%)**	
FeO	71,0 (Fe)	42-45
SiO_2	0,7	33-42
K_2O	0,02	-
Al_2O_3	0,3	2,0-5,0
CaO	0,2	2,0-5,0
MgO	0,3	0,5-1,5
MnO	0,05	0,4-0,6 (Mn)
TiO_2	0,3	-
V_2O_5	0,3	-
Zn	-	0,8
Cu	-	0,5-0,8
Cr	-	0,2-0,4
P	0,01	-
S	-	0,5-0,7

Copper smelter slag can be categorised as sharp grains with a size ranging from a few micrometres to a few millimetres [18]. Information about the shape magnetite fines were not available and are thus missing in this report. Magnetite fines are assumed to have the same shape as copper smelter slag in calculations. Table 3 presents the accumulated particle size distribution for the materials, as received data from LKAB and Boliden. Values for magnetite fines were provided by LKAB and for copper smelter slag the values are the set product target values [18].
The materials were sieved to obtain a material with particle size of 90-212μm. Magnetite could be sieved directly while copper smelter slag required further processing to obtain the required amount material. Copper smelter slag was alternately crushed and sieved before the target particles size was obtained. The particle size distribution for magnetite fines and copper smelter slag was calculated from the mass for each particle size interval, for which data is shown in figure 1. Based on the particle size distribution was the mean particle size, d_p, calculated to 137,0μm for magnetite fines and to 10,8μm for copper smelter slag. Furthermore was the material bulk

Table 3: *Accumulated material weight fraction for different particle sizes for magnetite fines and copper smelter slag, as received from LKAB and Boliden.*

	Magnetite fines	Copper smelter slag
Particle size	**Accumulated weight%**	
<63μm	1,2	2
<90μm	2,6	-
<125μm	9,8	2
<180μm	32,0	-
<250μm	60,9	5,0
<500μm	99,9	20
<1.0mm	100	70
<2.0mm	100	98
<4.0mm	100	100
<5.6mm	100	100

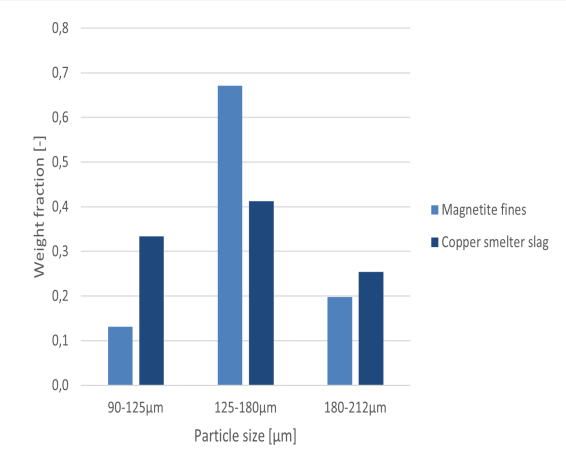

Figure 1: *Particle size distribution for magnetite fines and copper smelter slag after crushing and sieving.*

density, ρ_s, measured with a volume of ISO standard $3923 - 1 : 2008$. Magnetite fines measured a bulk density of 2482,8 kg/m^3 and the value for copper smelter slag was 1663,3 kg/m^3. Table 4 in section 3.2.1 lists these values for magnetite fines and copper smelter slag.

3.2.1 Calculations of properties for bed material

Calculations for additional properties for the bed materials can be done from the results of the measurements of particle size and bulk density. Depending on the particle density, particle size and the fluidization gas, each material has a minimum fluidization velocity. The minimum fluidization velocity is the gas velocity at which the drag force by upward moving gas is equal to the weight of particles [1]. Calculations of the material specific minimum fluidization velocity, u_{mf}, is made according to the method presented by Wen and Yu [19]. The minimum fluidization velocity is related to the Reynolds number as shown in equation 4[3].

$$Re_{mf} = \frac{d_p u_{mf} \rho_g}{\mu} \tag{4}$$

Re_{mf} is the Reynolds number at minimum fluidization velocity and d_p is the mean particle diameter in millimetre. ρ_g and μ are the density and viscosity of air at a given bed temperature. Re_{mf} is further related to the Galiteo expression, N_{Ga},

$$Re_{mf} = \sqrt{33.7^2 + 0.0408 N_{Ga}} - 33.7 \tag{5}$$

which is determined experimentally and N_{Ga} stands for the expression in equation 6

$$N_{Ga} = \frac{d_p^3 \rho_g (\rho_s - \rho_g) g}{\mu^2} \tag{6}$$

where d_p is the mean particle size and ρ_s is the solid material bulk density. Table 4 presents the calculated value for u_{mf}, together with the other measured and calculated parameter values for magnetite fines and copper smelter slag.

Table 4: *Parameter values for magnetite fines and copper smelter slag after preparations. Calculations are based on the particle size distribution and physical properties at 800°C.*

	d_p (μm)	ρ_{bulk} (kg/m^3)	ρ_p (kg/m^3)	u_{mf} (cm/s)	m_{bed} (g)
Magnetite fines	137,0	2484,8	2482,7	1,99	1616,6
Copper smelter slag	130,8	1663,3	2466,7	1,22	1082,1

3.2.2 Chemical reactions

The two investigated materials contains iron oxides which can be oxidised between different chemical forms binding more or less oxygen. Which oxidation state the different materials have is unknown in this project. However, generally is magnetite an iron oxide of the form Fe_3O_4 where one iron ion is ferrous (II) and two are ferric (III). The oxidized state of magnetite is then hematite, according to the oxidation reaction 7. Hematite is then reduced back to magnetite in the reaction with fuel. Reaction 8 shows the reduction reaction of hematite with syngas. The reduction with methane is more complex but can be simplified to reaction 9 for this project [20].

$$2Fe_3O_4 + {}^1\!/_2 O_2 \rightarrow 3Fe_2O_3 \tag{7}$$

$$6Fe_2O_3 + CO + H_2 \rightarrow 4Fe_3O_4 + CO_2 + H_2O \tag{8}$$

$$Fe_2O_3 + CH_4 \rightarrow Fe_3O_4 + CO_2 + H_2O \tag{9}$$

Reaction 8 gives a mole relation of 6:1 for oxidised magnetite to syngas, while reaction 9 is unbalanced. However is one (1) mole oxygen required for conversion of each mole CO and H_2. Conversion of methane requires four (4) mole oxygen for each mole methane.
One alternative form of iron oxide is ferrous oxide Fe(II)O which is oxidised to hematite according to reaction 10

$$4FeO + 3O_2 \rightarrow 2Fe_2O_3 \tag{10}$$

The material is most likely reduced back to Fe_3O_4 according to reaction 8 and 9

3.3 Experimental setup for CLC operation

The bed materials ability to operate as an oxygen carrier in a fluidized bed was evaluated through experiments for CLC operation like the one presented by Tsuji [6]. The previous study by Tsuji used ilmenite as bed material for experiments in the reactor current for this study. The experiments by Tsuji were carried out at a bed temperature at 840°C with two different fuels, syngas and carbon monoxide CO. Results from the experiment showed that the fuels were converted during the reduction step and oxidised when in contact with air. No ignition occurred that could indicate that air was mixed with fuel. It could be concluded that the experimental process used successfully demonstrate a lab-scale CLC batch configuration. Therefore a similar experimental process was used in this study to investigate the chemical reactivity of magnetite fines and coppers smelter slag. The total gas velocity was reduced in this study to a value that have been shown to give a stable bubbling fluidized-bed in the reactor [7]. The total gas velocity was set to 0.2 m/s for both CLC and OCAC experiments. Previous experiments by Tsuji were done at a bed temperature of 840°C, which is at the lower temperature range for CLC usually operating between 840-1040 °C. To evaluate if there were any difference in behaviour of the bed materials depending on the operational temperature were three different bed temperatures investigated in this study. The bed temperatures evaluated were 840°C, 890°C and 940°C.
To identify the chemical reactivity the fuel conversion of syngas and methane were observed during the reduction step in a number of CLC cycles. The dry gas composition was measured at the top of the reactor at measurement point H8, representing the flue gas outlet, see table 1. Also the temperature and pressure were continuously measured at this position to identify changes in the fluidization quality. A description of the experimental procedure is given below.
The air flow was set to 6 nlpm (normal litre per minute) and the material was added to the reactor. The flow was increased to 14 nlpm which gave a flow of 0,2 m/s at 900°C. Initially was the bed material heated to a temperature of 900°C and was left to operate for one hour. During this step the material was expected to oxidise to its oxidised state and combustible components (such as any residue from the production process) to be burnt of, as well as water to vaporise from the solids. Afterwards was

the electric furnace temperature set to the target bed temperature and regulated if needed to reach the target bed temperature. When the bed temperature was reached and stable, as well as the pressure was stable at point H8, the gas flow was changed to 10 nlpm of N_2. The bed was fluidized with N_2 until the oxygen level was below 0,75% in the reactor. The reduction step was then started by introducing the fuel flow (syngas or methane) at 0.2m/s for one (1) minute. Then the fuel flow was stopped and replaced by N_2 at 10 nlpm for three (3) minutes, or longer until no CO or CO_2 were detected at the outlet. Hence one cycle follows the steps for: oxidation with air, inert N_2, reduction with fuel, inert N_2, which is given in detail in table 5 for syngas fuel and table 6 for methane fuel. The oxidation step was then repeated, followed by the inert flow and reduction step, which together is one cycle for CLC operation. The CLC cycle was then repeated at least three (3) times.
When the targeted number of cycles were done the bed temperature was changed by regulating the electric furnace temperature during the oxidation step. The air flow was changed according to table 5 for operation with syngas and table 6 for methane to sustain a flow rate of 0,2 m/s during the oxidation and reduction steps. Due to limitation of the methane flow at 10 nlpm the flow of methane was set to two thirds of the total mass flow and the rest was inert nitrogen gas, N_2.

Table 5: *Gas flow and operational time for CLC cycle steps with syngas, CO/H_2 at the bed temperature of 840°C, 890°C and 940°C.*

	Oxidation	**Inert**	**Reduction**	**Inert**
Bed temp.			**Gas flow**	
	Air	**N_2**	**CO/H_2**	**N_2**
(°C)	(nlpm)	(nlpm)	(nlpm)	(nlpm)
840	15,06	10,00	15,06	10,00
890	14,41	10,00	14,41	10,00
940	13,82	10,00	13,82	10,00
Operational time for each cycle step				
	10 min	4 min	1 min	3 min

Table 6: *Gas flow and operational time for CLC cycle steps with methane at the bed temperature of 840°C, 890°C and 940°C.*

	Oxidation	**Inert**	**Reduction**		**Inert**
Bed temp.			**Gas flow**		
	Air	**N_2**	**CH_4**	**N_2**	**N_2**
(°C)	(nlpm)	(nlpm)	(nlpm)	(nlpm)	(nlpm)
840	15,06	10,00	10,00	5,06	10,00
890	14,41	10,00	9,57	4,84	10,00
940	13,82	10,00	9,18	4,64	10,00
Operational time for each cycle step					
	10 min	4 min	1 min		3 min

3.4 Experimental setup for OCAC operation

Current study used the same reactor and experimental set up as in previous study by Stenberg et al., to investigate the behaviour of magnetite fines and copper smelter slag in OCAC operation. Methane was used as gaseous fuel. Experiments with magnetite fines were done for six temperatures, 600°C, 700°C, 750°C, 800°C, 850°C and 900°C while copper smelter slag was only investigated at three 600°C, 750°C and 850°C due time limitation for the project. The procedure for OCAC experiments is described below.

After finished CLC experiments for one bed material, the bed material was kept in the reactor when the bed temperature was regulated to 600°C and the air flow to 17,46 nlpm. Once the bed temperature had reached the target bed temperature methane was added to the inlet gas flow to obtain an air to fuel ratio of 1.05. When the system reached steady state measurements of temperature, pressure and dry air composition were examined for a minimum of two (2) minutes for each measurement point, H1-H8. Similar measurements were done for the different bed temperatures. Table 7 lists the gas flows used for the corresponding bed temperatures to give an air to fuel ratio of 1.05.

Table 7: *Parameters for OCAC experiments. The gas flows for each bed temperature calculated for an air to fuel ratio at 1,05.*

Bed temp.	**Gas flow**		
	Total	**Air**	**CH_4**
(°C)	(nlpm)	(nlpm)	(nlpm)
600	19,20	17,46	1,74
700	17,23	15,67	1,56
750	16,39	14,90	1,49
800	15,62	14,21	1,42
850	14,93	13,57	1,35
900	14,29	12,99	1,30

3.5 Evaluation of fuel gas conversion

The materials ability to transfer oxygen is evaluated through the conversion of fuel during the combustion processes of CLC and OCAC operations. Fuel conversion is expressed by the CO_2 gas yield, γ_{CO2} according to reaction 11

$$\gamma_{CO2} = \frac{y_{CO2}}{y_{CO2} + y_{CO} + y_{CH4}} \tag{11}$$

where y_i indicates the gas fraction of component i at the reactor outlet [21]. Mass based oxygen carrier conversion is another measure of how well the bed material is oxidised and reduced in the combustion process. It is symbolised with ω and is the ratio between the reduced form of the material, m, and the mass of the oxidised form of the material, m_{ox}.

$$\omega = \frac{m}{m_{ox}} \tag{12}$$

The oxygen carrier mass cannot be measured during operation ans is therefore calculated as a function of time and the instantaneous mass balance over the reactor outlet [21] . The following two reactions describes the time integral for operation with syngas and methane respectively

$$\omega_t = \omega_{t-1} - \int_{t-1}^{t} \frac{\dot{n} M_o}{m_{ox}} [2x_{CO2} + x_{CO} - x_{H20}]\, dt \tag{13}$$

$$\omega_t = \omega_{t-1} - \int_{t-1}^{t} \frac{\dot{n} M_o}{m_{ox}} [4x_{CO2} + 3x_{CO} - x_{H20}] dt \tag{14}$$

where $\dot{n}$ is the molar flow rate at the reactor outlet, M_o is the molar mass of oxygen and y_i is the gas fraction of component i. The oxygen carrier conversion is expected to have the value of one (1) at the beginning of the cycle. Furthermore, the concentration of H_2O is not possible to measure and is therefore calculated from a mass balance over the reactor.

4

Results

Results from experiments in a lab-scale fluidized-bed reactor is presented in this section. First are results presented for CLC operation with magnetite fines as bed material, with syngas and methane as fuel, respectively. Secondly are results for copper smelter slag for CLC operation with syngas followed by the case with methane as fuel. In a following section are the results from CLC experiments discussed. Later are results from OCAC experiments presented and discussed for magnetite fines followed by the case with copper smelter slag. At last are the results for physical properties presented and discussed together with potential errors of the study.

4.1 Chemical activity in CLC

4.1.1 Chemical activity of magnetite fines

In this section the results for the CLC experiments with magnetite fines are presented. The results are then discussed together with the results for CLC experiments for copper smelter slag in section 4.1.4.

4.1.1.1 Reactivity with syngas

Chemical reactivity of magnetite fines with syngas was investigated at 840°C, 890°C and 940°C in a series CLC cycles. Conversion of syngas resulted in the reaction products CO_2 and H_2O in two parallel reactions of CO and H_2. Results from experiments with magnetite fines and syngas at 840°C are presented in figure 2 where figure 2a presents the CO_2 dry gas concentration during the reduction stage for the different cycles. The concentration of CO_2 is similar over time for all cycles with the highest value about 77 vol% of the total gas volume measured. Figure 2b presents the related concentration of CO, which is measured between 9,5-12 vol%. Only a few percentage points in gas concentration differs between the cycles which implies potential of repetitive fuel conversion with magnetite fines at 840°C. Figure 3 shows the mean dry gas concentration of CO and CO_2 for the different cycles and for each bed temperature investigated. As expected are magnetite fines reactive at the higher temperatures and the mean dry gas concentration of CO_2 increase with higher temperature, indicating higher fuel conversion with increased temperature. The results also show repetitive cycles for these temperatures, see figure A.1-A.6 in appendix.

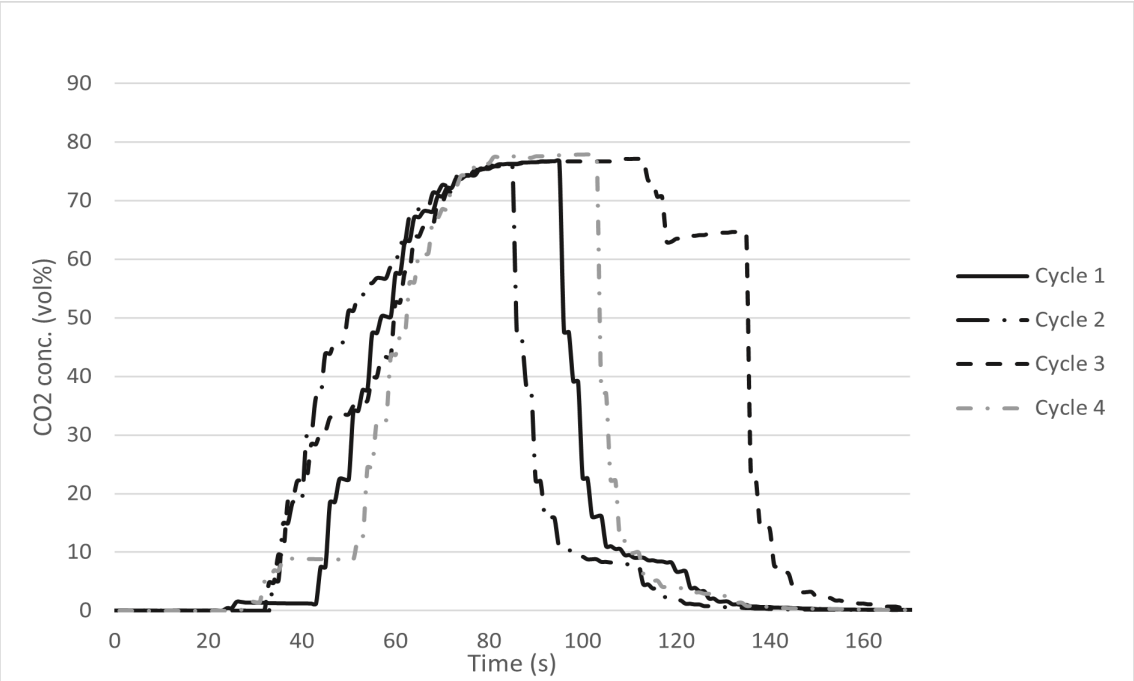

(a) CO_2 *concentration over time.*

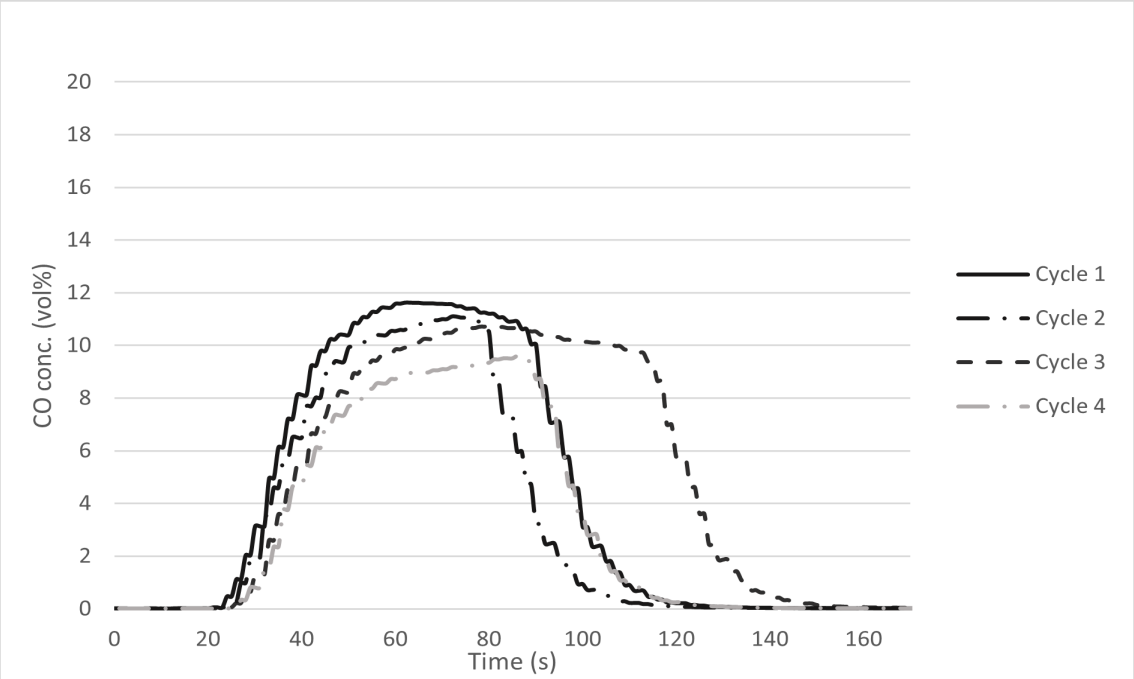

(b) CO concentration over time.

Figure 2: *Dry gas concentration over time during reduction stages in CLC cycle for magnetite fines at 840°C.*

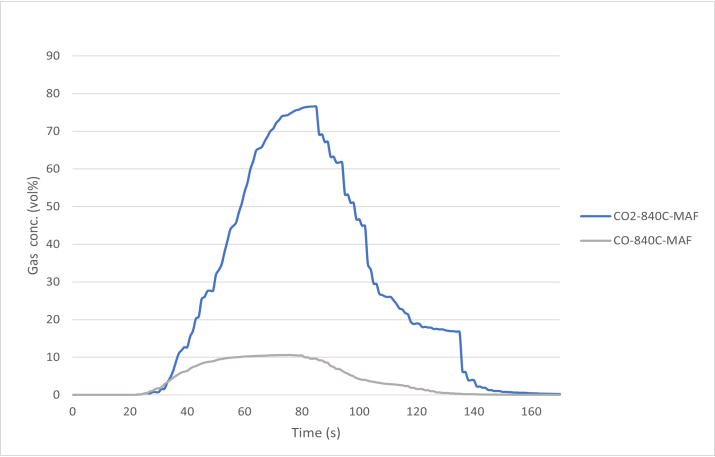

(a) Bed temperature 840°C.

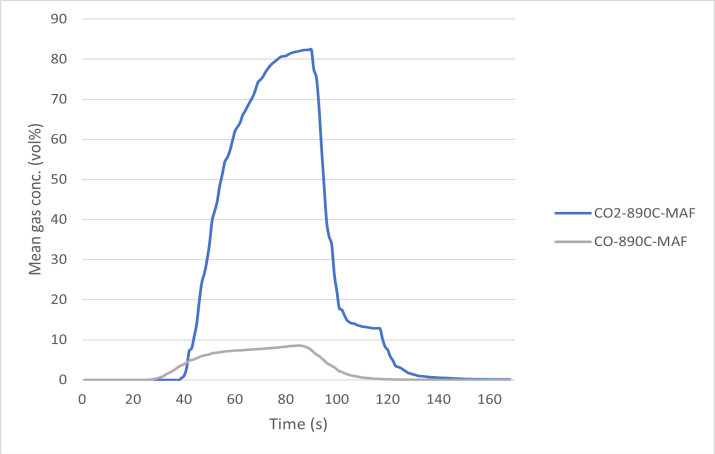

(b) Bed temperature 890°C.

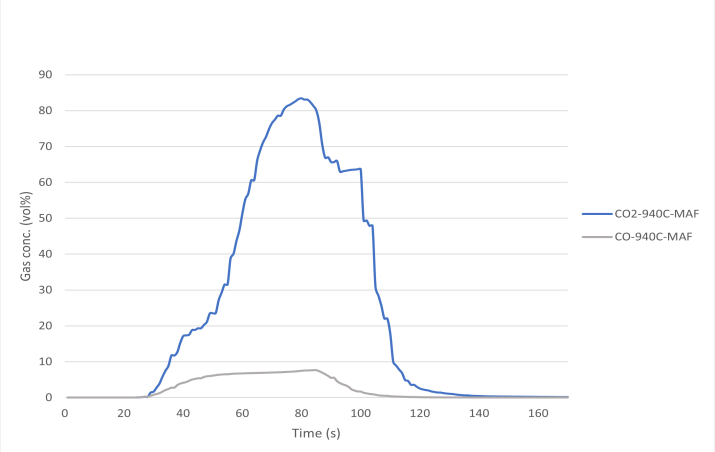

(c) Bed temperature 940°C.

Figure 3: *Mean dry gas concentration for CLC cycles with magnetite fines as bed material and syngas as fuel, for bed temperatures 840°C, 890°C and 940°C.*

Concentration of CO_2 was significantly higher than of CO for all bed temperatures when operating with syngas which shows that magnetite fines was chemically active

with high conversion for CLC operations with syngas. Peak value for concentration of CO_2 was measured to 83.0%76 at both 890°C and 940°C, while the peak value for 840°C was 76.0vol% for 840°C. The trend of increased fuel conversion with higher bed temperature can also be identified from figure 4, showing the yield of CO_2 as function of the oxygen carrier conversion for different bed temperatures. It is expected that the fuel conversion increases with the bed temperature. The experiments show up to 0,92 gas yield for CO_2.

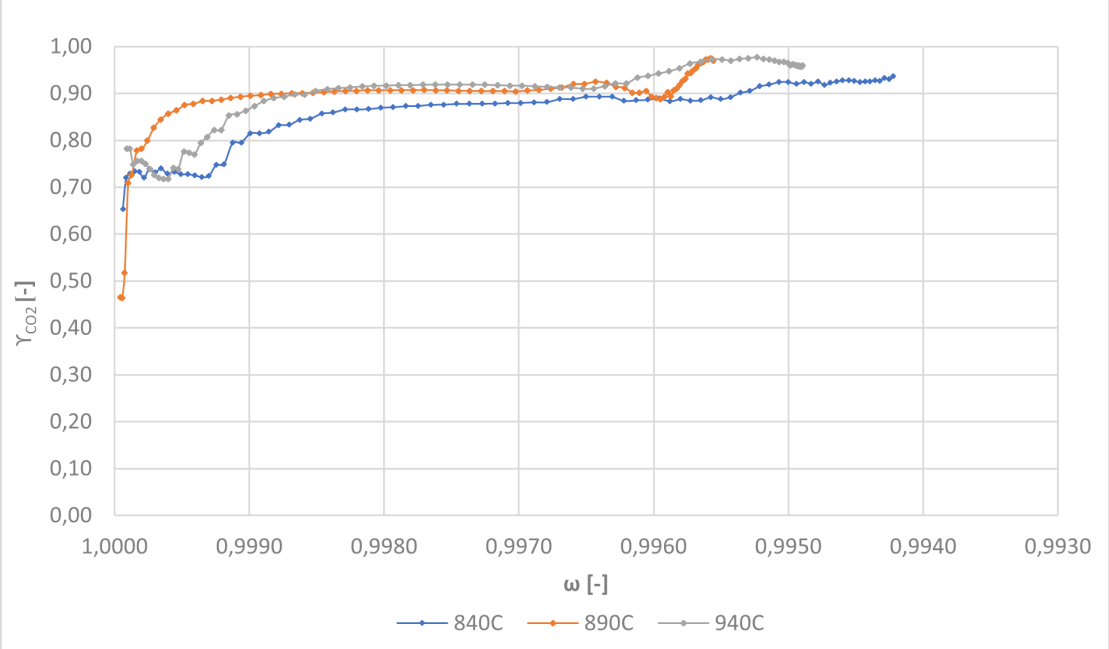

Figure 4: *CO_2 yield as function of the mass based oxygen carrier conversion of magnetite fines for combustion with syngas, at different bed temperatures.*

4.1.1.2 Reactivity with methane

When operating with methane as fuel for CLC the conversion was expected to be lower than that of the more reactive syngas. Note that data from experiments at 890°C is missing, due to loss of data during operation. Unlike the case with syngas, formation of CO is an indication for incomplete combustion when operating with methane. The mean dry gas concentration for bed temperature 840°C and 940°C are presented in figure 5. The orange coloured line is the CH_4 concentration which clearly is lower at 940°C than for 840°C. Likewise one can notice the CO_2 and the CO is higher at 940°C than for 840°C. Hence the endothermic two-phase reaction in the bed is favoured at higher bed temperature. Further more does the results show that the cycles repeats similar fuel conversion over time. Note that the gas concentrations in figure 5 is not directly comparable with the concentration for operation with syngas in figure 3 since operation with methane also have a flow of N_2 during the reduction step. The graph in figure 6 confirms the trend of increased fuel conversion for higher bed temperature, showing increased CO_2 yield for higher bed temperatures as a function of oxygen carrier conversion.

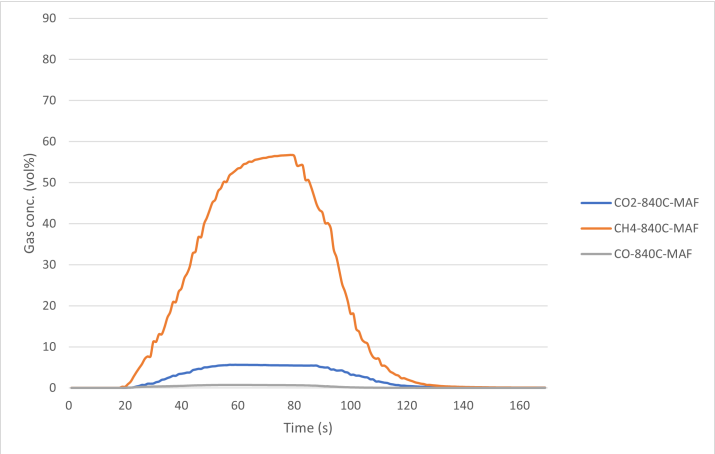

(a) *Bed temperature 840°C.*

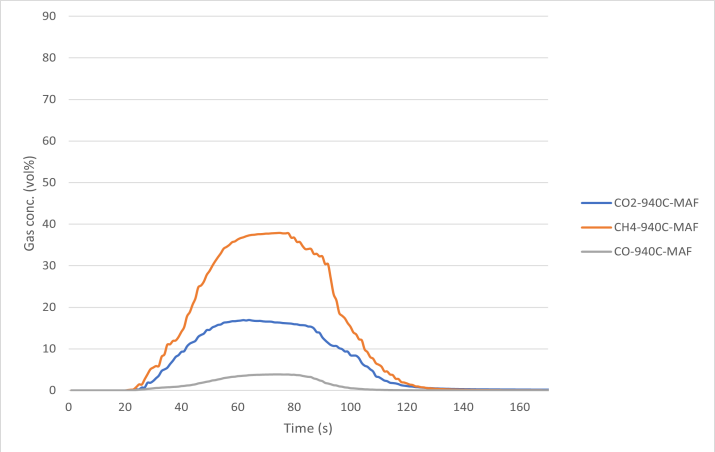

(b) *Bed temperature 940°C*

Figure 5: *Mean dry gas concentration for CLC cycles with magnetite fines as bed material and methane as fuel, for bed temperatures 840°C and 940°C.*

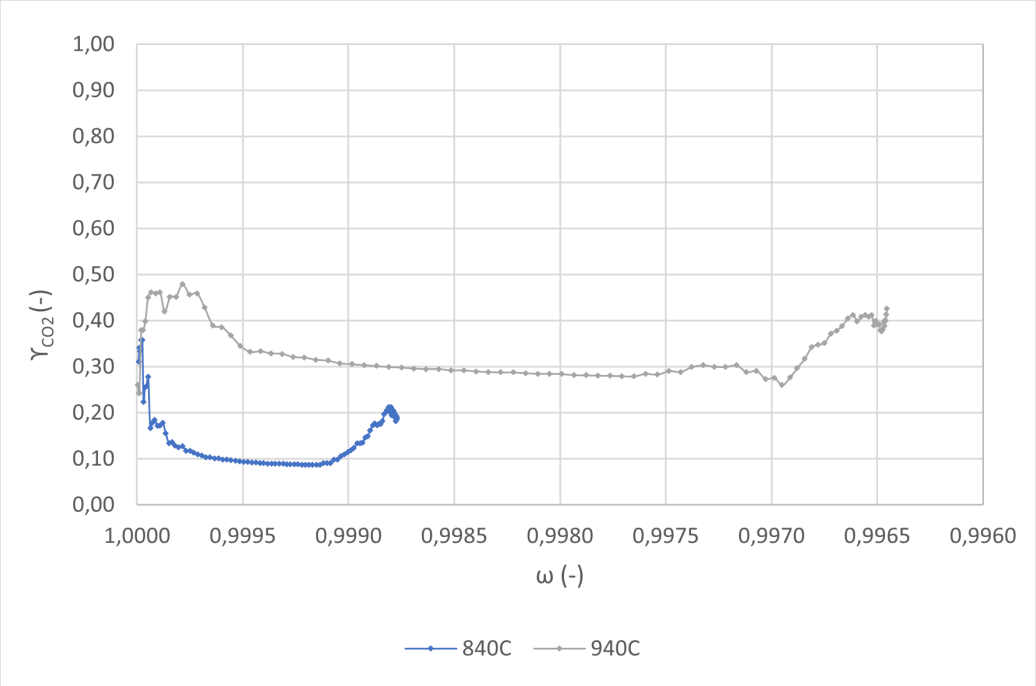

Figure 6: *CO_2 yield as function of the mass based oxygen carrier conversion of magnetite fines for combustion with methane, at different bed temperatures.*

4.1.2 Chemical activity of copper smelter slag

Chemical activity was also investigated for copper smelter slag, which was more cumbersome to prepare for experiments in a fluidized bed boiler.

4.1.2.1 Reactivity with syngas

Like the experiments with magnetite fines was the chemical reactivity with syngas the first experiment in the test series for copper smelter slag. Figure 7 presents the outlet gas concentration for CLC experiment at 840°C with syngas as fuel. The CO_2 concentration was reduced with the number of cycles, but the curves shows similar appearances with a value between 66-82 vol%, while the CO concentration was found to be more or less constant at 30 vol% for all cycles. Values for cycle 1 are deviant to the other cycles in time and area under the graph. This may be caused if the start of syngas flow was delayed and run for a longer operational time than 1 minute. It can also be because the oxygen carrier was more oxidized at the first cycle due to the long time it been exposed for oxygen during the previous step of heat up of the furnace and boiler. Furthermore, results show that the operation is recitative for higher bed temperature too. At 940°C was a slight tendency noticed of decreased CO_2 concentration with the number of cycles, in contrast of corresponding increase of CO. Figure 8 shows the mean dry gas concentrations for operation with copper smelter slag and syngas at all three bed temperatures. Mean gas concentration of CO_2 was found to be increasing with higher bed temperature, indicating higher conversion rate for 940°C than for the lower temperatures. The same trend can be noticed in figure 9, showing the CO_2 yield as a function of oxygen carrier conversion. The CO_2 yield is higher for increased bed temperature for the related value of oxygen carrier conversion.

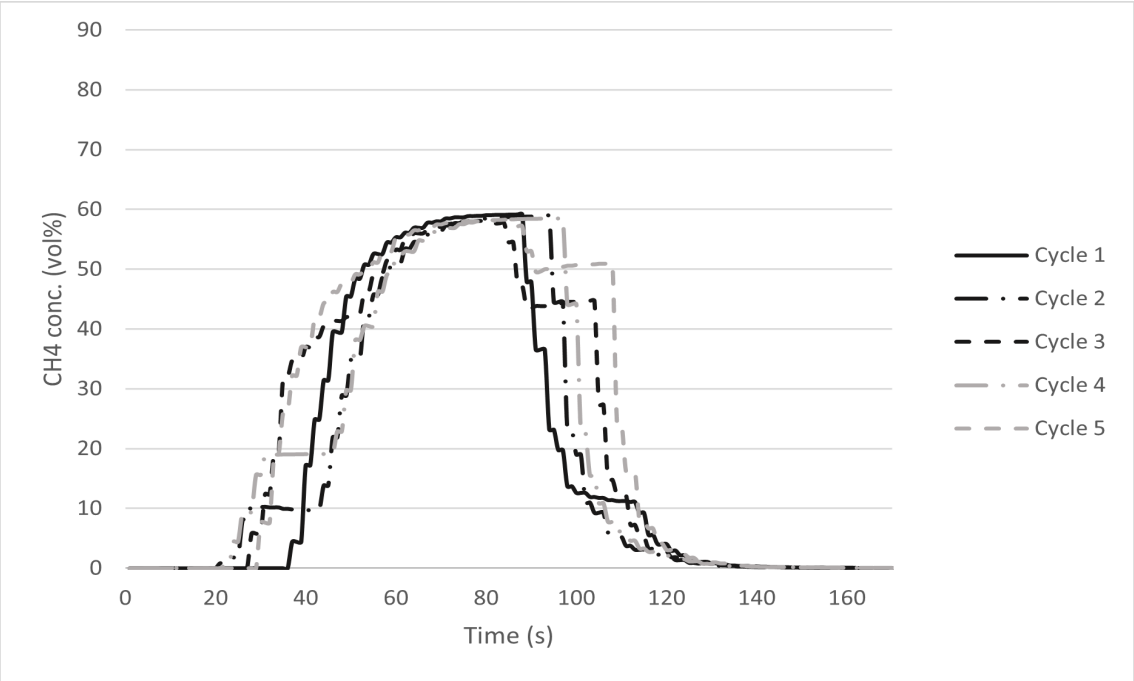

(a) CO_2 concentration over time.

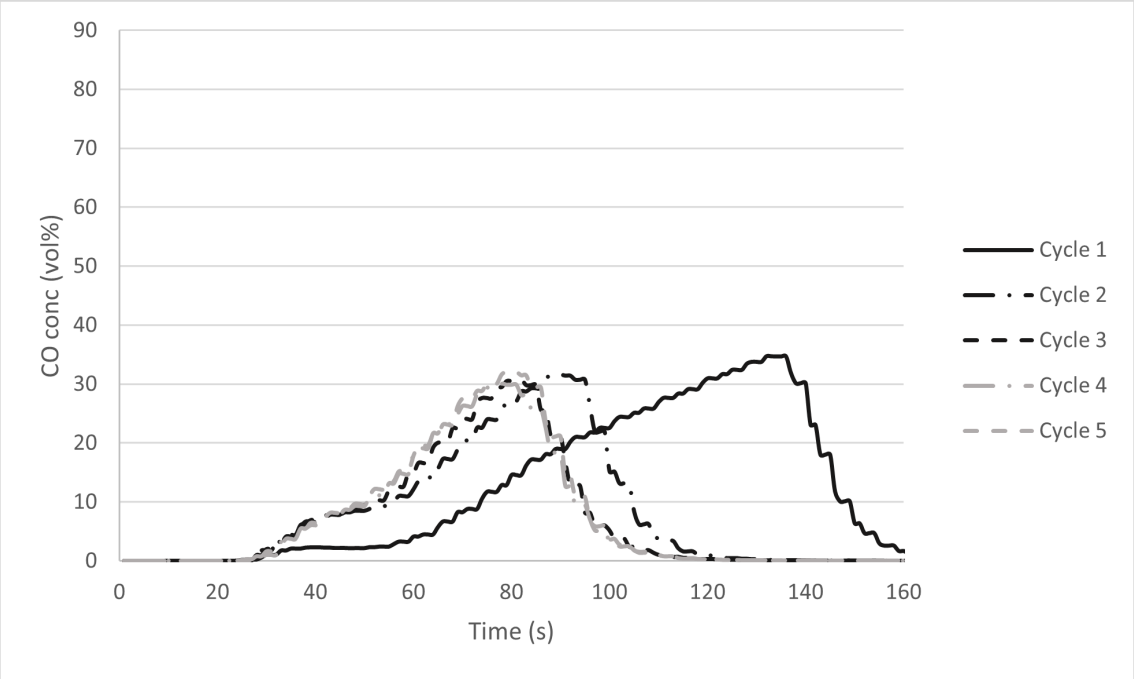

(b) CO concentration over time.

Figure 7: *Dry gas concentration over time during reduction with syngas in CLC cycle for copper smelter slag at 840°C.*

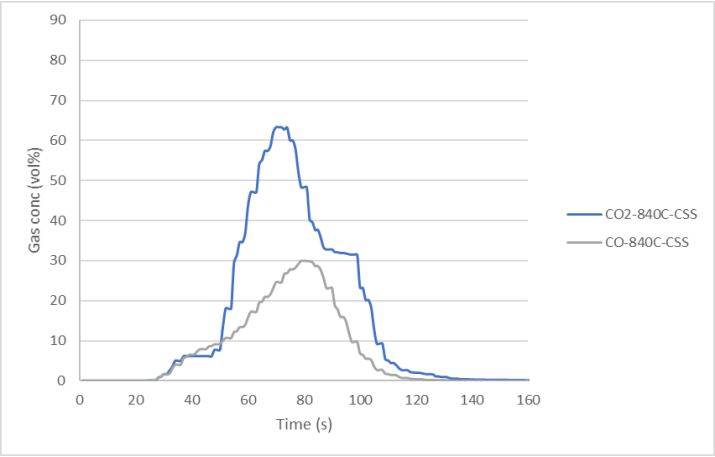

(a) Bed temperature 840°C.

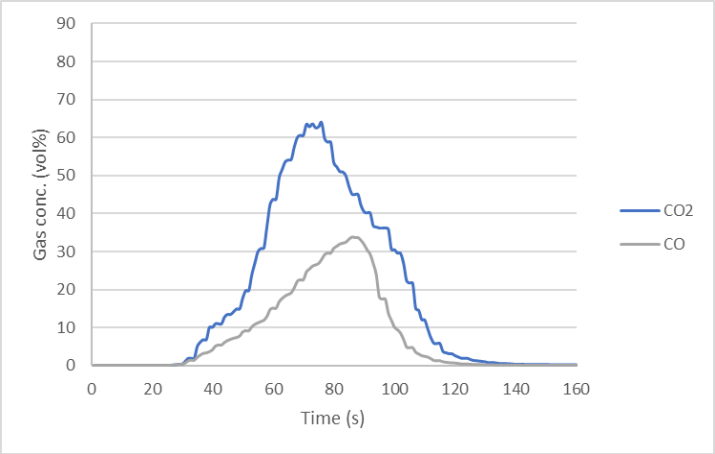

(b) Bed temperature 890°C.

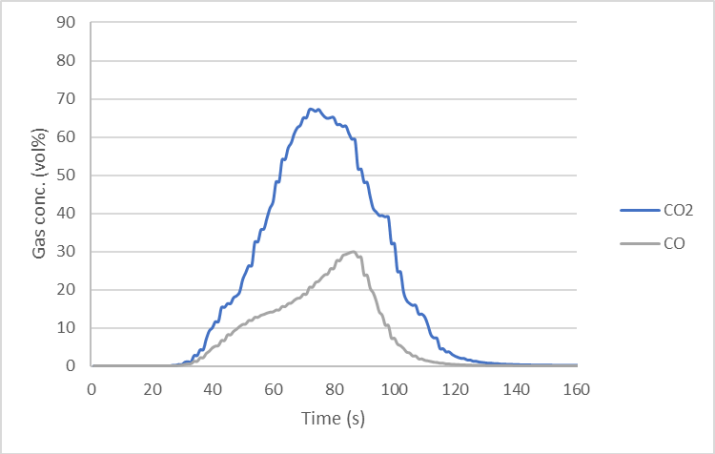

(c) Bed temperature 940°C.

Figure 8: *Mean dry gas concentration for CLC cycles with copper smelter slag as bed material and syngas as fuel, for bed temperature s 840°C, 890°C and 940°C*

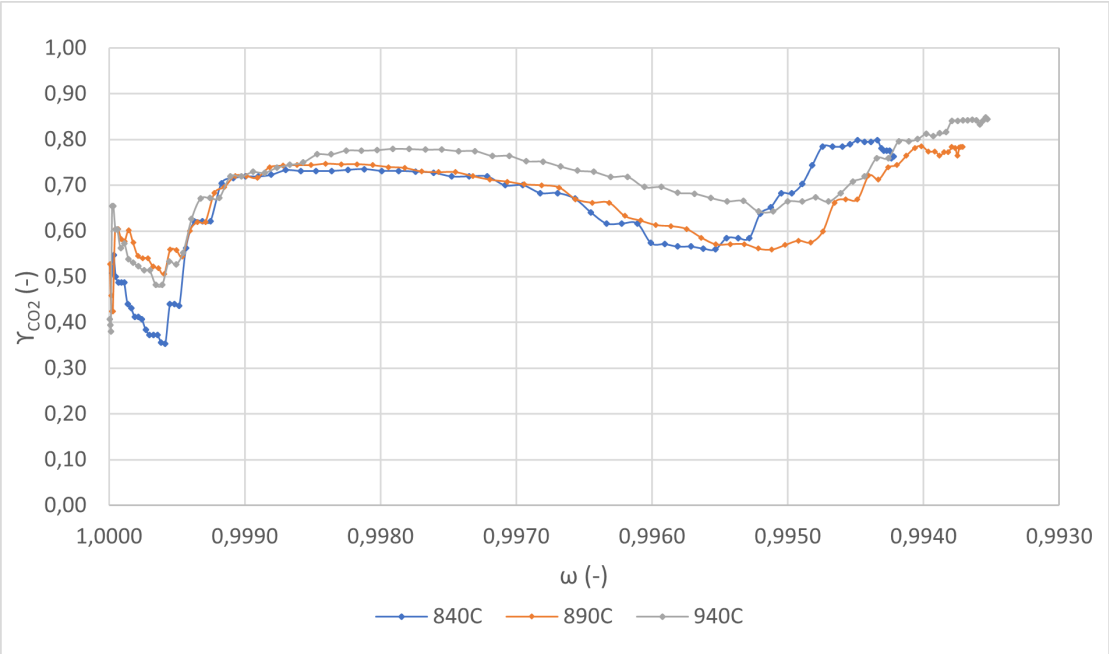

Figure 9: *CO_2 yield as function of the mass based oxygen carrier conversion of copper smelter slag for combustion with syngas, at different bed temperatures.*

4.1.2.2 Reactivity with methane

Figure 10 show the dry gas concentration of CH_4, CO_2 and CO for CLC operation with copper smelter slag and methane. The results show conversion of methane fuel to CO_2 and CO for all bed temperatures and all cycles during the experiment. General trends for all bed temperatures noticed were highest concentration of CO_2 for the first or second cycle and decreased for every following cycles. In contrary was the CO concentration increasing with the number of cycles. Furthermore, it can be noticed that the CO concentration increase towards the end of the cycle while CO_2 was highest at the beginning and thereafter decreased. While the CH_4 value increased at the end of the cycle. Figure 11 shows the mean dry gas concentration for cycle 2-5, for each bed temperature. The CH_4 concentration was lower for high bed temperature with a difference of 10 percentage points between the lowest and highest temperature. That trend is expected and can further be seen in figure 12 where the value for CO_2 yield at bed temperature 940°C is significantly higher than for 840°C. Further more can it bee seen that the oxygen carrier conversion reaches a lower value at higher bed temperature, indicating higher reactivity at this temperature, as expected.

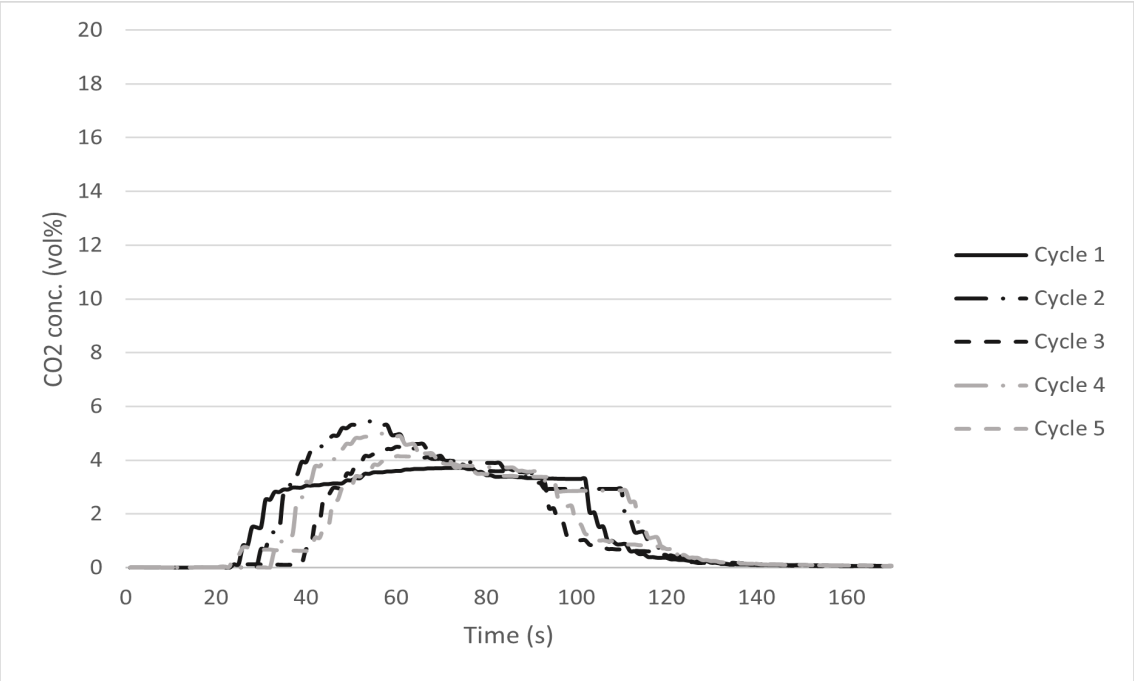

(a) *CO_2 concentration over time during reduction with methane in CLC cycle for copper smelter slag at 840°C*

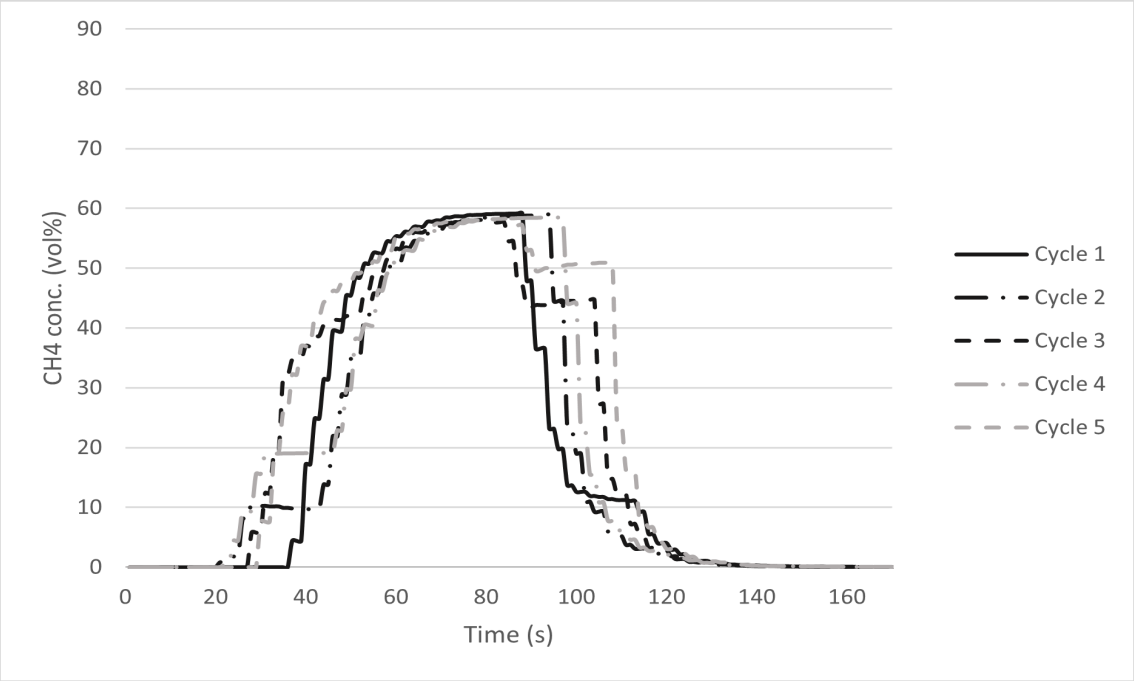

(b) *CH_4 concentration over time during reduction with syngas in CLC cycle for copper smelter slag at 840°C*

Figure 10: *Dry gas concentration over time during reduction with methane in CLC cycle for copper smelter slag at 840°C.*

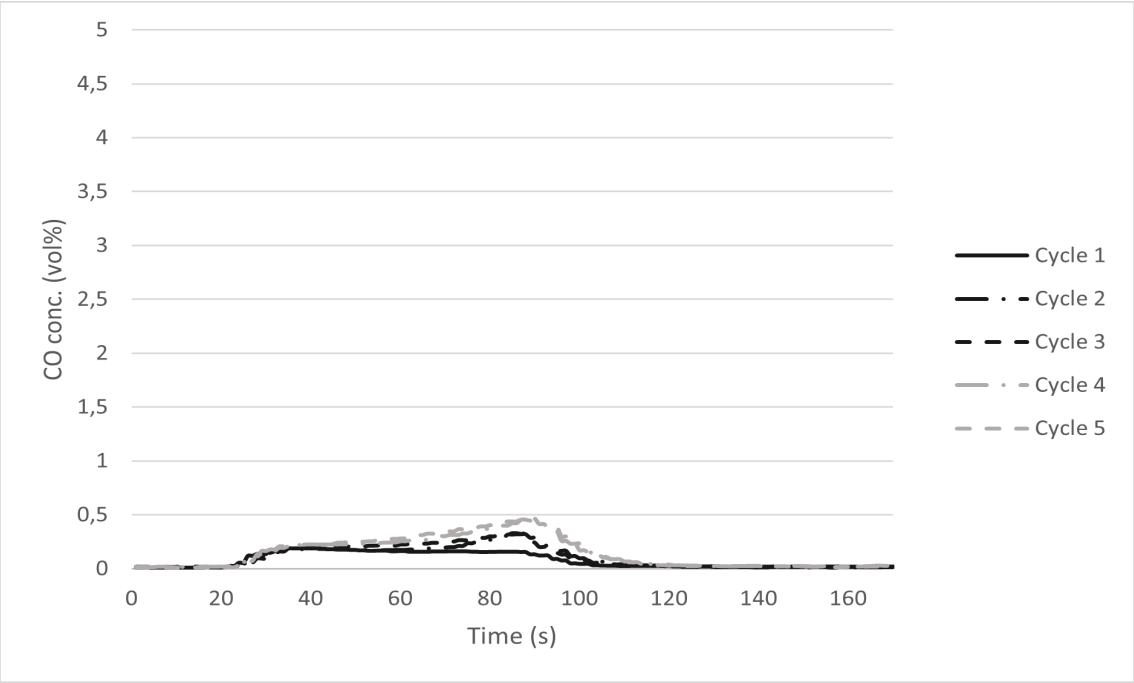

(c) CO concentration over time during reduction with syngas in CLC cycle for copper smelter slag at 840°C

Figure 10: *Dry gas concentration over time during reduction with methane in CLC cycle for copper smelter slag at 840°C.*

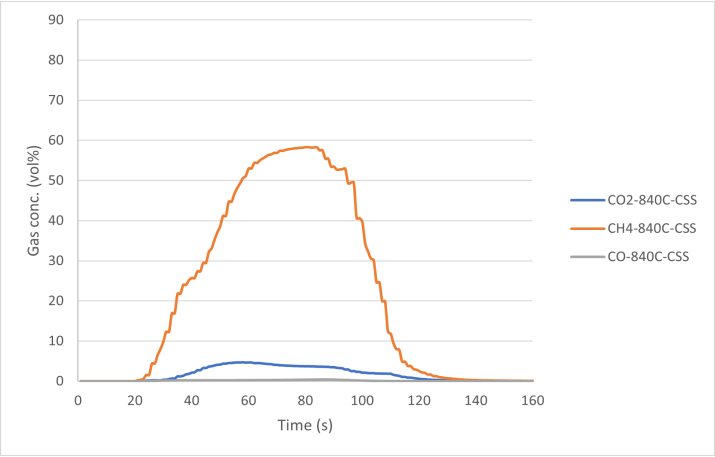

(a) Bed temperature 840°C.

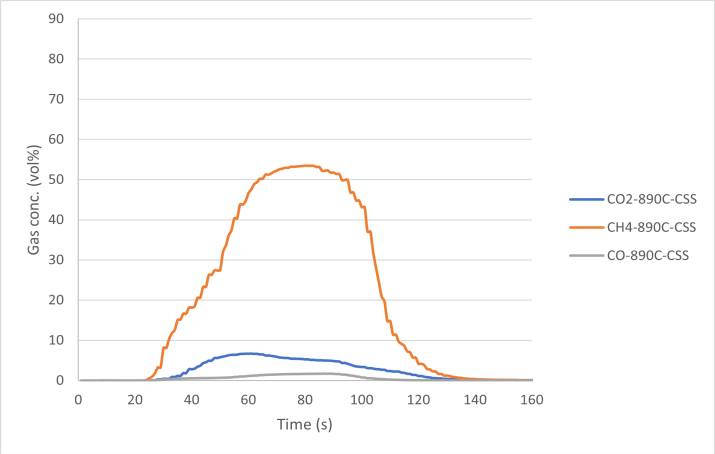

(b) Bed temperature 890°C.

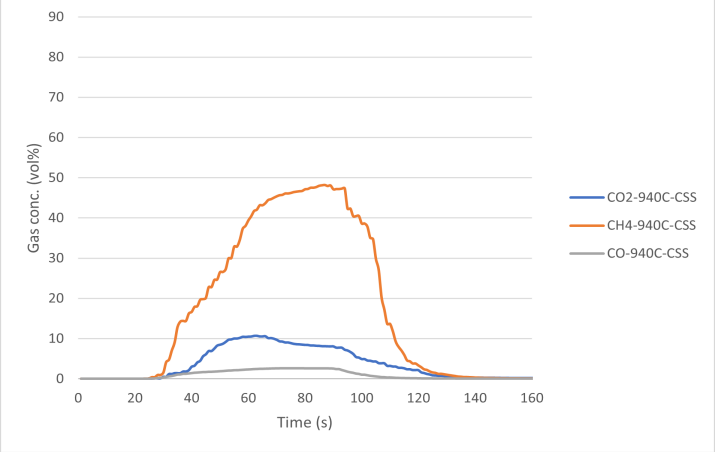

(c) Bed temperature 940°C.

Figure 11: *Mean dry gas concentration for CLC cycles with copper smelter slag as bed material and methane as fuel, for bed temperature s 840°C, 890°C and 940°C*

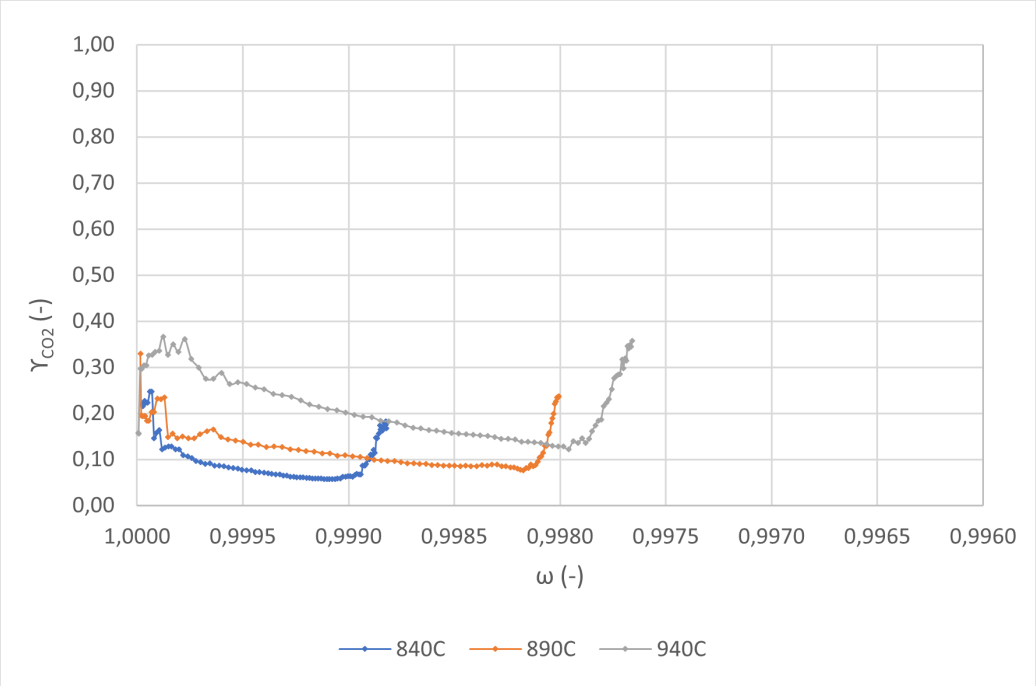

Figure 12: *CO_2 yield as function of the mass based oxygen carrier conversion of copper smelter slag for combustion with methane, at different bed temperatures.*

4.1.3 Discussion CLC operation

Magnetite fines and copper smelter slag both show chemical activity in the CLC experiments presented. Both materials converts syngas fuel to CO_2 and H_2O already at the lower temperature of 840°C and the conversion increased for higher bed temperatures. The conversion was, as expected, lower for operation with methane fuel, for which both the materials showed increased conversion for higher temperature. However methane was not fully converted to CO_2 for any bed material or temperature, showing formation of CO. Incomplete combustion of methane is expected due to the chemical properties of the methane molecule and the chemical stability of methane during the relatively short operational time. However it is positive that some conversion of methane occur since it then can be possible to use the materials for applications with combustion of biomass and other solid fuels.
Furthermore, the results in fuel conversion is similar between the cycles which indicates that the reactivity may be stable with the number of cycles. This is different from the reactivity of ilmenite, which reactivity increase with the number of cycles initially. It is not possible to compare the absolute reactivity of ilmenite with the results from this study since the reactivity depends on several design and operational parameters. However the stable reactivity of magnetite fines and copper smelter slag is positive for operation in CLC. The experiments in this study only investigated the trends from a few number of cycles (4-6 cycles) and this may be too few for a reliable perception on the matter of stability. Further experiments with increased number of cycles are needed in order to settle this matter.
The CO_2 yield for combustion for magnetite fines is significantly higher than for

copper smelter slag, for both syngas and methane combustion, see figure 4, 6, 9, 12. The value of CO_2 yield for magnetite fines are also more stable with decreased oxygen carrier conversion, than for copper smelter slag. This result was expected since magnetite fines have a higher Fe oxide content than copper smelter slag, which is the oxygen carrying component in the material.

4.2 Chemical activity in OCAC

To further investigate the chemical activity of the materials experiments for OCAC operation were carried out at different bed temperatures between 600°C and 900°C. Methane was used as fuel with an air to fuel ratio of 1.05. Results for experiments with magnetite fines as bed material is presented in the section below, before the results from operation with copper smelter slag is presented.

4.2.1 Magnetite fines for OCAC

Experiments for magnetite fines were examined at the bed temperatures 600°C, 700°C, 750°C, 800°C, 850°C and 900°C. The concentration profile of methane for the different heights over the distribution plate for different bed temperatures are presented in Figure 13. It can be observed that the methane concentration decreases with increasing bed temperature for all measurement point. This general trend is expected for methane due to its limited reactivity. The chemical reaction is more likely to occur at higher temperature. At 600°C the concentration is the same as the inlet concentration for H4 to H8, which indicates that there are no significant combustion at this temperature. 600°C is a relatively low temperature for conversion of methane and no conversion at this temperature is expected. However, the concentration at H1, H2 and H3 is lower than it is above the bed which could indicate that some conversion of methane takes place in the bed already at this low temperature. The same trend is observed for all other temperatures. The lower methane concentration in the bed is expected to be caused by the gas-solid interaction in the emulsion phase of the bed, causing methane conversion to carbon dioxide and water. However, this trend was not observed at as low temperature as 600°C in an earlier study by Stenberg et al [7]. Concentration at H1 in that study was the same as for all other measurement points at 600°C. Furthermore was it lower for higher bed temperature with a trend to decrease between H1 and H3 which is not the same as observed for magnetite fines. This may indicate that some fuel conversion occur directly above the distribution plate when operating with magnetite fines before the reactivity decrease through the lower part of the bed at H2, which can be seen in figure 13 where the CH_4 concentration increase between the first and second measurement point. However, for the higher bed temperatures is it expected that the conversion may decrease higher up in the bed, at H3 and H4, since it is expected that larger bubbles are formed here which in turn decrease the heat and mass transfer between the bubbles and the emulsion phase. For bed temperature 800-900°C can it be noticed that the CH_4 concentration decreases from H2 to H3, which shows that the conversion is not effected by the formation of larger bubbles.

Measurements of CO have been analysed to identify if the conversion of methane is complete or if formation of CO occur as indication of incomplete combustion. Figure 14 presents the concentration of CO at the different measurement points for different bed temperatures. The first important observation is that CO concentration at the reactor outlet, H8, is close to zero for all be temperatures. Since the concentration of CH_4 also goes to zero at the outlet, figure 13, has the fuel been fully converted to CO_2 before leaving the reactor. The peak concentrations of CO are low for the three lower temperatures, 600-750°C, where the fuel conversion is generally low. At 800°C the concentration increases and peaks at H4. The same peak is observed for 850°C and 900°C. The deviant peak values can possibly depend on where the gas sampling is made. Gas sampling tube at H4 is located in the free board of the bed, where the gas sampling is made from the gas surrounding the particles. While down in the bed is it possible that the gas sampling tubes are located either in the emulsion phase where fuel conversion can occur, or inside the bubble phase, containing mainly methane gas. The difference in gas concentration between H2, H3 and H4 can also indicate that the conditions for formation of CO is favoured in the free board where the gas bubbles of methane and the emulsion phase with oxygen carriers are mixed together again. It also indicates that the emulsion phase reaction in the bed favours formation of CO further down in the bed while at H3 is full conversion to CO_2 higher. One possible explanation to the formation of CO further down in the bed is that CO is the chemical intermediate in the conversion reaction of CH_4 to CO_2 and is therefore the first reaction to occur down in the bed, H2. At H3 does CO react to CO_2.

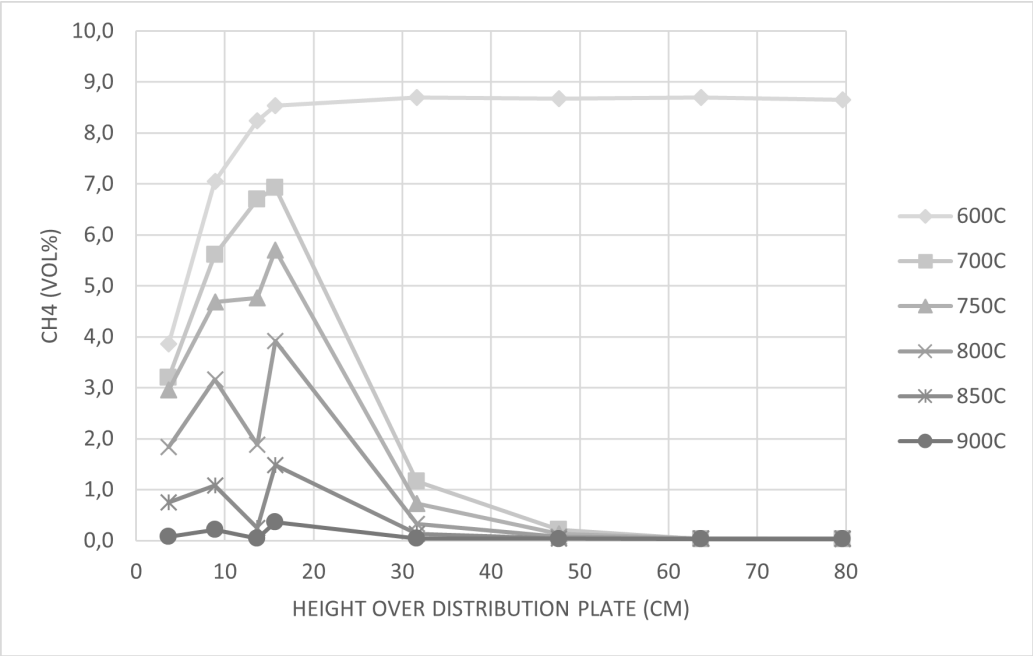

Figure 13: *Dry gas concentration of CH_4 measured at different height over the distribution plate at bed temperatures 600°C, 700°C, 750°C, 800°C, 850°C and 900°C for magnetite fines in OCAC.*

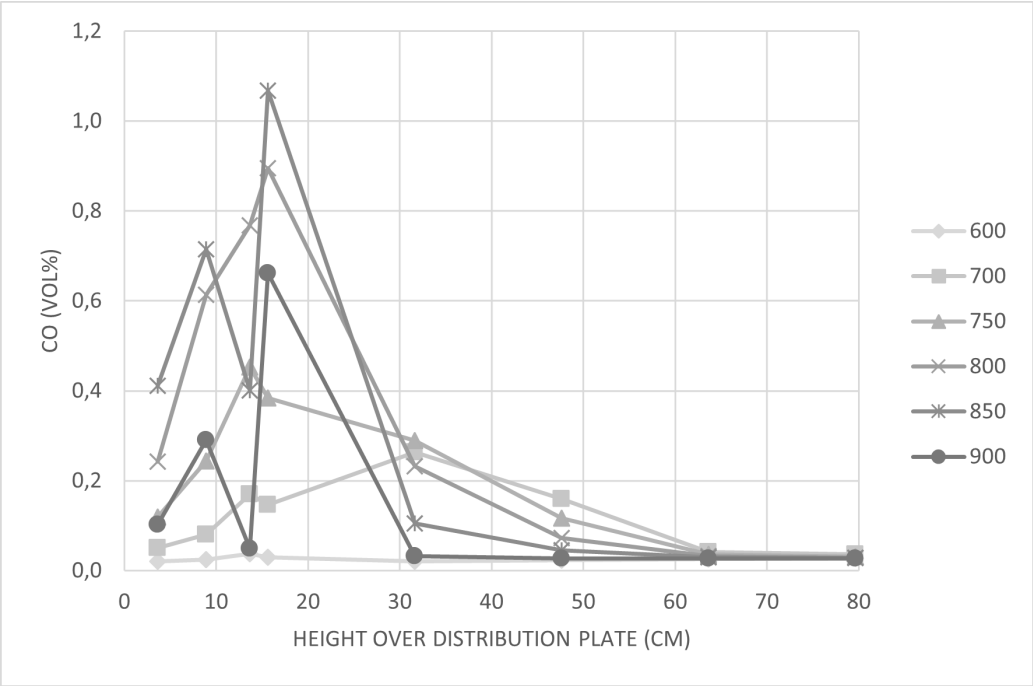

Figure 14: *Dry gas concentration of CO measured at different height over the distribution plate at bed temperature 600°C, 750°C and 850°C for magnetite fines in OCAC.*

4.2.2 Copper smelter slag in OCAC

Experiments with copper smelter slag in OCAC were done for three bed temperatures 600°C, 750°C and 850°C. Figure 15 presents the methane concentration for the different measurement points for all bed temperatures. First it can be noticed that the methane concentration decreases with increasing bed temperature both in the free board and the bed, which is the same result as discussed earlier for magnetite fines. At 600°C the values at all measurement points but two, H0 and H1, are about the inlet concentration, indicating no conversion of CH_{44}. During heating of the reactor from 600°C to 750°C ignition in the reactor was observed at 700°C. For 750°C there is a change in concentration from H2 to H3 which indicates that combustion occur in the upper part of the bed. There is a slight increase from H3 to H4 where the gas from emulsion phase is mixed with the gas from the bubbles. The significant decrease of methane is however detected in the free board between H4 and H6. Measurements for 850°C shows the same trend as for 750°C even though the methane concentration is significantly lower already in the bed. Furthermore, for 600°C are the values for H3 and H6 lower than the expected value for inlet concentration. Since the values presented are a mean value over 120 seconds the values over the time interval have been reviewed. During the first 24 seconds the methane concentration decreases from 8.65% gradually to 1.57% and thereafter increases back to 8.58% during additional 20 seconds. Even though the change in concentration is out of trend compared to values for the remaining 75 seconds, are the measurements one third of all data point and can therefore not be rejected in mean value calculations. Any explanation of this results is however uncertain. Measurements of other gases

did not change during the time interval. Looking at the concentration of CO for the different bed temperatures gives an indication whether methane is fully converted to CO_2 or not. Figure 16 shows the CO concentration throughout the reactor for the different bed temperatures investigated. The concentration is generally low for all three bed temperatures. However at 850°C is one peak of 1% observed at H2 difficult to explain. Most important to observe is that the concentration of CO is close to zero at H8, the top of the reactor. It proves that methane can be fully converted in an OCAC operation with copper smelter slag as bed material.

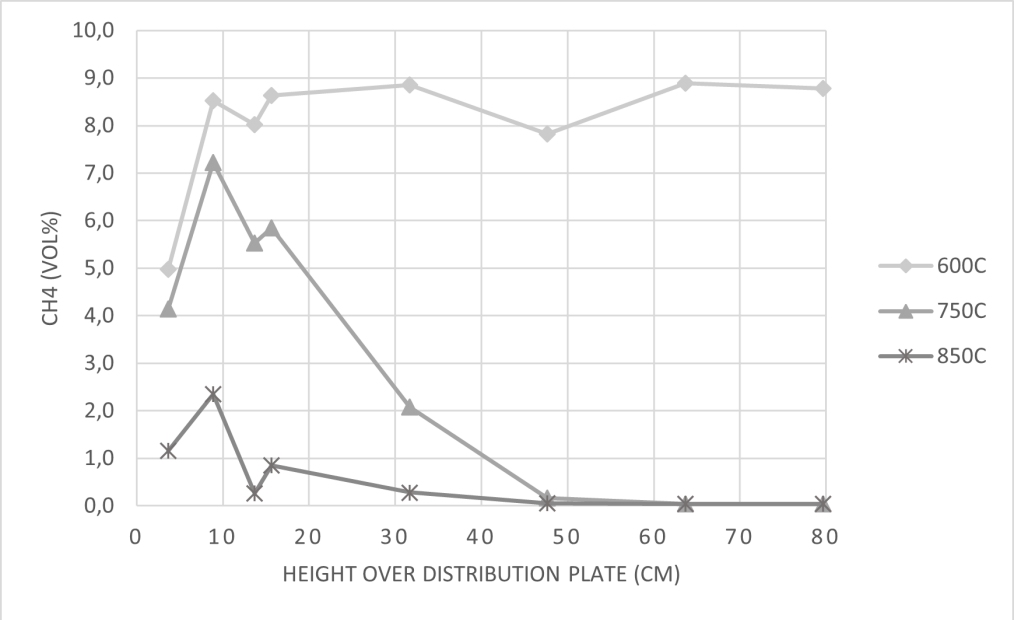

Figure 15: *Dry gas concentration of CH_4 measured at different height over the distribution plate at bed temperature 600°C, 750°C and 850°C for copper smelter slag in OCAC.*

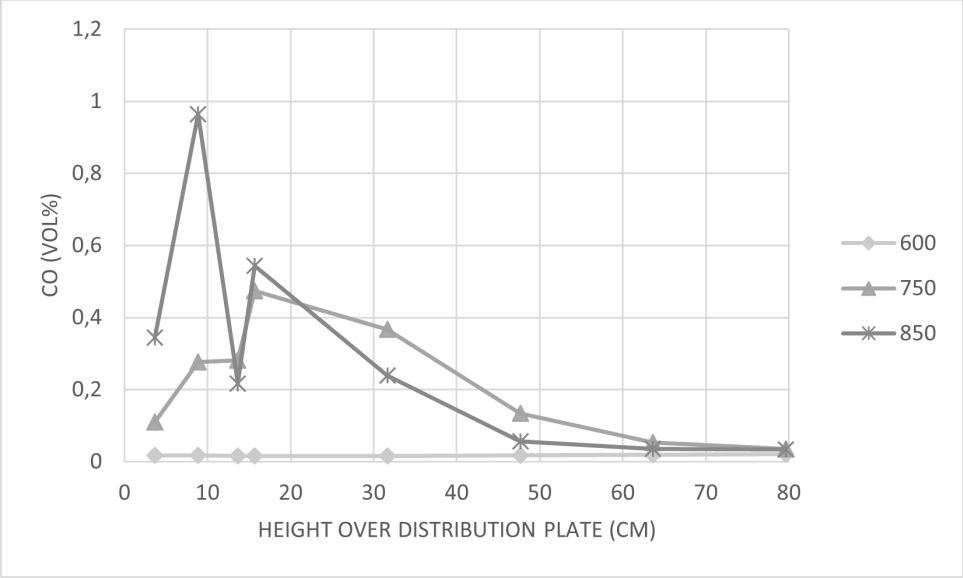

Figure 16: *Dry gas concentration of CO measured at different height over the distribution plate at bed temperature 600°C, 750°C and 850°C for copper smelter slag in OCAC.*

4.3 General observations

Visual inspection of the material was done after all CLC and OCAC experiments in order to identify tendencies for agglomeration or sintering. Magnetite fines did not show any tendency for formation of agglomerate or sintered material. However for copper smelter slag was a few lumps identified in the bed inventory. It is impossible to say if they were formed during CLC or OCAC, or during both experiments. Larger particles were noticed on the top of the reactor wall after OCAC, which was not seen after CLC experiments. One possible explanation can be that OCAC forms active combustion with flame formation, which causes high local temperature in the reactor, especially in the free board. The high temperature may effect the properties of the particles which makes them stick to the reactor wall. However, these larger particles where easily removed from the reactor wall and was easy to break apart again, indicating that no significant agglomeration or sintering occurred. Further investigations of the particle size distribution and particle structure are however needed for a more reliable data in this matter.
No visual observation of swelling of magnetite fines or copper smelter slag were done. Measurement of the bulk density after the experiments implies that copper smelter slag may have increased in particle size, hence showing a lower bulk density than the original material. Table 8 lists the mass of the bed interior and the bulk density before and after the experiments for magnetite fines and copper smelter slag. Copper smelter slag measured a bulk density at 1400,7 kg/m^3 after finished experiments compered to 2466,7 kg/m^3 for the original material. Further more is the bulk density for magnetite fines higher after the experiments compared to before, which can imply attrition of the particles when operating in the fluidized bed. The bulk density of smaller particles are generally higher than for larger particles. The bulk

density of a sample of magnetite fines was measured to 2673,4 kg/m^3 compered to 2484,8 kg/m^3 for the original material. Further information to investigate the effect of attrition is outside the scope of this study. Parameters to be investigated further would be particle size distribution, mean particle size and calculation of particle density.

Table 8: *interior material mass and bulk density before and after conducted experiments for magnetite fines and copper smelter slag.*

	Initial material		**Material after experiments**	
	m_{bed} (g)	ρ_{bulk} (kg/m^3)	m_{bed} (g)	ρ_{bulk} (kg/m^3)
Magnetite fines	1616,6	2482,7	1634,4	2673,4
Copper smelter slag	1082,1	2466,7	1053,2	1400,7

Limitations were observed for the technical equipment used for the experiments. There is an uncertainty in measurement of gas concentration at specific measurement points. The gas flow for the gas sampling tube should be about 30 litre per minute to fill the gas analyse chamber. The gas flow measured was less than 30 litre per minute for a number of measuring points, which is believed to be due to worn out gas sampling tubes or plugged filter at the tubes. This eventually affect measurements of the gas concentration at measurement point H2 and H6. Measurements from CLC experiments are not affected since only measurement point H8 was used. However, all measurement point were used for the OCAC experiments which results can be influenced by the low gas flow in the gas analyser. Observing figure 13 for gas concentration profile through the reactor, with magnetite fines, measurements at H6 are in line with measurements at H5, H7 and H8 for 600°C. It may indicate that the measurements at H6 are acceptable even though the gas flow is low. Corresponding measurements for copper smelter slag however, figure 15 show a deviant value for H6 at 600°C, which indicates there may be an effect on the results. Measurements at H6 at 750°C and 850°C for copper smelter slag is however showing the same trends as magnetite fines and earlier measurements by Stenberg [7].
One additional potential error of the reactor setup was the position of the gas sampling tubes. The sampling tubes was supposed to be placed inside the reactor at 2 cm from the inside of the reactor wall. When taking down the reactor after finished experiments with magnetite fines (both CLC and OCAC tests), it was noticed that two sampling tubes was at the wrong position. The tubes at height H5 and H7 was placed too fare out in the construction pipe holding the gas sampling tube in place, leaving an empty space at the opening of the construction pipe towards the reactor. The error in the position might have influenced the accuracy of the gas concentration measurement at H5 and H7. However, the values of gas concentration are at H7 in line with the values at H6 and H8 and the values for H5 are to expect compared to results by Stenberg in the same reactor [7]. The gas sampling tubes

at H5 and H7 were adjusted before continuing with tests for copper smelter slag. Results for CLC experiments is however not affected since no measurements were done at other heights than H8.
An other limitation for the equipment was that no measurements of the exact inlet gas concentrations was possible to get from current reactor design. There was no instant measurement of the gas concentration at the gas inlet. The inlet was regulated by an automatic vault which furthermore gave an unstable flow when mixing inlet gases. To get more accurate inlet gas concentration it would be of interest to have a gas sampling tube at the inlet, measuring the inlet gas concentration parallel to any of the other measurement points above the distribution plate. Then it would be possible to set up a mass balance over the reactor which may give more accurate values for the instant fuel conversion.
An other aspect with the two materials investigated is the product availability in the region. Since the materials are products and byproducts in the already existing metal industries in Sweden and Norway, the logistics to use them in northern Europe may be attractive as an alternative to ilmenite. However, a full analysis of the matter of available market, logistics and a life cycle perspective is not included in this study.

4.4 Future work on this topic

From current study is it possible to conclude that both magnetite fines and copper smelter slag are reactive with syngas and methane when operating in CLC and OCAC processes. To further investigate how the reactivity changes over time experiments in lab scale reactor can be done with longer operational time, both for CLC and OCAC operation. Experiments with longer operational time than done in this study may also be useful to identify behaviour of the material´s physical properties and chemical composition.
This study have only investigated the reactivity and properties operating in small scale lab reactor, which limits the application of the findings at large scale reactors. To further investigate the behaviour and effects in commercial fluidized bed boilers is it necessary to do experiments in a large scale reactor. Suggestion is to carry out a similar experimental setup as used in this study for OCAC in a large scale experimental boiler at Chalmers University of Technology, operating at 30 MW. However, the operational time should be longer than in this study to identify changes in the material´s reactivity and particle´s properties over time. Large scale reactors for CLC is not commercially available today and may therefore not be tested. However, the material´s reactivity and particle´s properties can be evaluated over a longer operational time in the same reactor as used in this study.
The material that been used in the reactor, in current study, can in future work be investigated to quantify elements and locate material properties within the particles. Relevant methods are X-ray diffraction (XRD) and Scanning electron microscope (SEM). XRD characterise segments of different solid phases in the particles corresponding to different crystalline elements. XRD can then quantify different metals and their oxidation phases in the particles which are of interest when calculating the reaction time and comparing with other materials. Location of different metal

phases and elements are detected with SEM. With this analyse method it is possible to see if the metal oxides are located in the centre of the particle or at the particle surface. The location of the metal oxides effect the availability for chemical reactions for the combustion process. Therefore SEM can be helpful to further understand the chemical reactivity and identifying potential changes in reactivity during operation. XRD and SEM can together also give knowledge about unwanted elements that may effect the reactivity, toxicity and eventual waste disposal processes of the bed material. Material used in additional experiments with longer operational time may also be investigated with XRD and SEM since changes in the material composition and location of elements can occur after longer operational time than used in this study.
Future work also includes experiments for OCAC with solid fuel and biomass fuel. The commercial application of OCAC is energy generating fluidized bed boilers with solid fuel, municipal solid waste or biomass. Since magnetite fines and copper smelter slag in this study show reactivity with methane in OCAC experiments there are potential to be reactive with solid waste and biomass. Experiments with solid waste and biomass fuel can potentially take place in the same lab scale reactor as used in this study. However it is necessary to construct a mechanical system that provides the solid waste to the reactor continuously during operation.

5
Conclusion

Two materials from the metallurgical industries of LKAB and Boliden AB have been investigated as potential oxygen carriers for CLC and OCAC. The materials are magnetite fines and copper smelter slag. Experiments have been conducted in a lab-scale fluidized bed boiler at Chalmers University of Technology to evaluate if the materials are reactive with syngas and methane. Experiments for CLC operation have been investigated the fuel conversion at three bed temperatures 840°C, 900°C and 940°C. An experimental setup for OCAC operation was carried out at bed temperatures between 600°C and 900°C.

- Lab-scale experiment of CLC with syngas shows that magnetite fines and copper smelter slag are reactive with both oxygen and the fuel components H_2 and CO, at the bed temperature between 840-940°C.
- Magnetite fines and copper smelter slag are moderate reactive with methane, CH_4, at the bed temperatures between 840-940°C.
- When operating in OCAC configuration magnetite fines and copper smelter slag shows potential to move fuel conversion down in the bed already at moderate bed temperatures and have potential to decrease the excess air flow needed for combustion.
- Magnetite fines do not show any tendency for agglomeration from visual inspection after CLC operation and OCAC operation up to 940°C.
- Copper smelter slag show tendency for agglomeration after visual inspection after CLC operation and OCAC operation up to 940°C.
- Enrichment sand in its natural form is not suitable as fluidized bed material due to its poor physical properties.

Bibliography

[1] Daizo Kunii and Octave Levenspiel. *Fluidization engineering*. Butterworth-Heinemann, 1991. ISBN: 0409902330.

[2] Tobias Mattisson and Anders Lyngfelt. "Applications of chemical-looping combustion with capture of CO 2". In: *Control* 1 (2001), pp. 46–51.

[3] Ray Cocco, S. B.Reddy Karri, and Ted Knowlton. "Introduction to fluidization". In: *Chemical Engineering Progress* 110.11 (2014), pp. 21–29. ISSN: 03607275.

[4] Magnus Rydén, Malin Hanning, and Fredrik Lind. "Oxygen Carrier Aided Combustion (OCAC) of wood chips in a 12 MWth circulating fluidized bed boiler using steel converter slag as bed material". In: *Applied Sciences (Switzerland)* 8.12 (2018). ISSN: 20763417. DOI: 10.3390/app8122657.

[5] Anders Lyngfelt, Bo Leckner, and Tobias Mattisson. "A fluidized-bed combustion process with inherent CO2 separation; Application of chemical-looping combustion". In: *Chemical Engineering Science* 56.10 (2001), pp. 3101–3113. ISSN: 00092509. DOI: 10.1016/S0009-2509(01)00007-0.

[6] Yukari Tsuji. "Experimental studies on Chemical-looping combustion in a packed-fluidized bed". In: (2021).

[7] Viktor Stenberg et al. "Experimental investigation of oxygen carrier aided combustion (Ocac) with methane and psa off-gas". In: *Applied Sciences (Switzerland)* 11.1 (2021), pp. 1–25. ISSN: 20763417. DOI: 10.3390/app11010210.

[8] Felicia Störner, Fredrik Lind, and Magnus Rydén. "Oxygen Carrier Aided Combustion in Fluidized Bed Boilers in Sweden—Review and Future Outlook with Respect to Affordable Bed Materials". In: *Applied Sciences* 11.17 (2021), p. 7935.

[9] A. Lyngfelt, M. Johansson, and T. Mattisson. "Chemical-looping combustion - Status of development". In: *CFB 2008 - Proceedings of the 9th Int. Conference on Circulating Fluidized Beds, in Conjunction with the 4th International VGB Workshop "Operating Experience with Fluidized Bed Firing Systems"* (2008).

[10] Henrik Leion et al. "The use of ilmenite as an oxygen carrier in chemical-looping combustion". In: *Chemical Engineering Research and Design* 86.9 (2008), pp. 1017–1026. ISSN: 02638762. DOI: 10.1016/j.cherd.2008.03.019.

[11] Henrik Thunman et al. "Using an oxygen-carrier as bed material for combustion of biomass in a 12-MWth circulating fluidized-bed boiler". In: *Fuel* 113.x (2013), pp. 300–309. ISSN: 00162361. DOI: 10.1016/j.fuel.2013.05.073. URL: http://dx.doi.org/10.1016/j.fuel.2013.05.073.

[12] Boliden. *Användningsområden Järnsand*. URL: http://jarnsand.boliden.com/sa-har-anvander-du-jarnsand/.

[13] LKAB. *Avfall och Deponi*. URL: https://www.lkab.com/sv/hallbarhet/miljo/avfall-och-deponi/.

[14] M. Kramp et al. "The role of attrition and solids recovery in a chemical looping combustion process". In: *Oil & Gas Science and Technology–Revue d'IFP Energies nouvelles* 66.2 (2011), pp. 277–290.

[15] A Cabello et al. "On the attrition evaluation of oxygen carriers in Chemical Looping Combustion". In: *Fuel Processing Technology* 148 (2016), pp. 188–197.

[16] Dennis P. Nolan. "Physical Properties of Hydrocarbons and Petrochemicals". In: *Handbook of Fire and Explosion Protection Engineering Principles* (2014), pp. 55–77. DOI: 10.1016/b978-0-323-31301-8.00004-0.

[17] Viktor Stenberg. "Experimental Study of the Hydrodynamics of a Lab-scale Chemical Looping Combustion System A study in preparation for a CLOU (Chemical Looping with". In: (2015).

[18] Boliden AB. *Jänsand*. URL: https://www.boliden.com/globalassets/operations/products/by-products/335-7128-jarnsand-produktblad_se8.pdf.

[19] C.Y. Wen and Y.H. Yu. "A generalized method for predicting the minimum fluidization velocity". In: *AIChE Journal* 3 (1966), pp. 610–612.

[20] Ronald W. Breault and Esmail R. Monazam. "Analysis of fixed bed data for the extraction of a rate mechanism for the reaction of hematite with methane". In: *Journal of Industrial and Engineering Chemistry* 29 (2015), pp. 87–96. ISSN: 22345957. DOI: 10.1016/j.jiec.2015.03.020. URL: http://dx.doi.org/10.1016/j.jiec.2015.03.020.

[21] Henrik Leion, Volkmar Frick, and Fredrik Hildor. "Experimental method and setup for laboratory fluidized bed reactor testing". In: *Energies* 11.10 (2018). ISSN: 19961073. DOI: 10.3390/en11102505.

A

Appendix A

A.1 Results for CLC operation

A.1.1 Results for magnetite fines with syngas

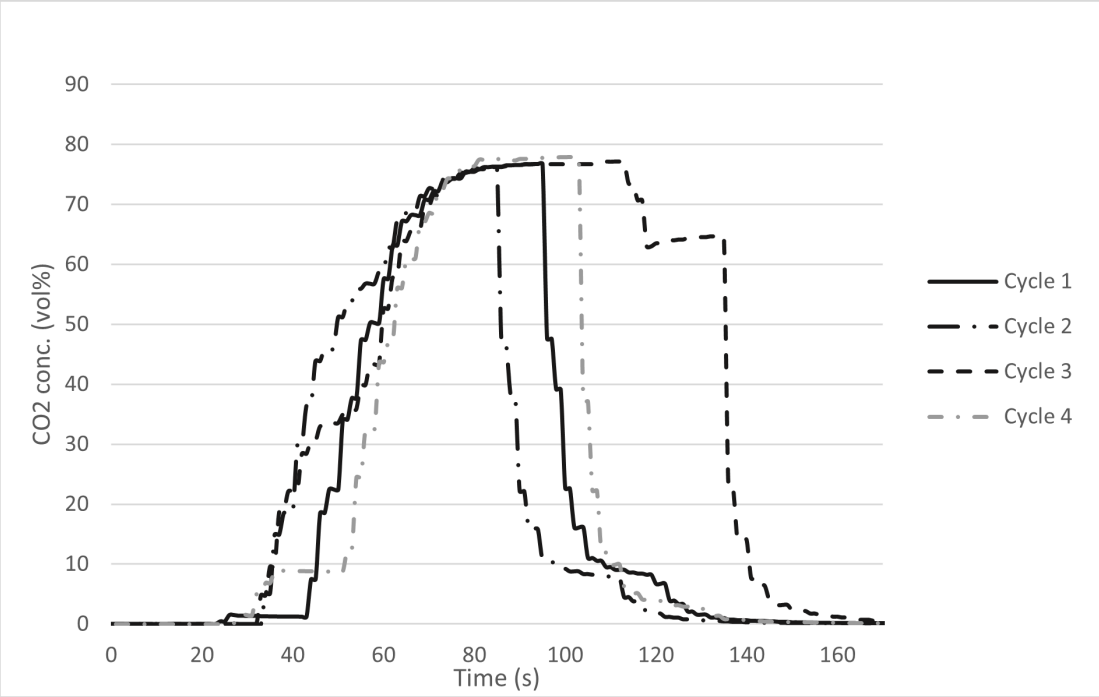

Figure A.1: *CO_2 concentration over time during reduction with syngas in CLC cycle for magnetite fines at 840°C*

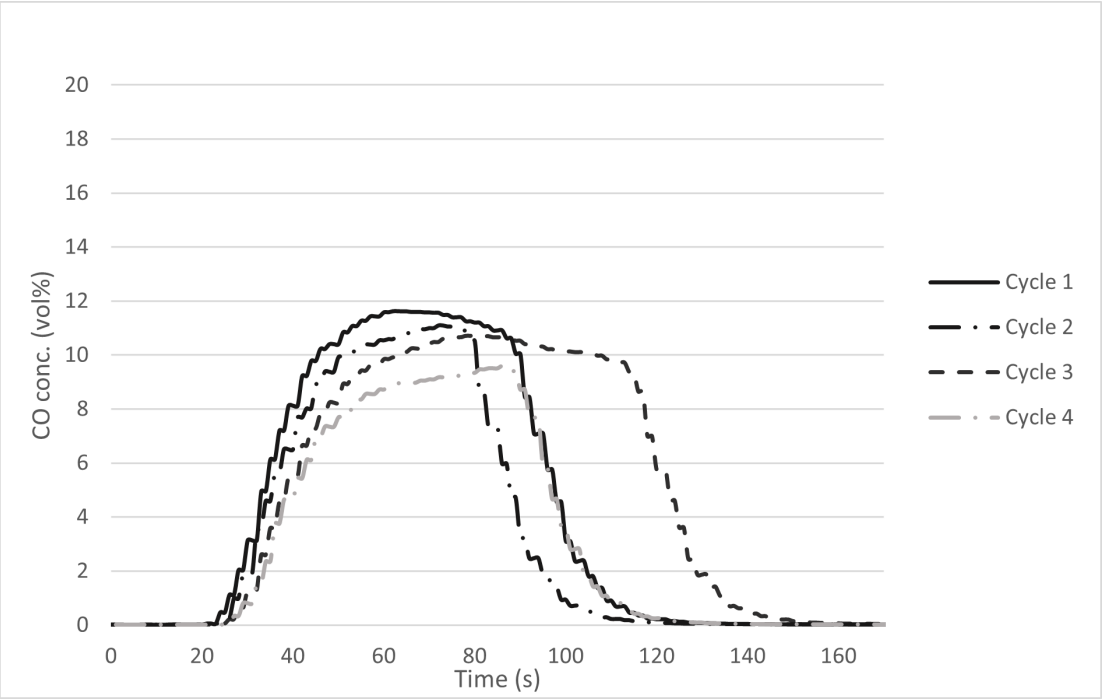

(a) CO concentration over time.

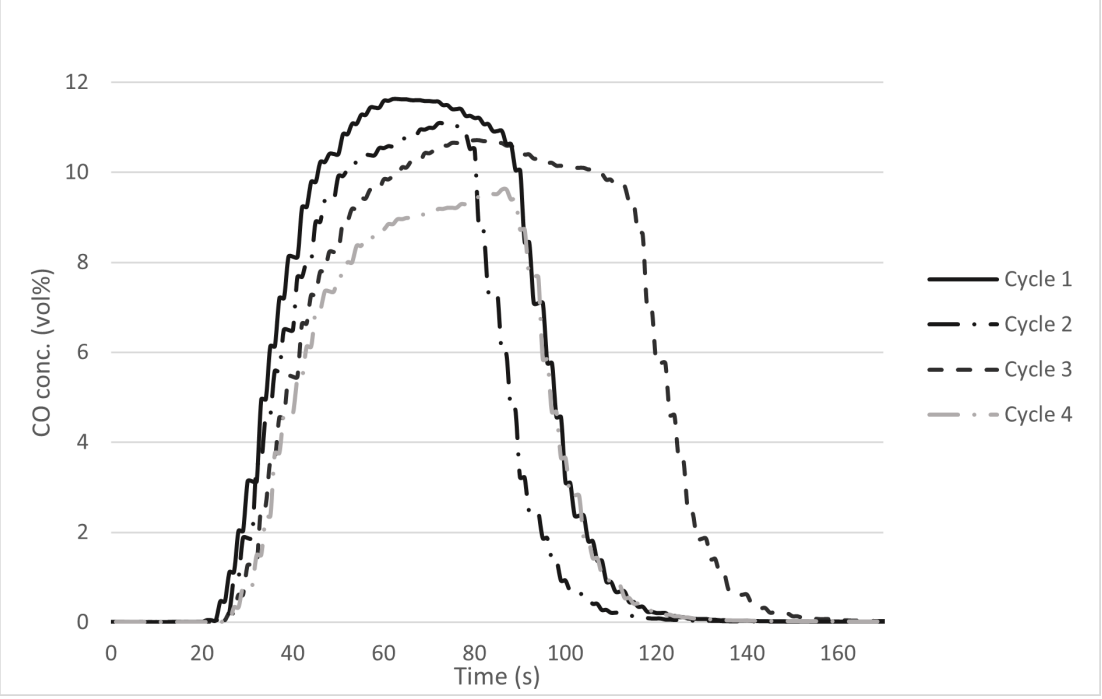

(b) CO concentration over time presented with zoomed y-axis.

Figure A.2: *CO concentration over time during reduction with syngas in CLC cycle for magnetite fines at 840°C*

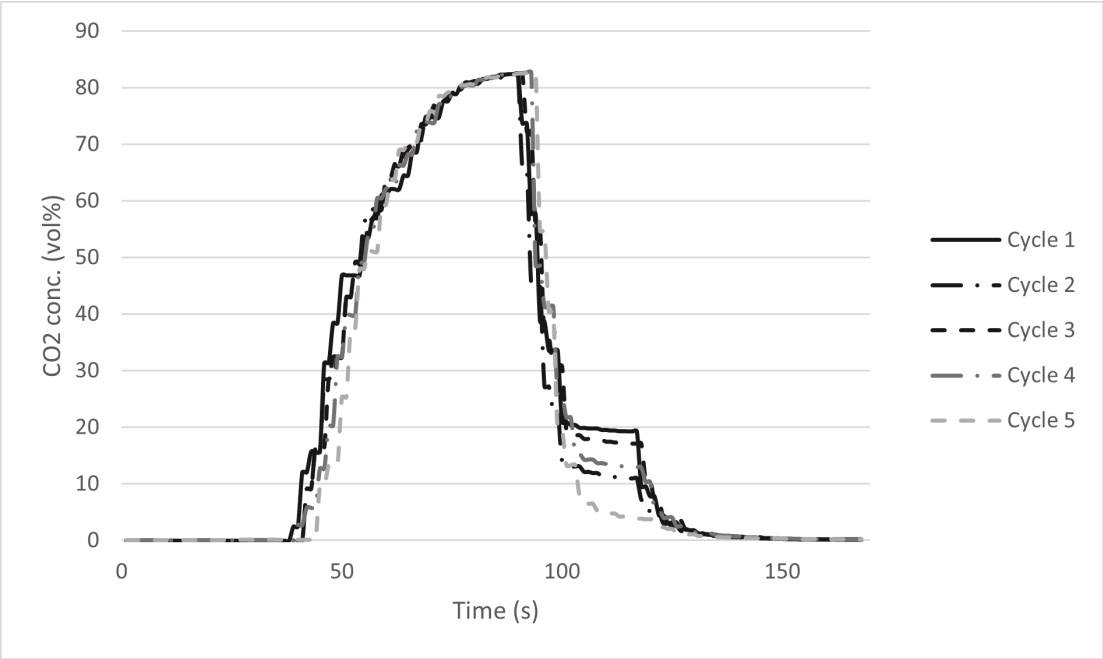

Figure A.3: *CO_2 concentration over time during reduction with syngas in CLC cycle for magnetite fines at 890°C*

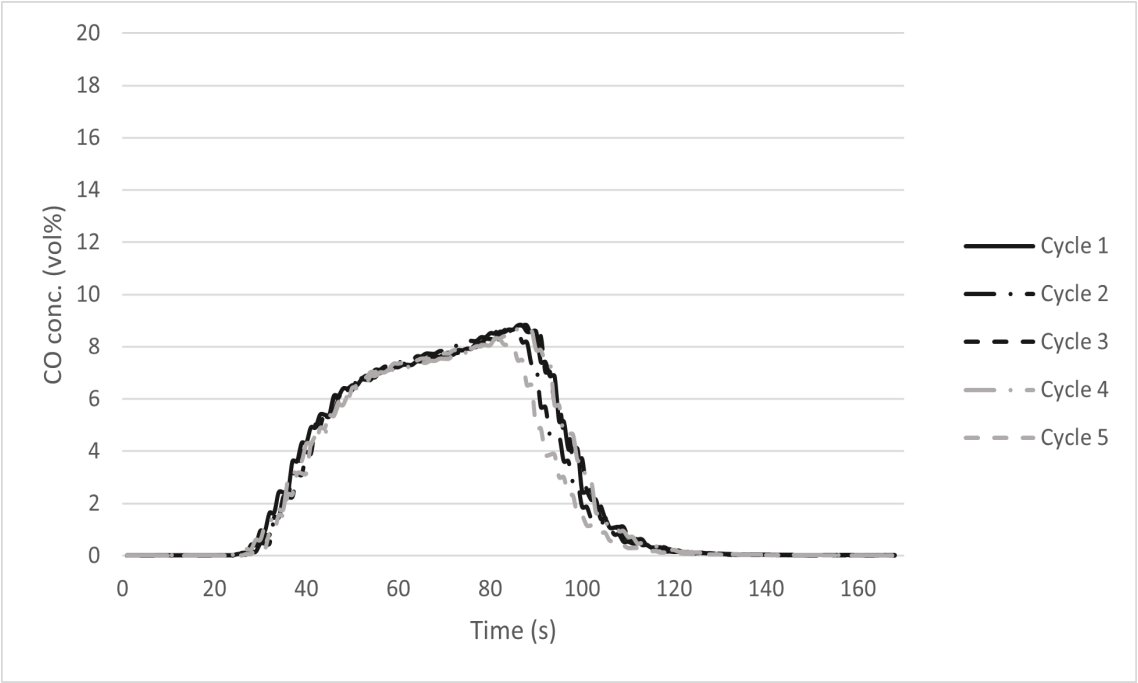

(a) CO concentration over time.

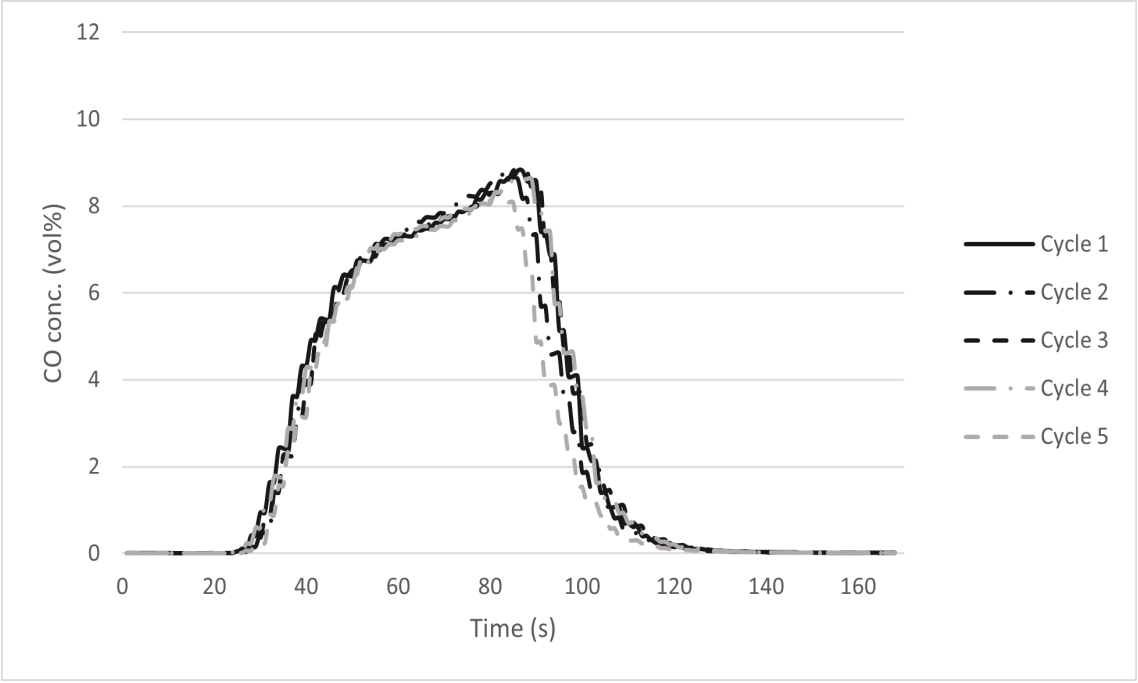

(b) CO concentration over time presented with zoomed y-axis.

Figure A.4: *CO concentration over time during reduction with syngas in CLC cycle for magnetite fines at 890°C*

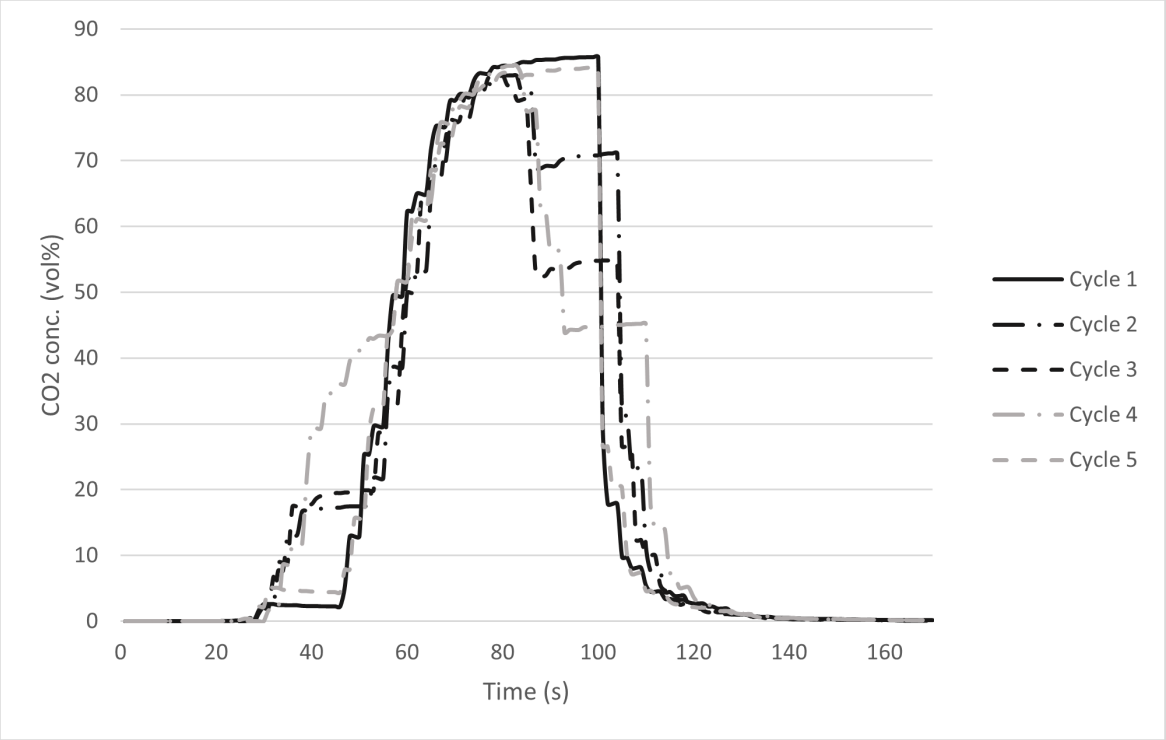

Figure A.5: *CO_2 concentration over time during reduction with syngas in CLC cycle for magnetite fines at 940°C.*

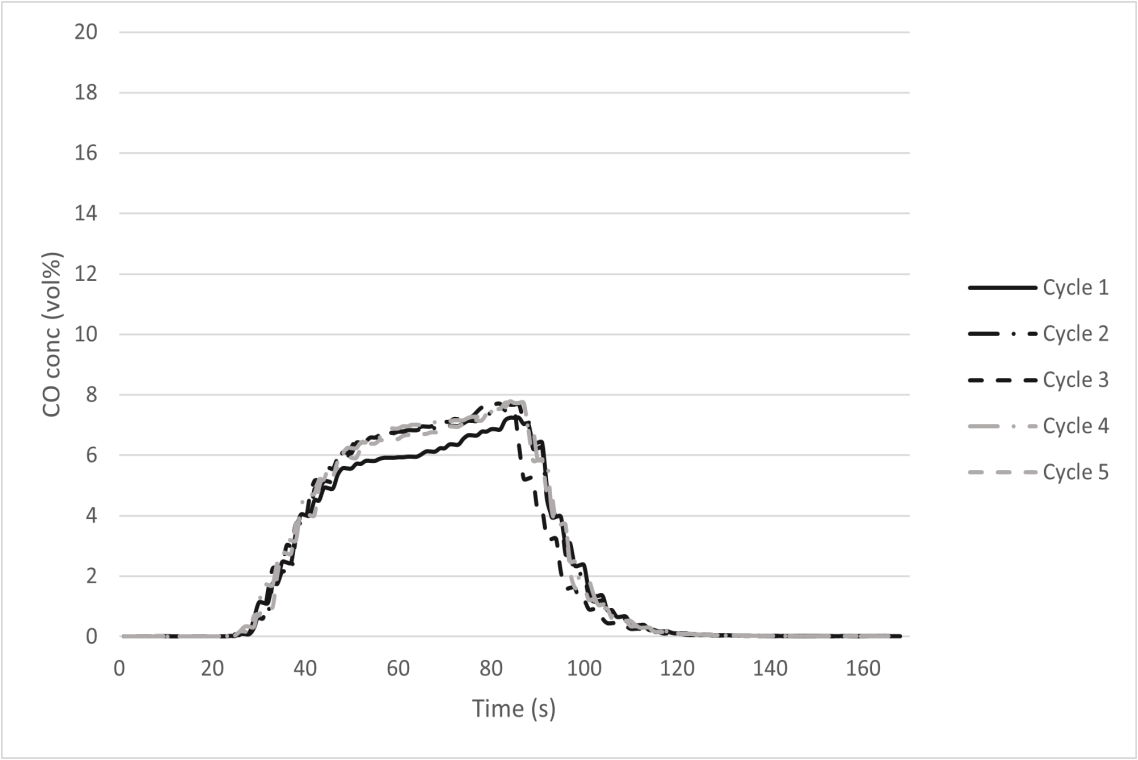

(a) CO concentration over time.

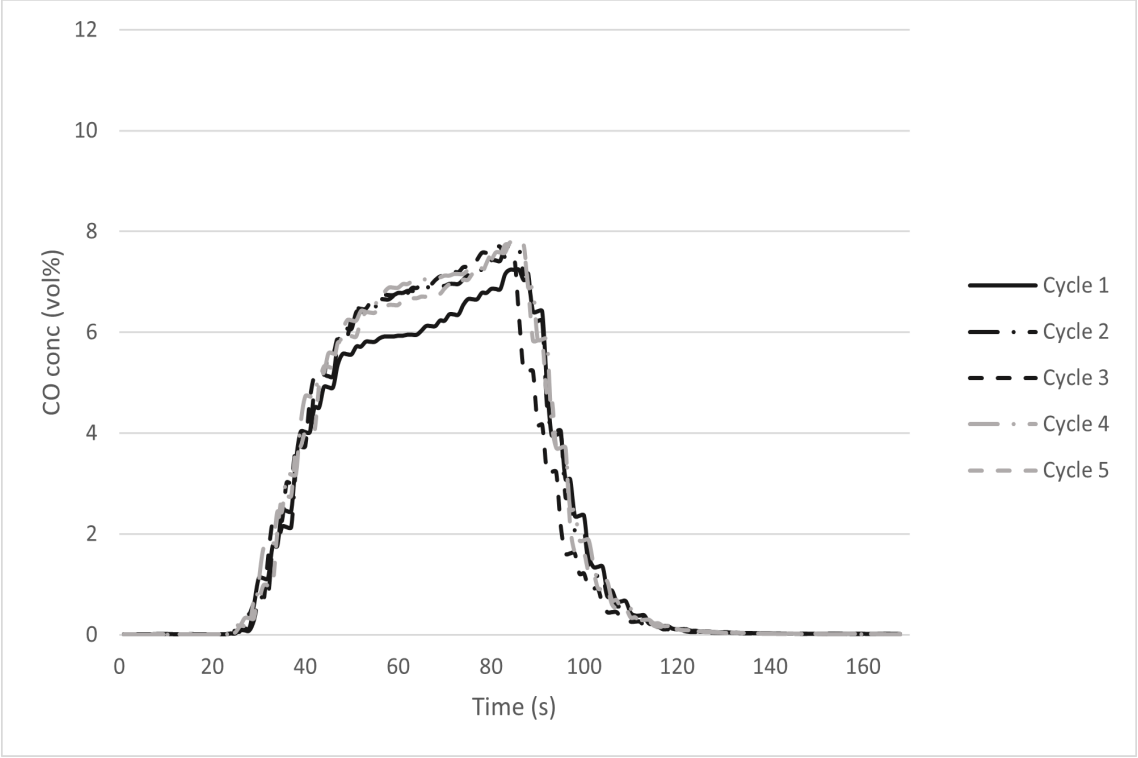

(b) CO concentration over time presented with zoomed y-axis.

Figure A.6: *CO concentration over time during reduction with syngas in CLC cycle for magnetite fines at 940°C.*

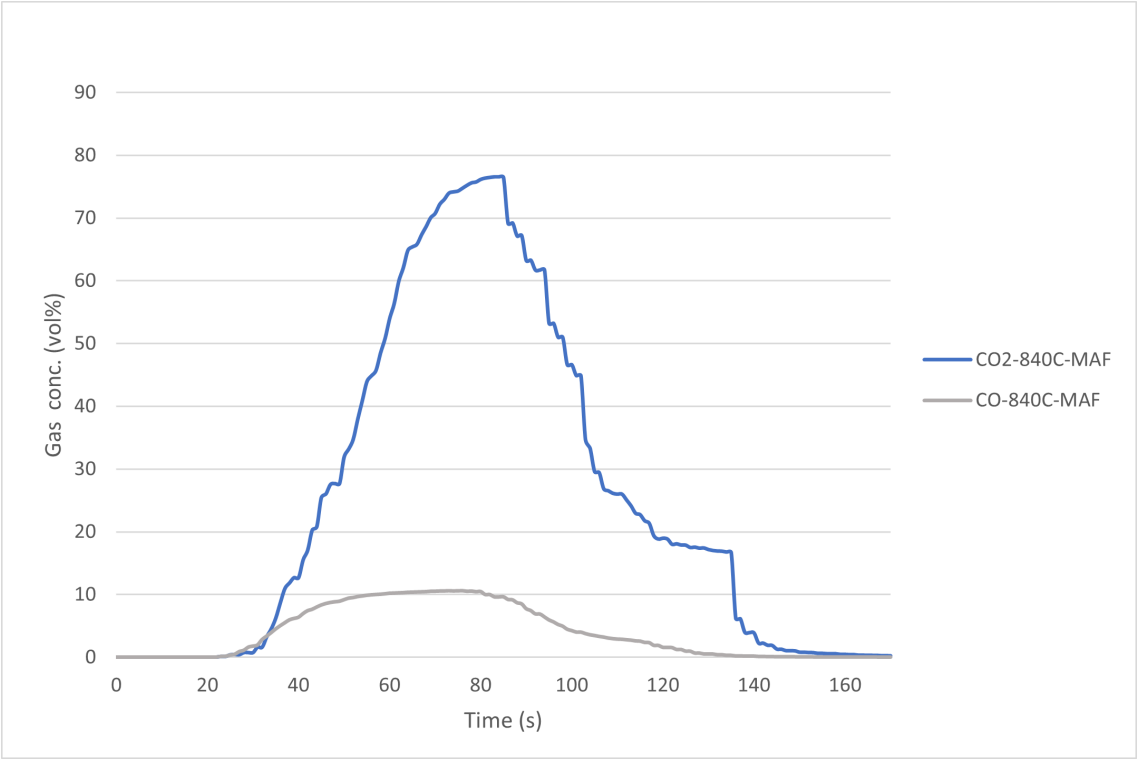

(a) Bed temperature 840°C.

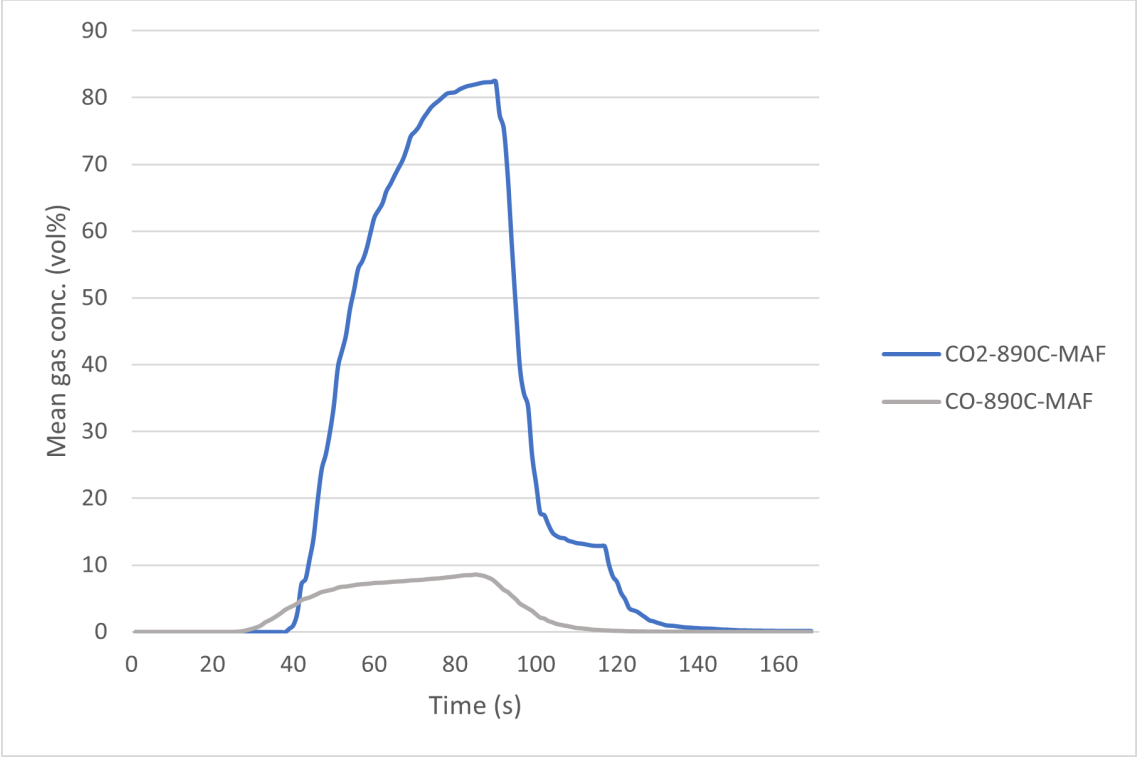

(b) Bed temperature 890°C

Figure A.7: *Mean dry gas concentration for CLC cycles with magnetite fines as bed material and syngas as fuel, for bed temperature s 840°C, 890°C and 940°C*

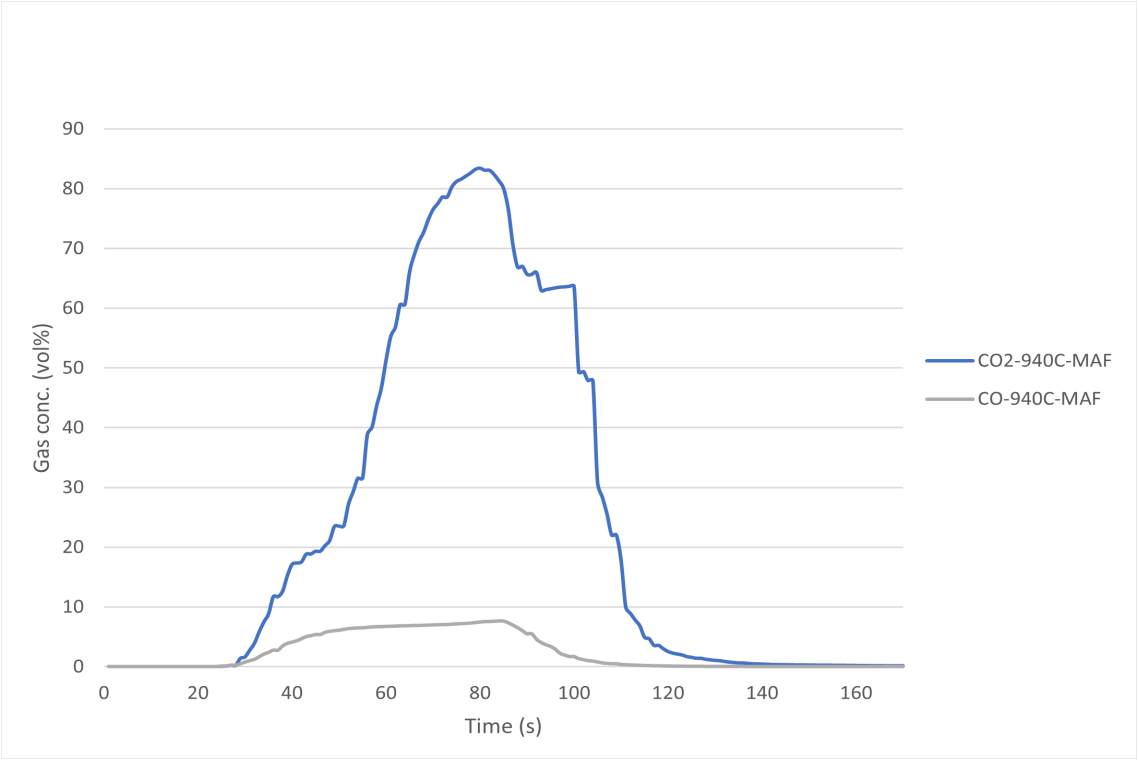

(c) Bed temperature 940°C

Figure A.7: *Mean dry gas concentration for CLC cycles with magnetite fines as bed material and syngas as fuel, for bed temperature s 840°C, 890°C and 940°C*

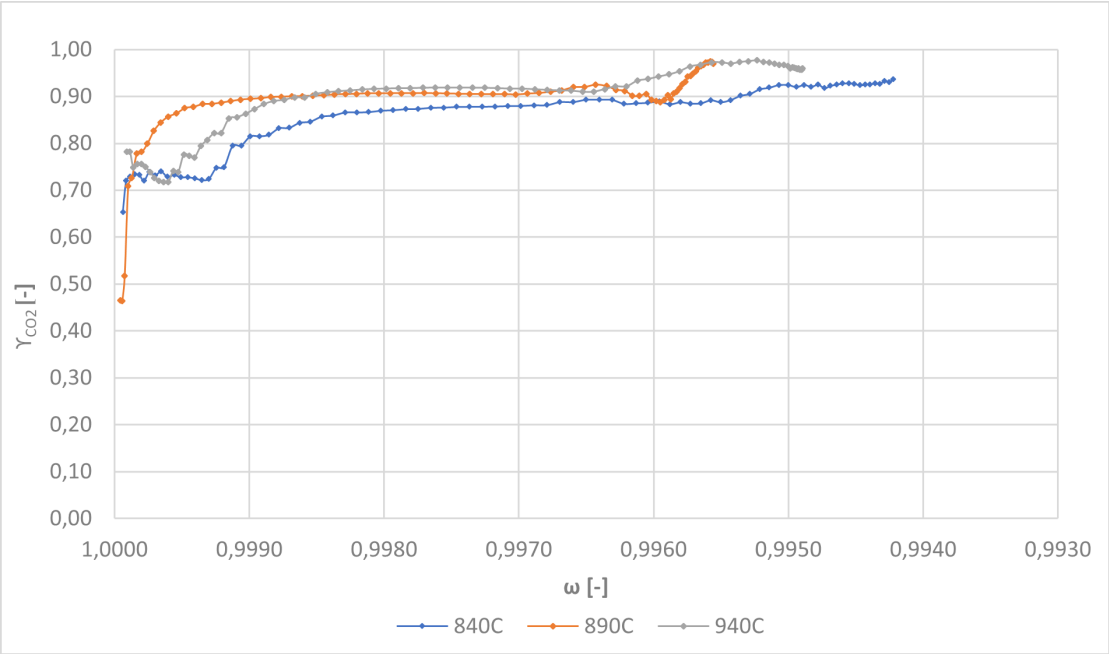

Figure A.8: *CO_2 yield as function of the mass based oxygen carrier conversion of magnetite fines for combustion with syngas, at different bed temperatures.*

A.1.2 Results for magnetite fines with methane

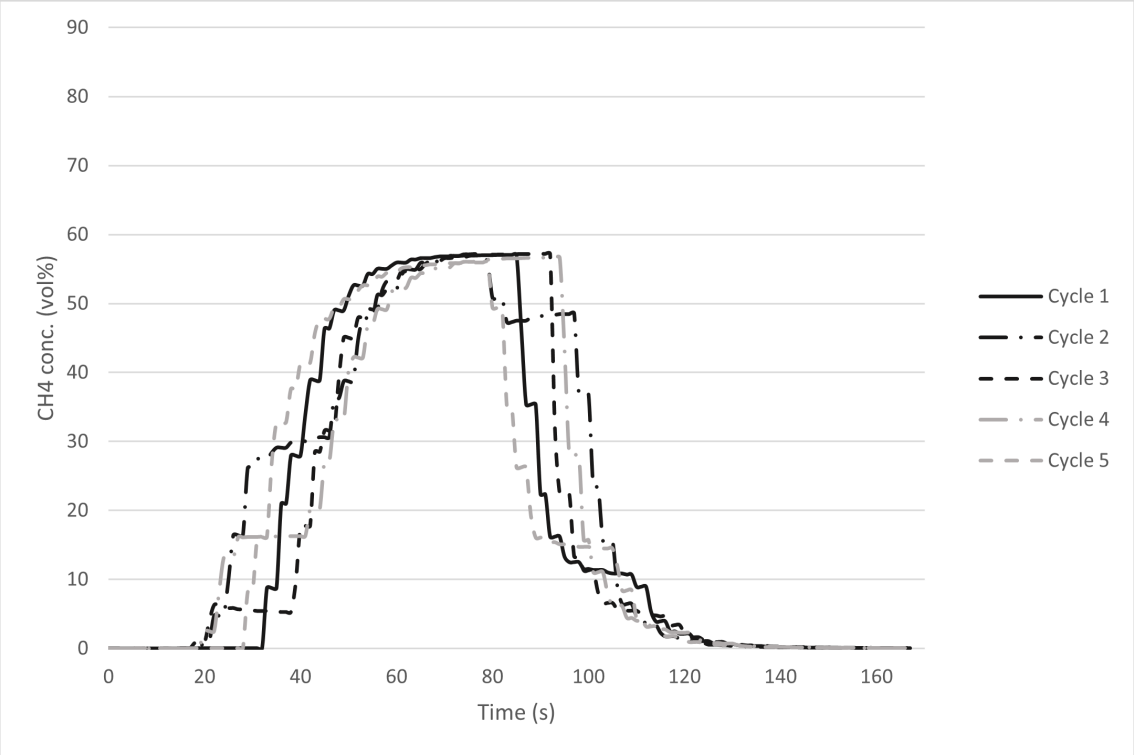

Figure A.9: *CH_4 concentration over time during reduction with methane in CLC cycle for magnetite fines at 840°C.*

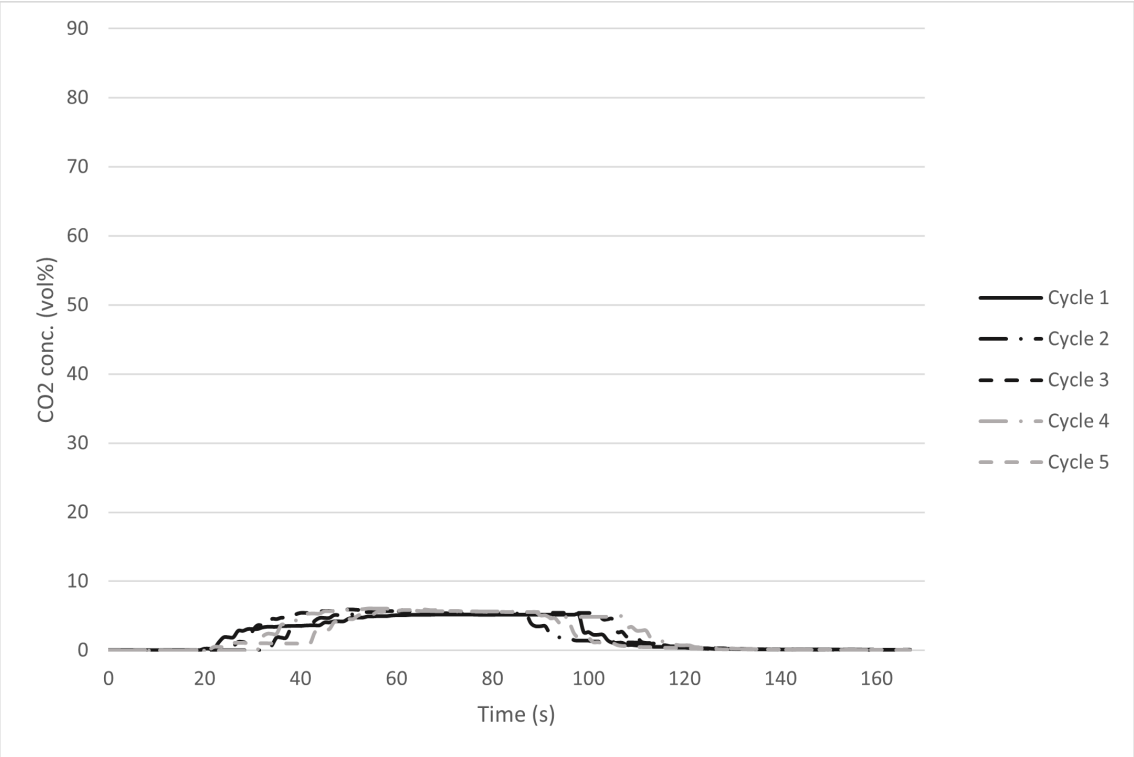

(a) CO2 concentration over time.

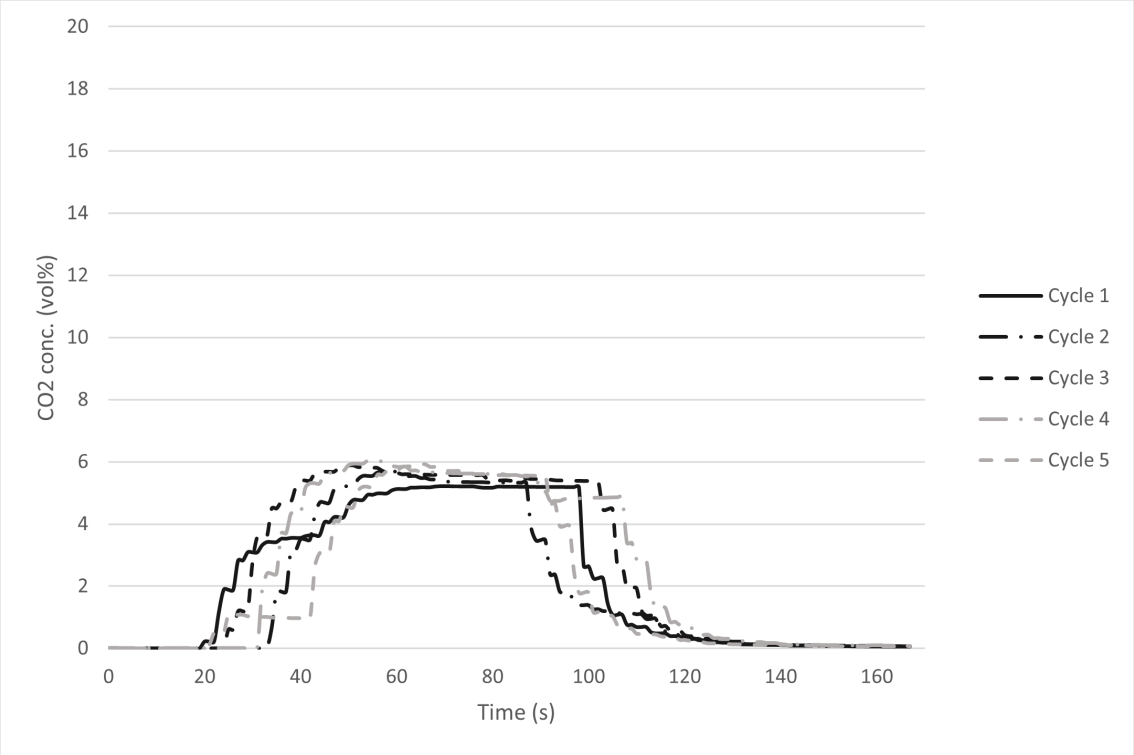

(b) CO2 concentration over time presented with zoomed y-axis.

Figure A.10: *CO2 concentration over time during reduction with methane in CLC cycle for magnetite fines at 840°C.*

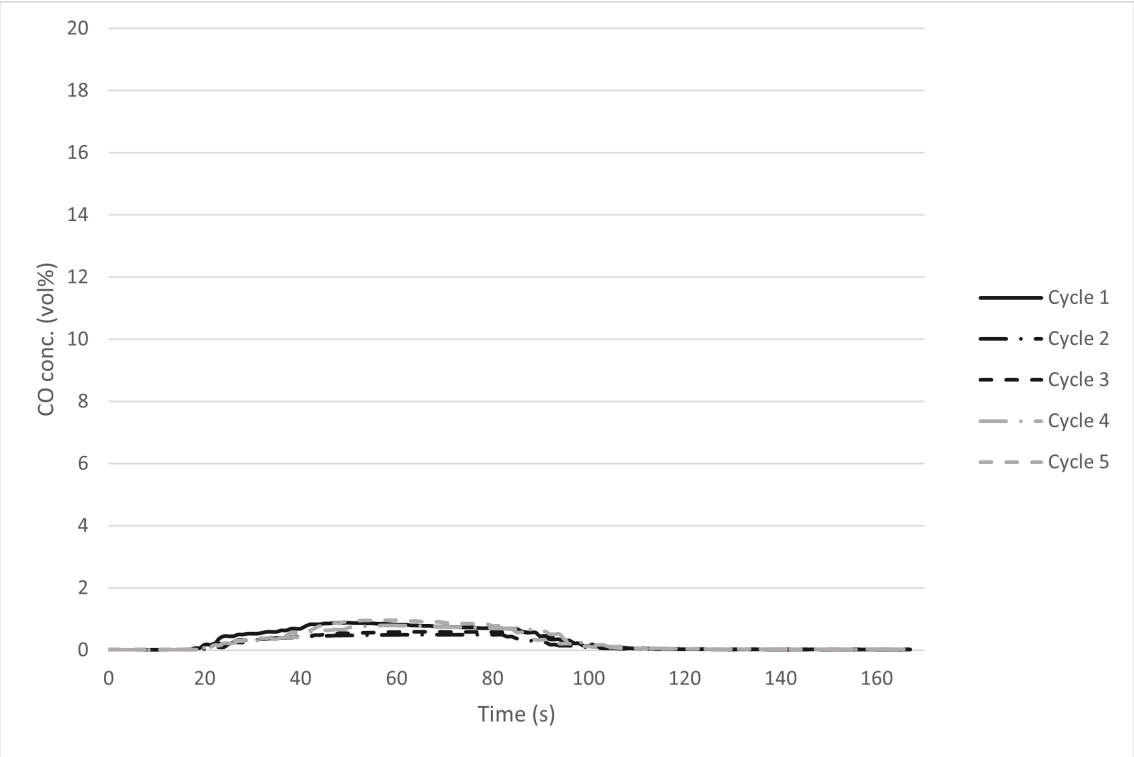

(a) CO concentration over time.

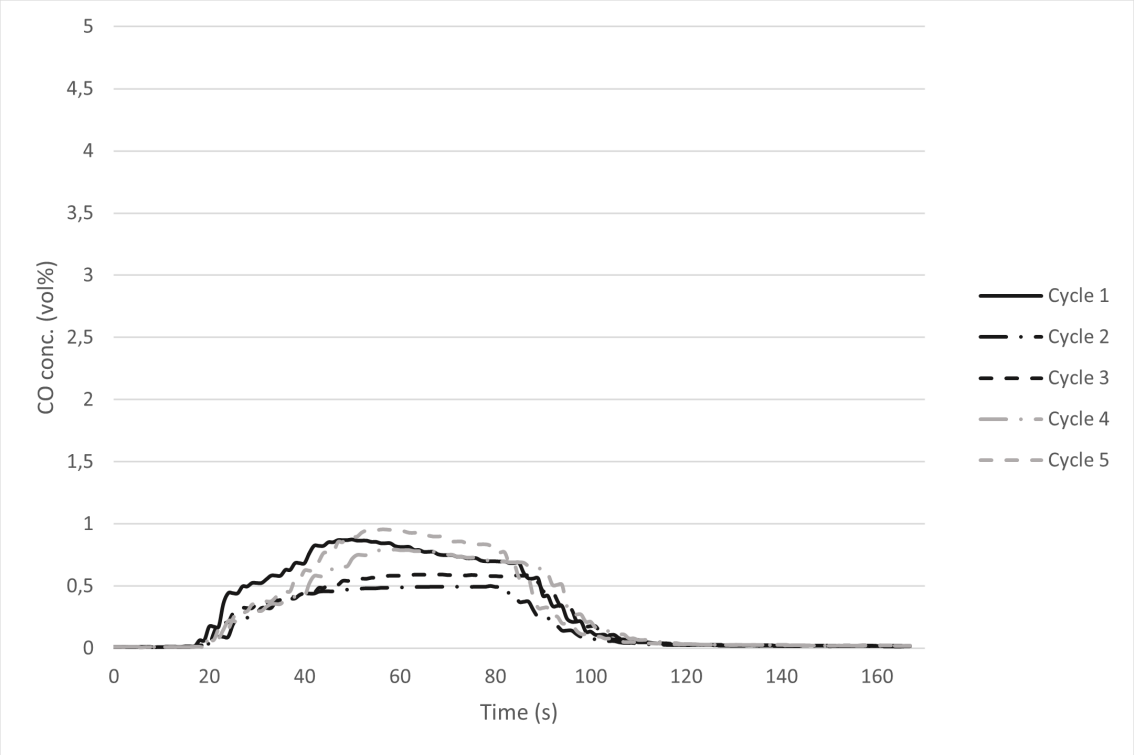

(b) CO concentration over time presented with zoomed y-axis.

Figure A.11: *CO concentration over time during reduction with methane in CLC cycle for magnetite fines at 840°C.*

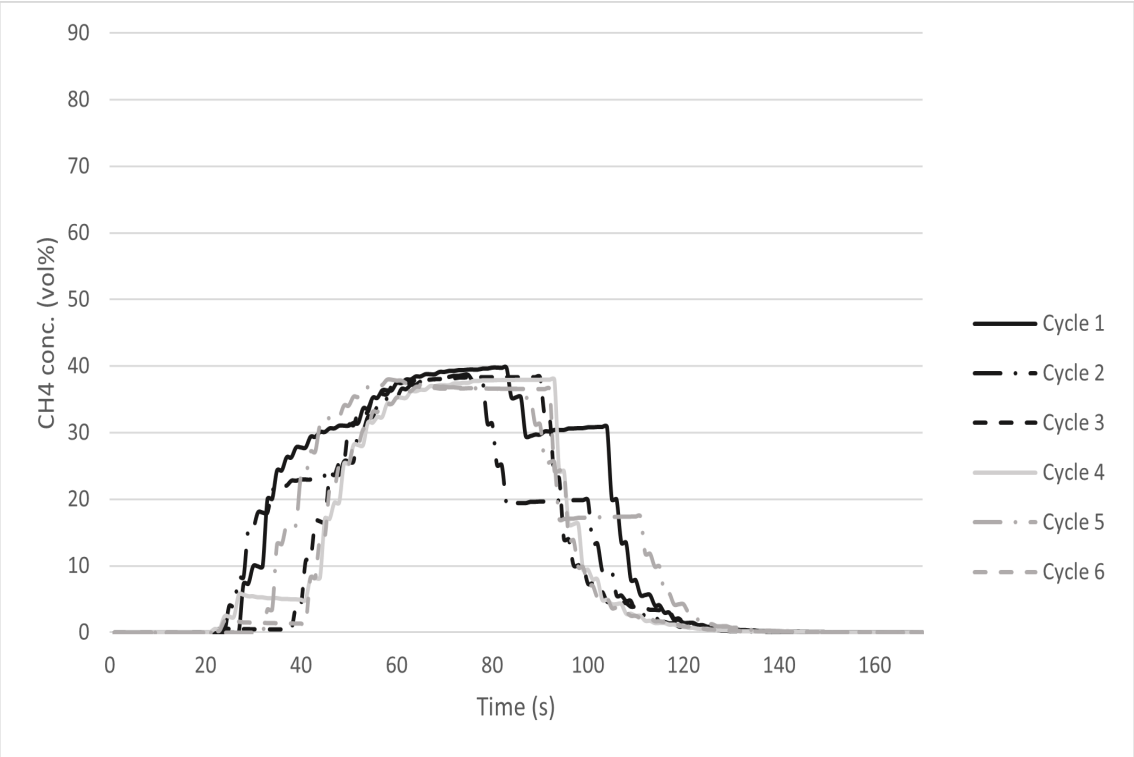

Figure A.12: *CH_4 concentration over time during reduction with methane in CLC cycle for magnetite fines at 940°C.*

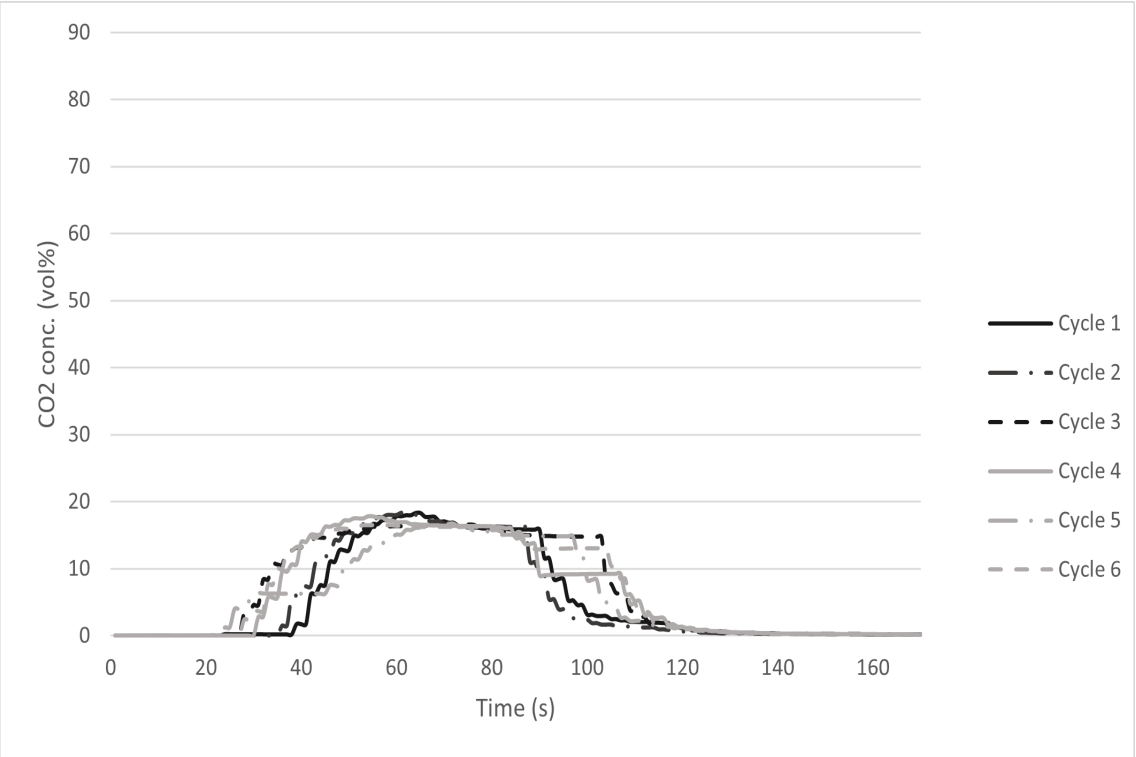

(a) CO2 concentration over time.

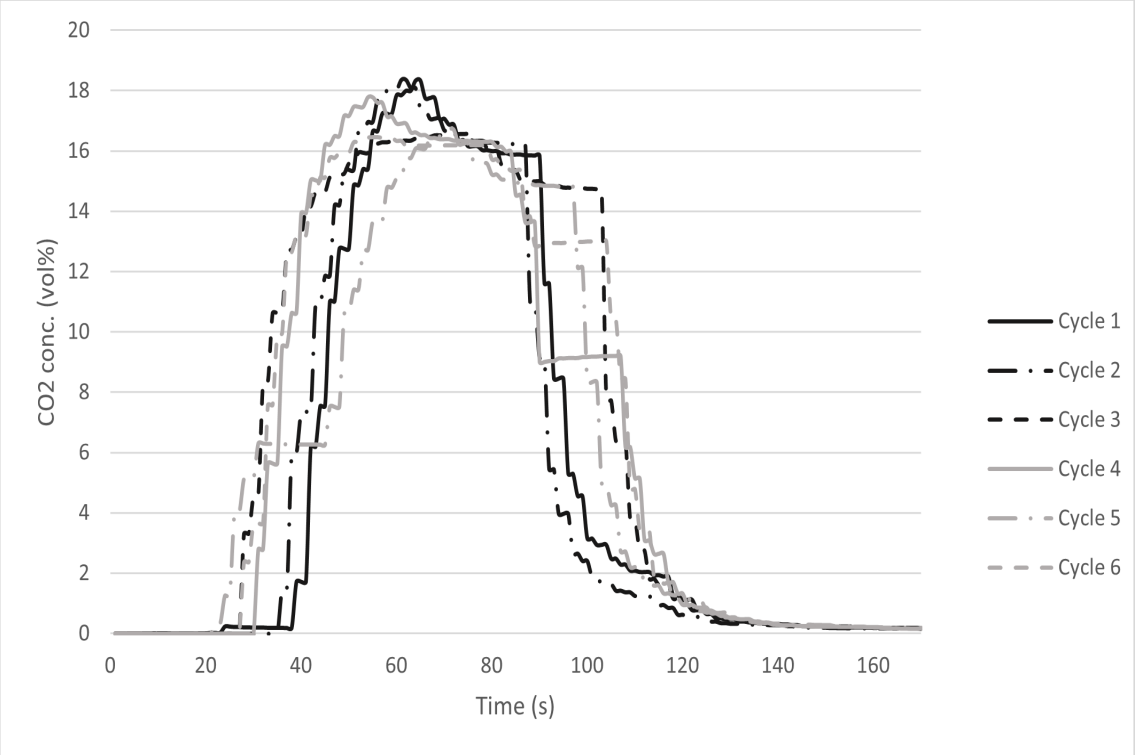

(b) CO2 concentration over time presented with zoomed y-axis.

Figure A.13: *CO2 concentration over time during reduction with methane in CLC cycle for magnetite fines at 940°C.*

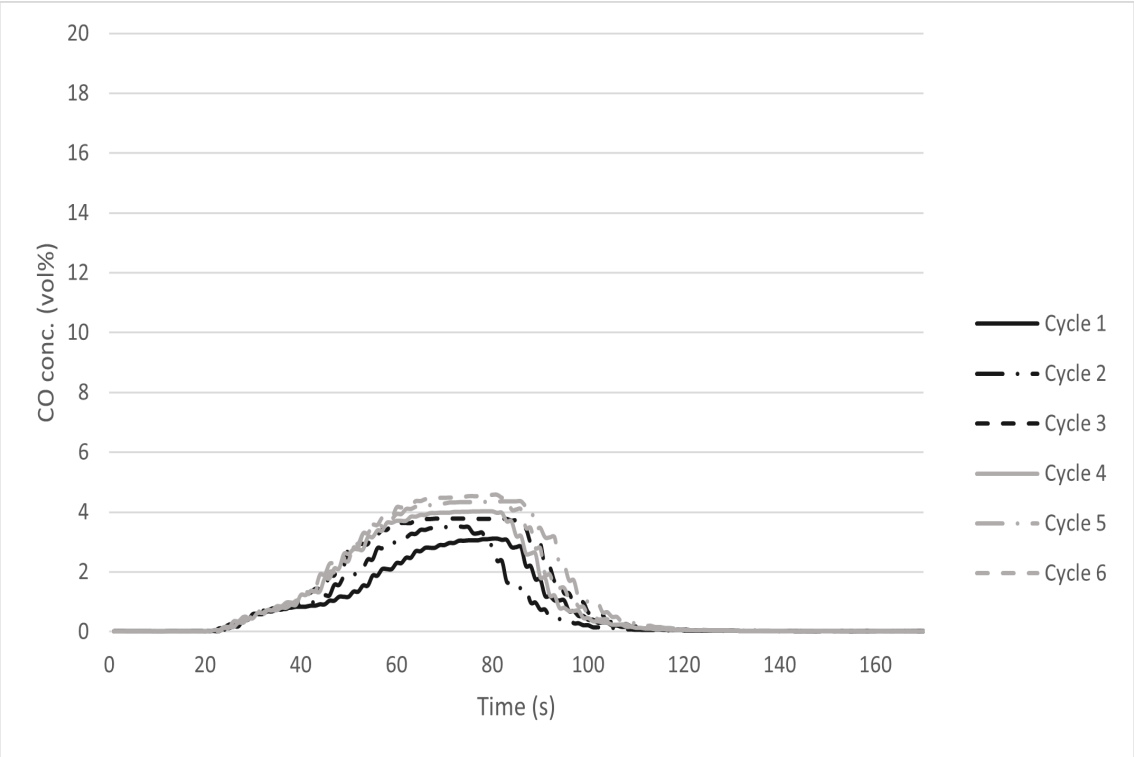

(a) CO concentration over time.

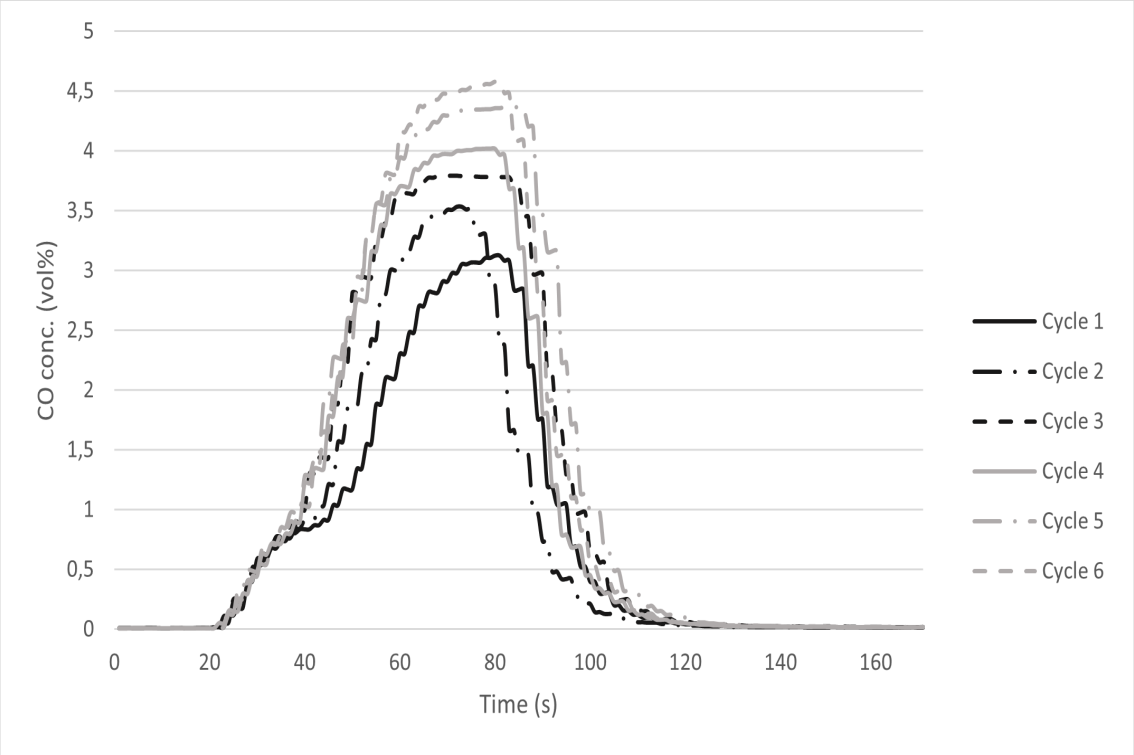

(b) CO concentration over time presented with zoomed y-axis.

Figure A.14: *CO concentration over time during reduction with methane in CLC cycle for magnetite fines at 940°C.*

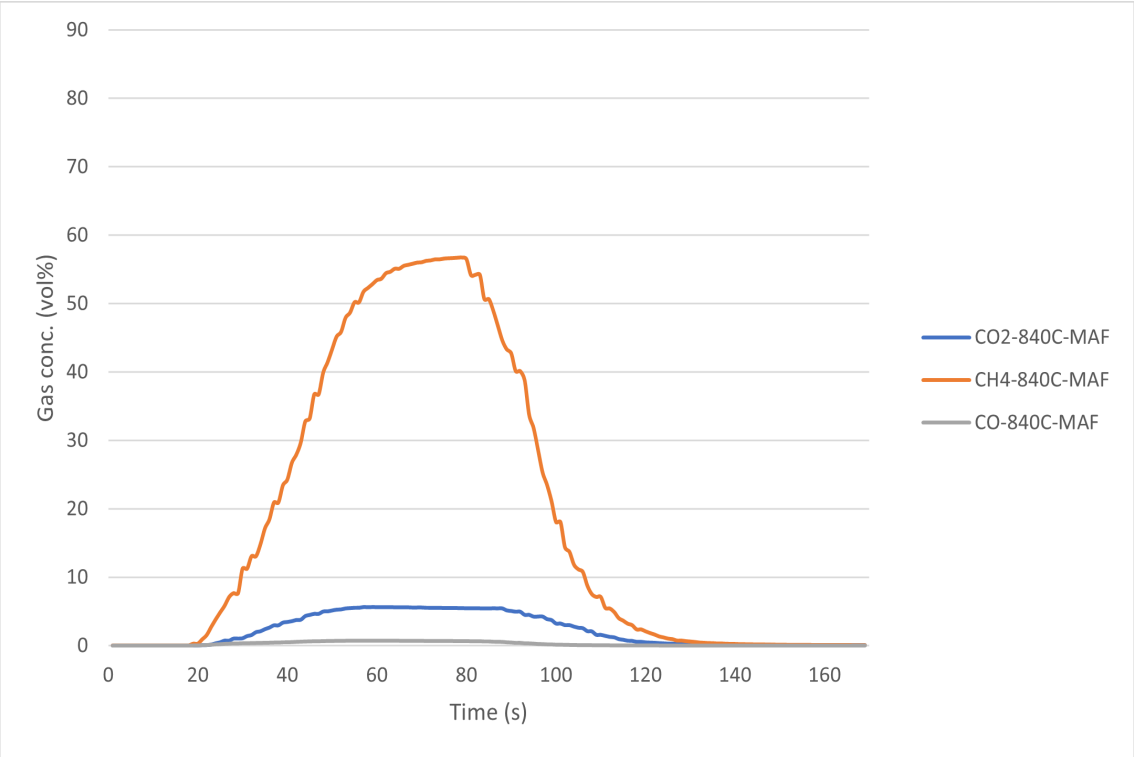

(a) Bed temperature 840°C.

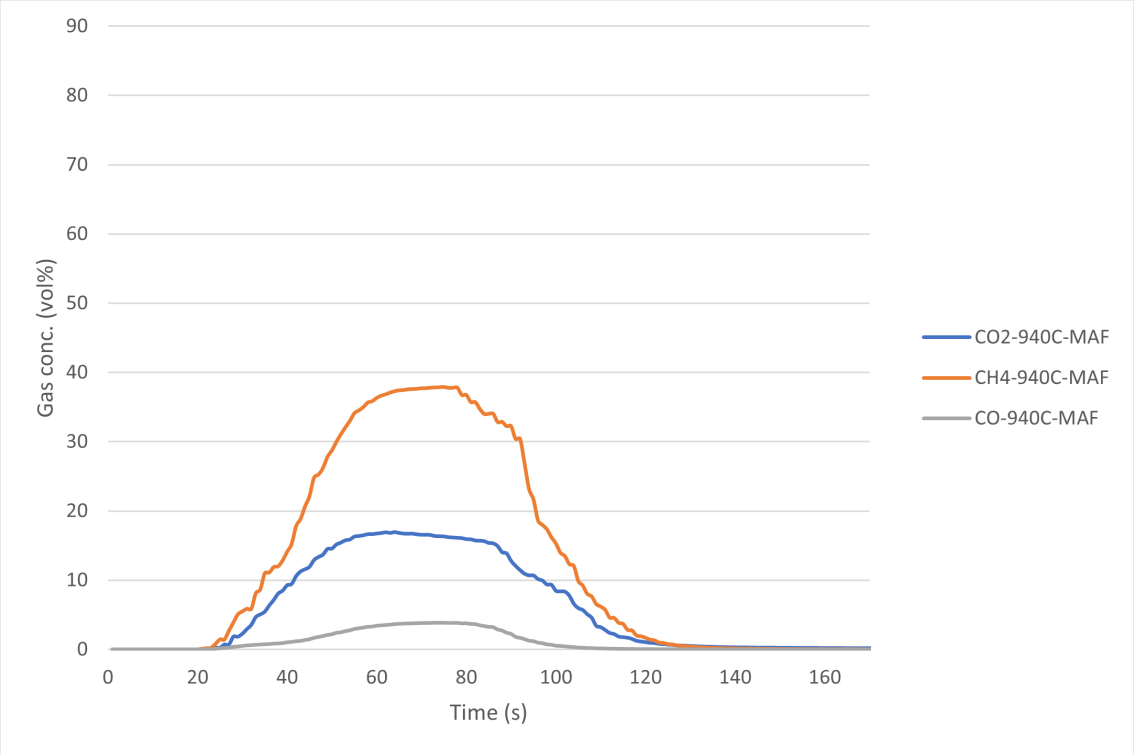

(b) Bed temperature 940°C

Figure A.15: *Mean dry gas concentration for CLC cycles with magnetite fines as bed material and syngas as fuel, for bed temperature s 840°C and 940°C*

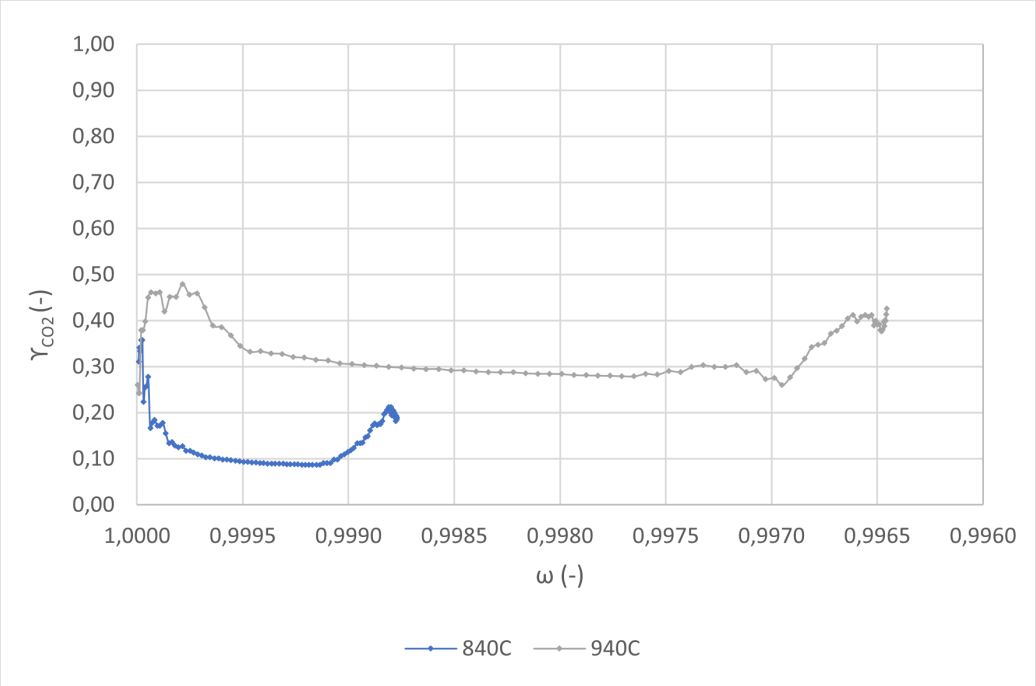

Figure A.16: *CO_2 yield as function of the mass based oxygen carrier conversion of magnetite fines for combustion with methane, at different bed temperatures.*

A.1.3 Results for copper smelter slag with syngas

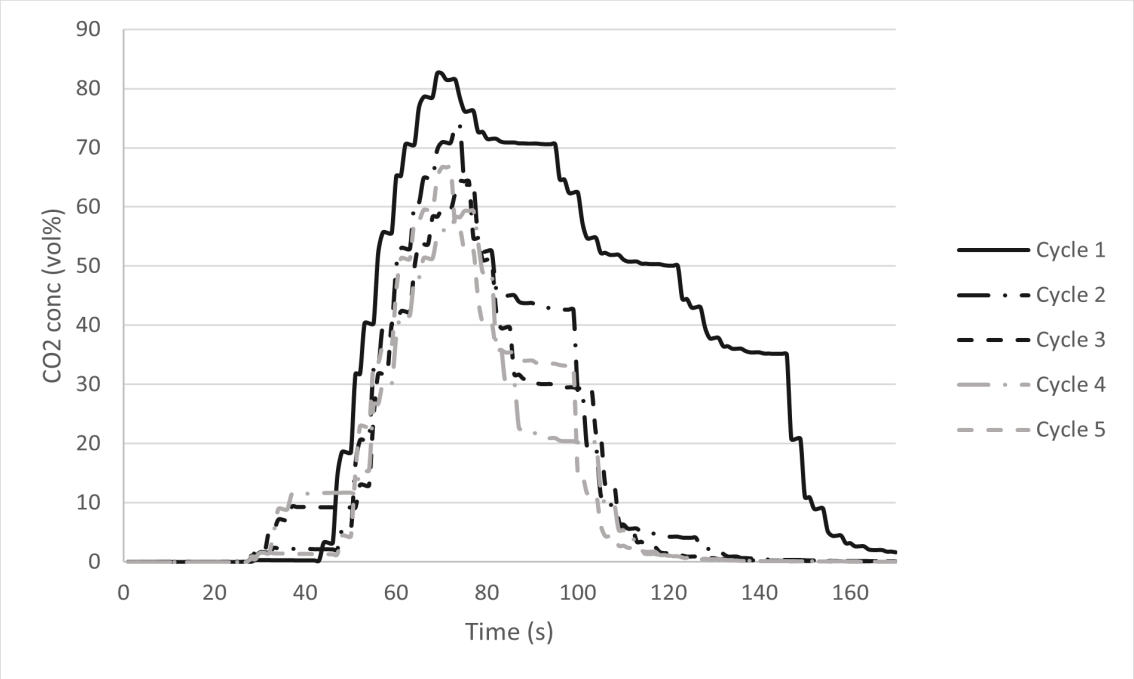

Figure A.17: *CO_2 concentration over time during reduction with syngas in CLC cycle for copper smelter slag at 840°C*

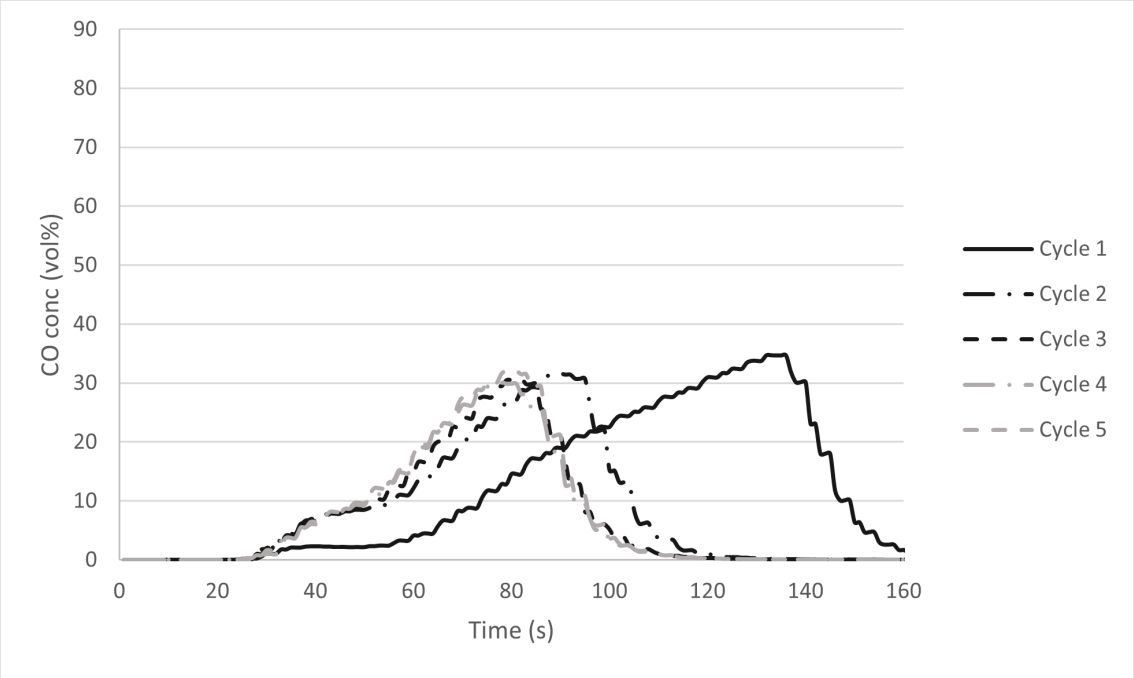

Figure A.18: *CO concentration over time during reduction with syngas in CLC cycle for copper smelter slag at 840°C*

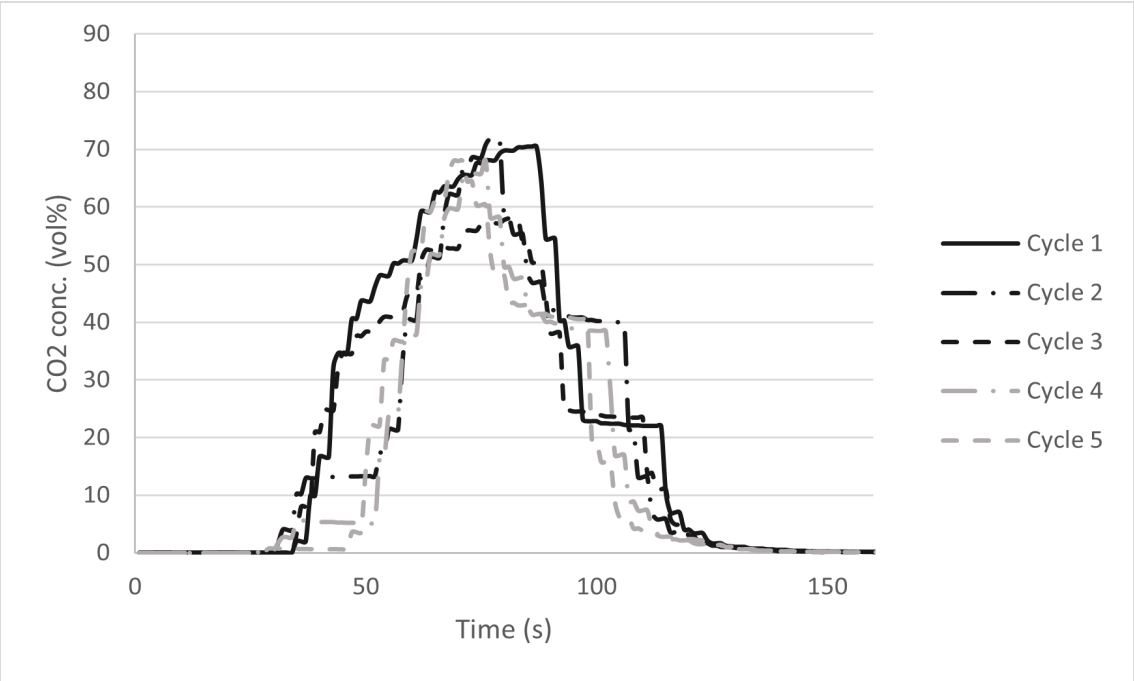

Figure A.19: *CO_2 concentration over time during reduction with syngas in CLC cycle for copper smelter slag at 890°C*

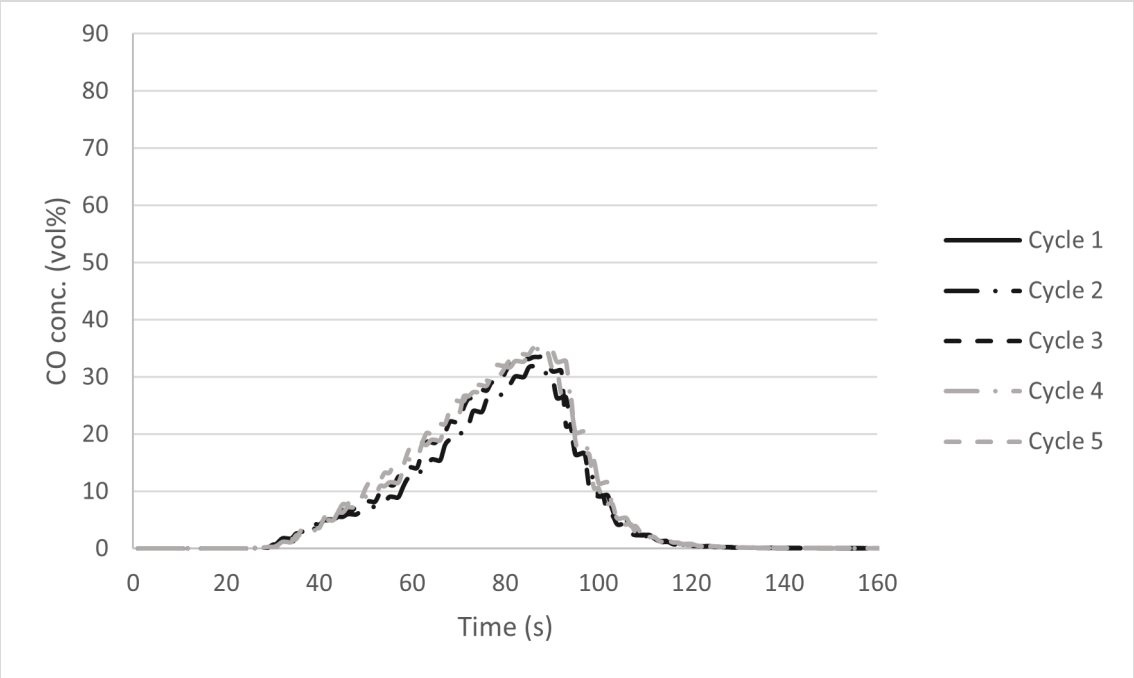

Figure A.20: *CO concentration over time during reduction with syngas in CLC cycle for copper smelter slag at 890°C*

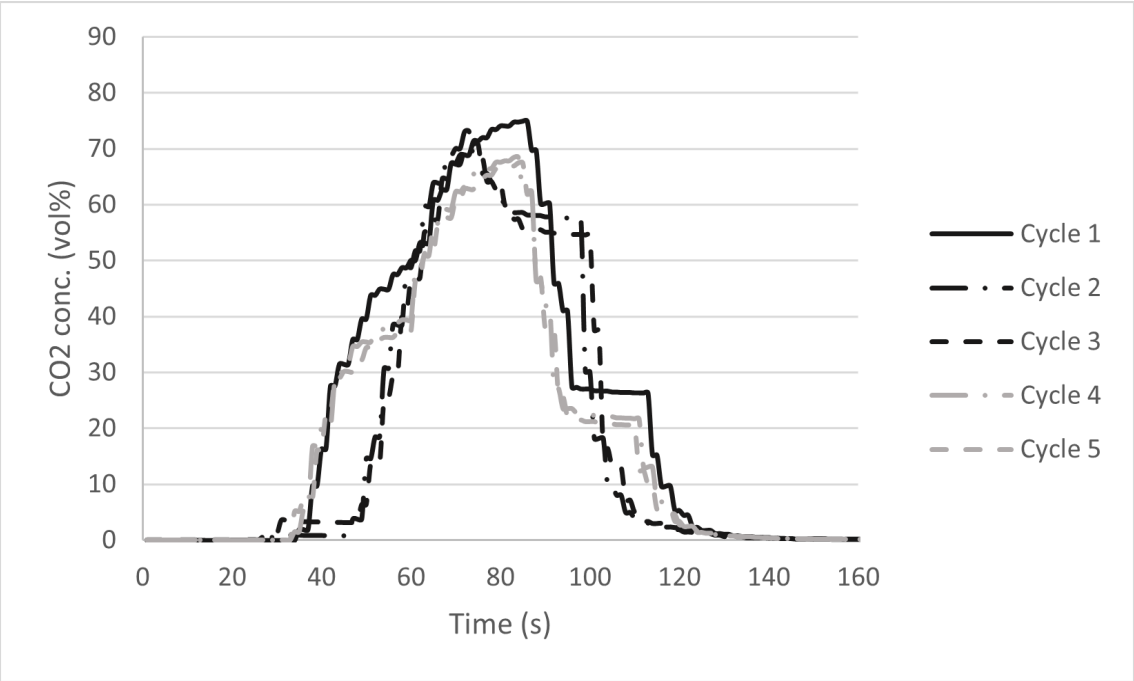

Figure A.21: *CO_2 concentration over time during reduction with syngas in CLC cycle for copper smelter slag at 940°C*

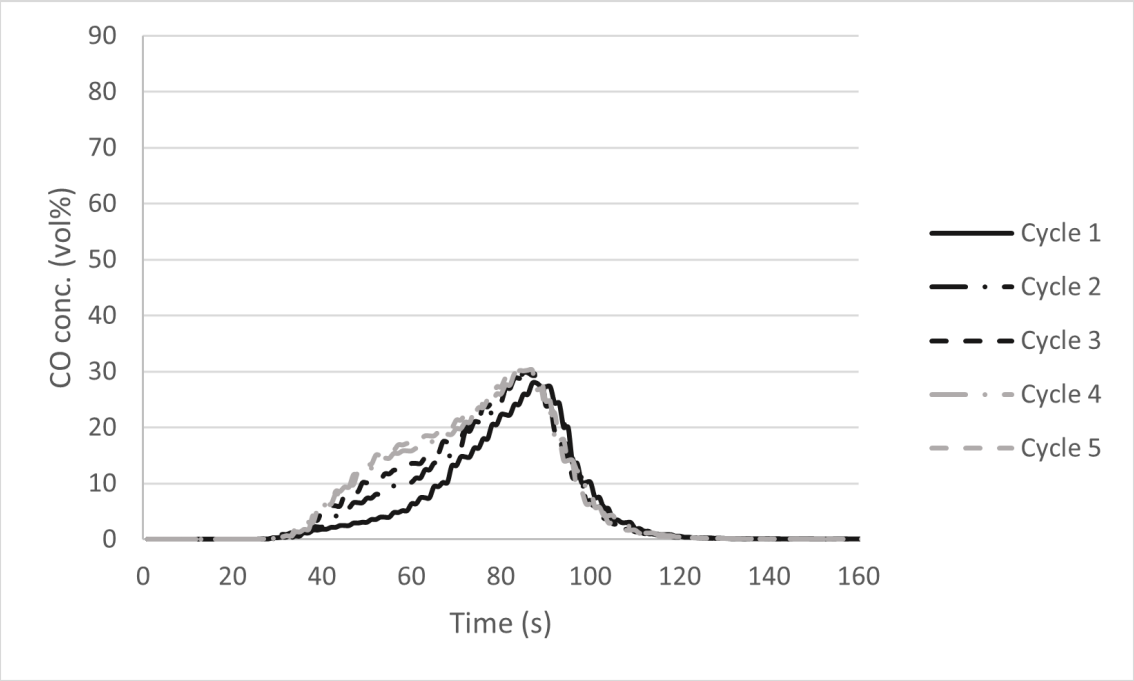

Figure A.22: *CO concentration over time during reduction with syngas in CLC cycle for copper smelter slag at 940°C*

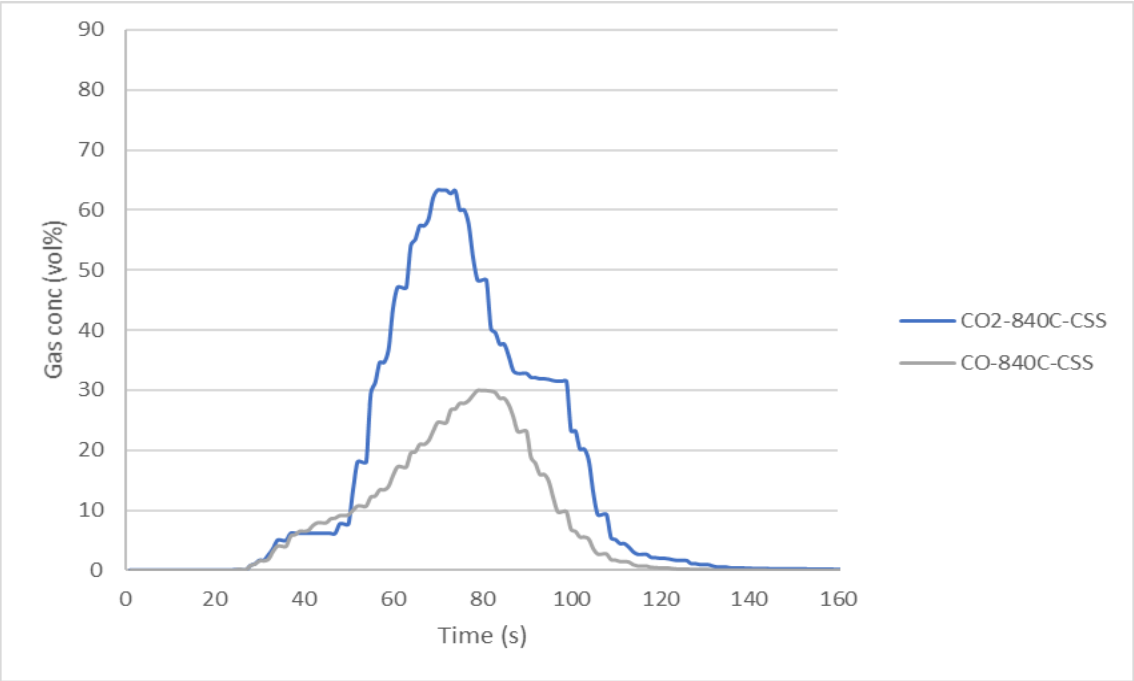

(a) Bed temperature 840°C.

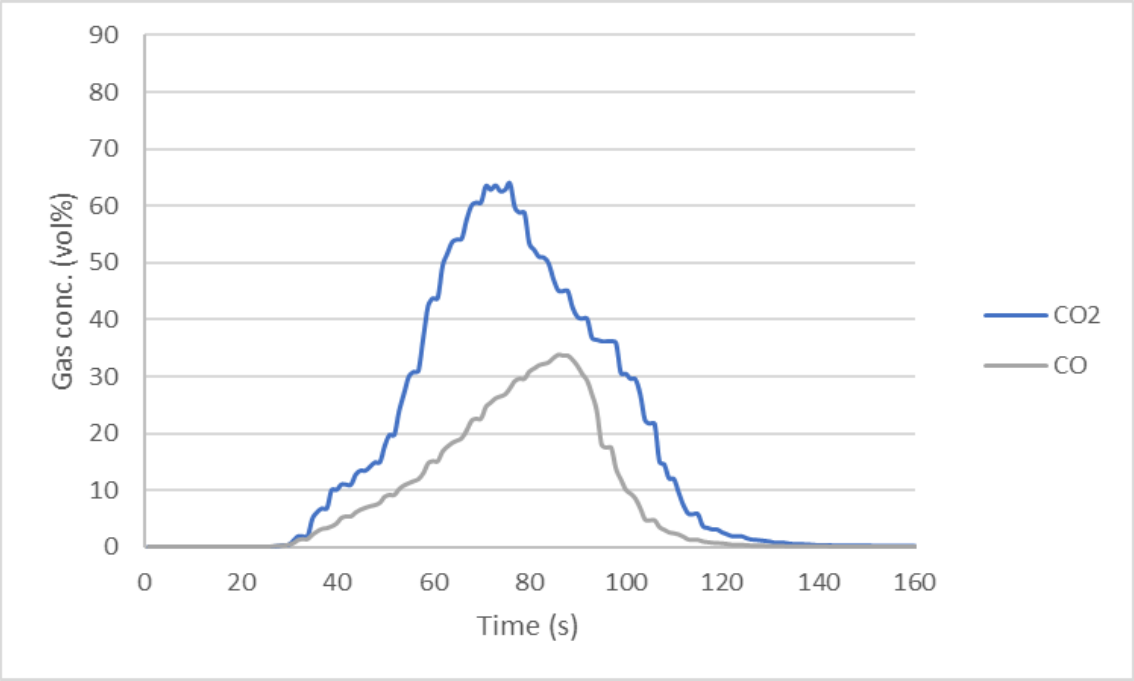

(b) Bed temperature 890°C.

Figure A.23: *Mean dry gas concentration for CLC cycles with copper smelter slag as bed material and syngas as fuel, for bed temperature s 840°C, 890°C and 940°C*

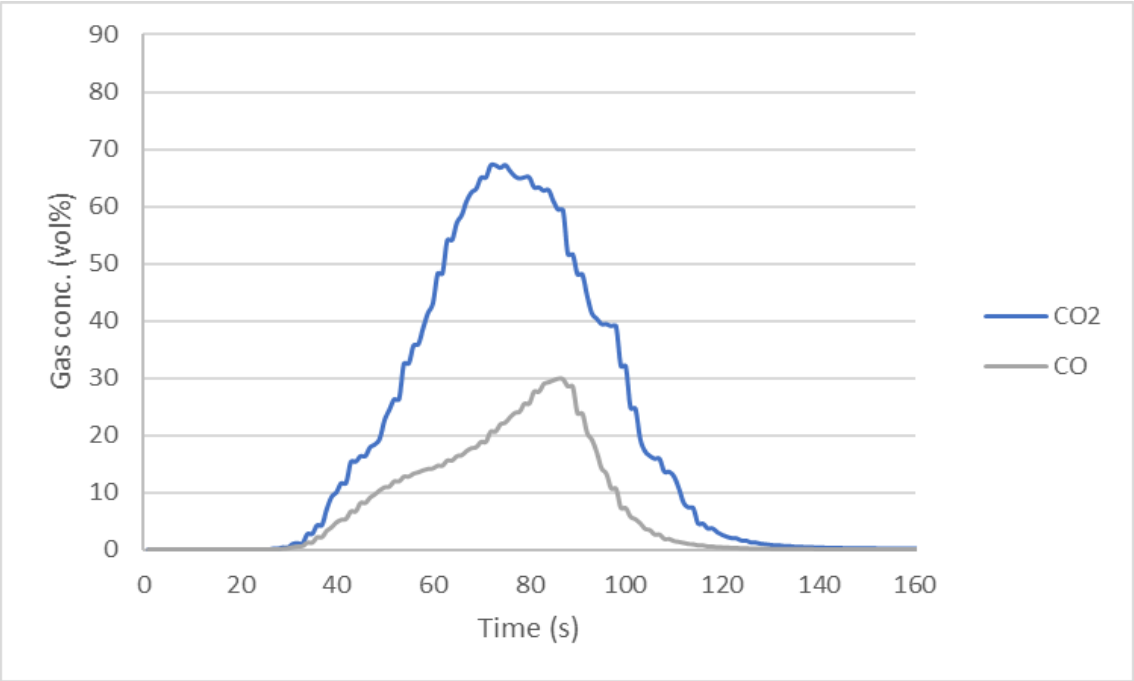

(c) Bed temperature 940°C.

Figure A.23: *Mean dry gas concentration for CLC cycles with copper smelter slag as bed material and syngas as fuel, for bed temperature s 840°C, 890°C and 940°C*

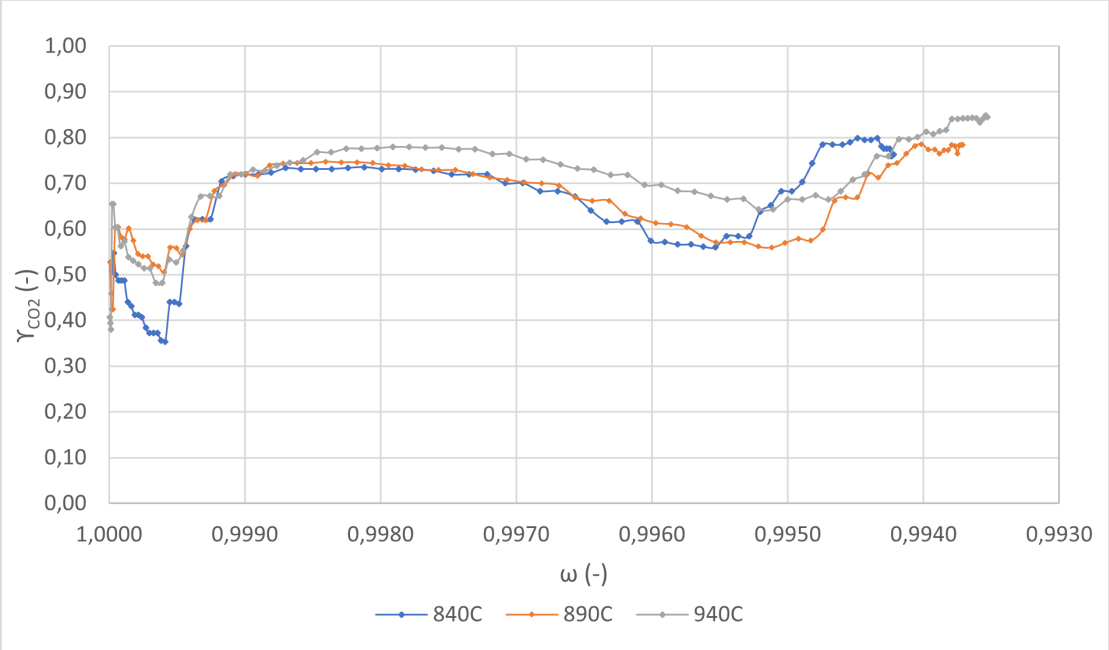

Figure A.24: *CO_2 yield as function of the mass based oxygen carrier conversion of copper smelter slag for combustion with syngas, at different bed temperatures.*

A.1.4 Results for copper smelter slag with methane

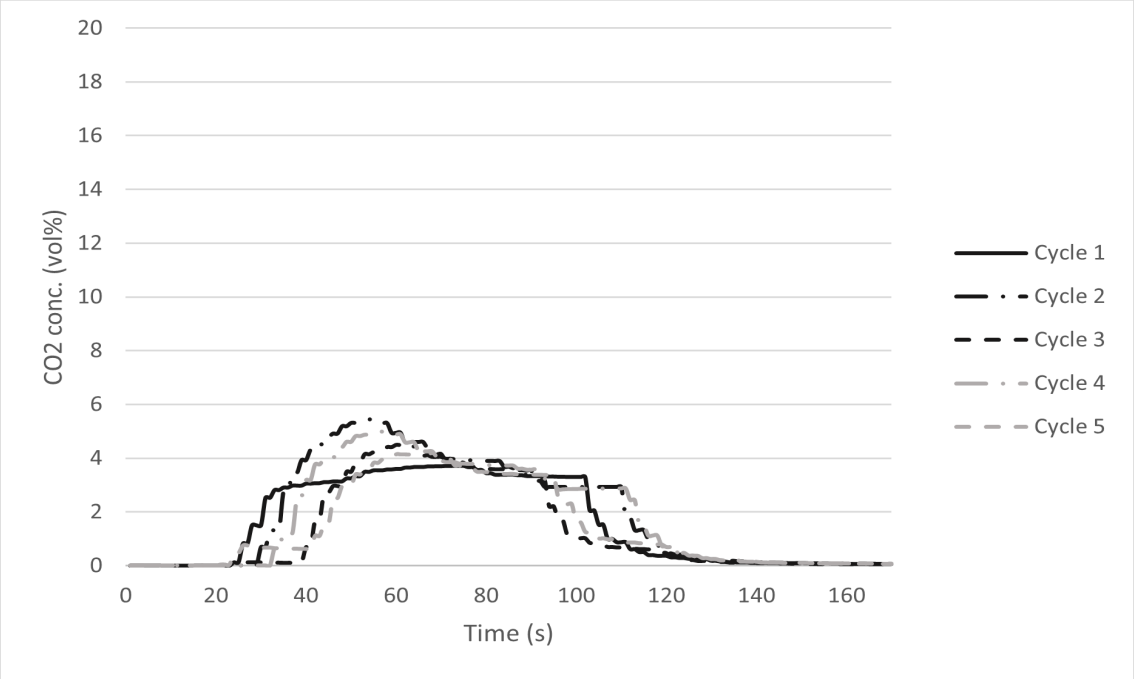

Figure A.25: *CO_2 concentration over time during reduction with methane in CLC cycle for copper smelter slag at 840°C*

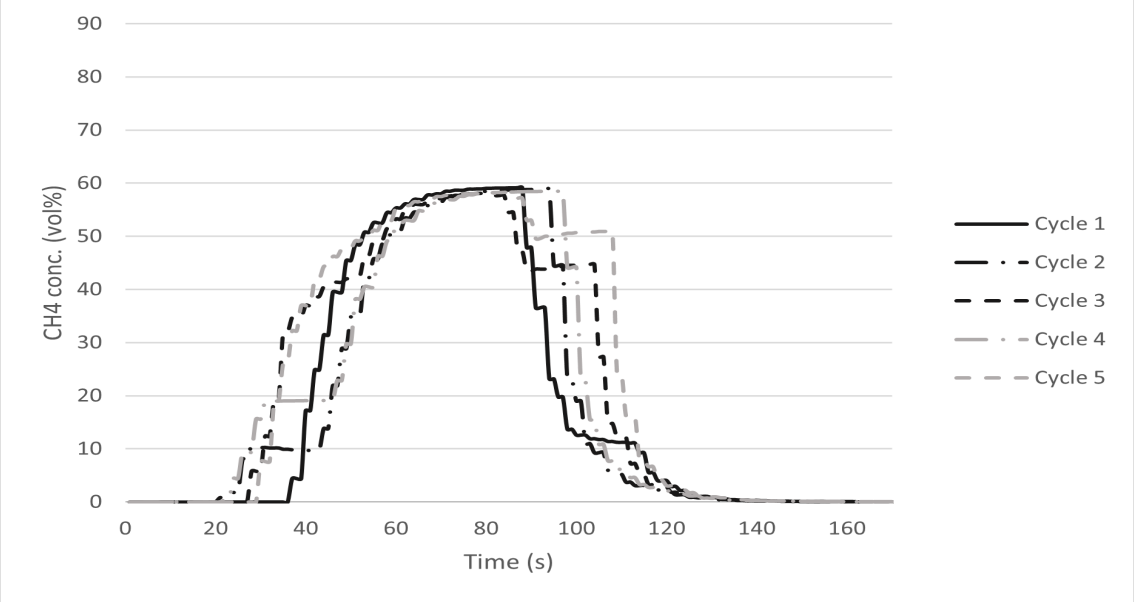

Figure A.26: *CH_4 concentration over time during reduction with syngas in CLC cycle for copper smelter slag at 840°C*

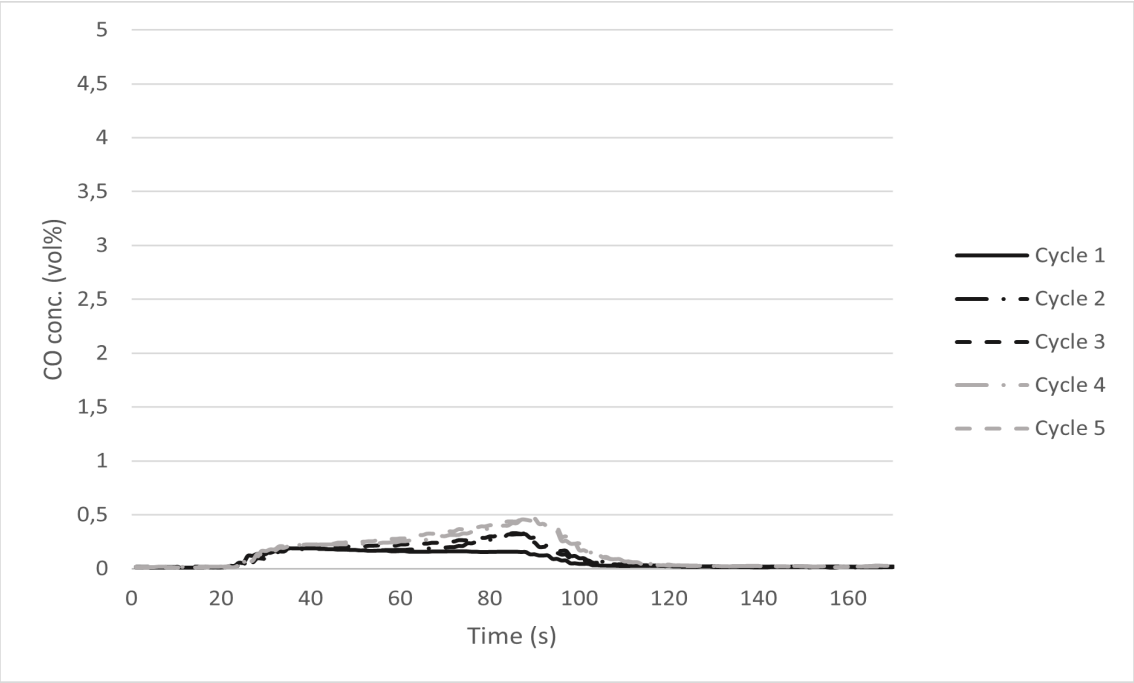

Figure A.27: *CO concentration over time during reduction with syngas in CLC cycle for copper smelter slag at 840°C*

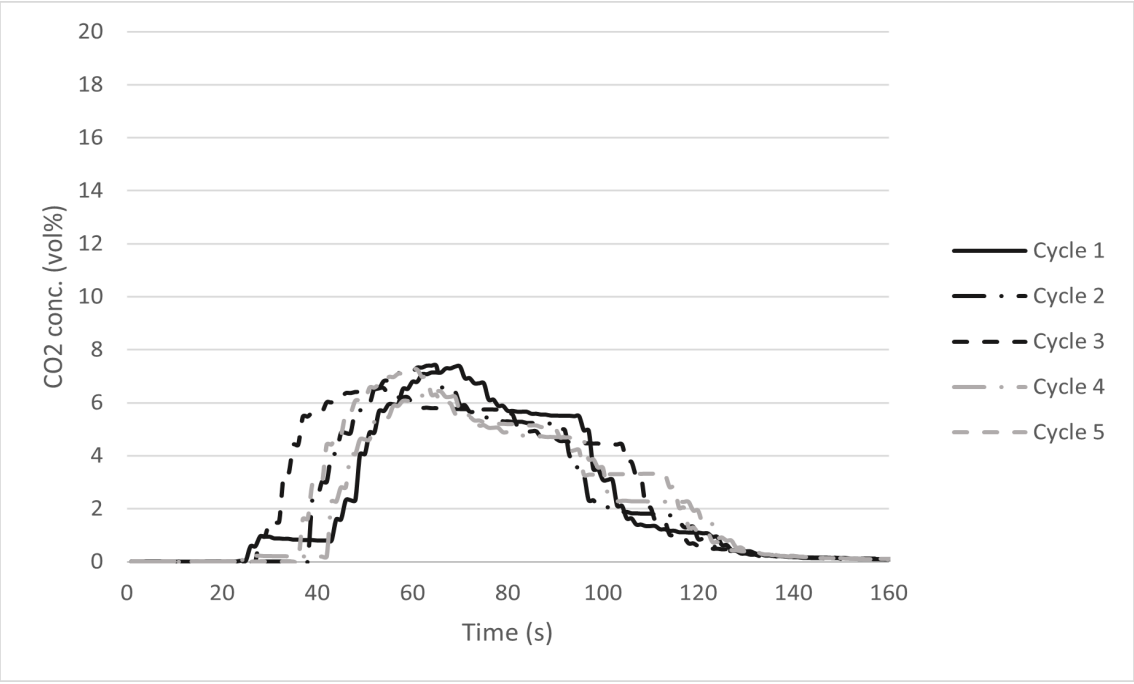

Figure A.28: *CO_2 concentration over time during reduction with syngas in CLC cycle for copper smelter slag at 890°C*

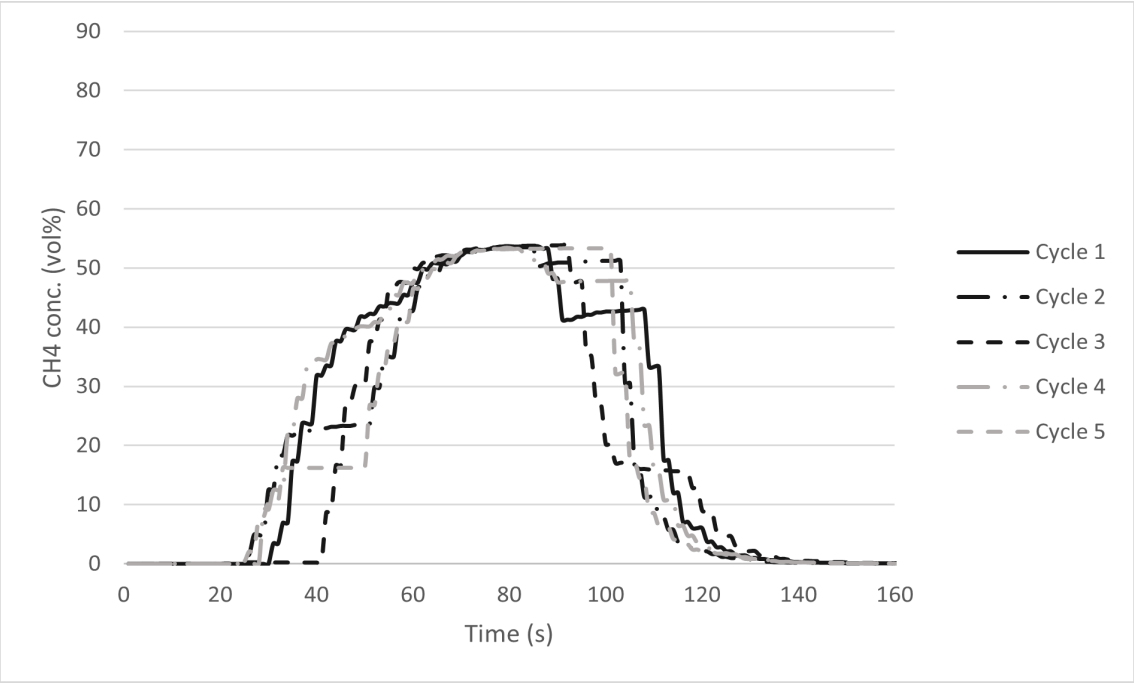

Figure A.29: *CH_4 concentration over time during reduction with syngas in CLC cycle for copper smelter slag at 890°C*

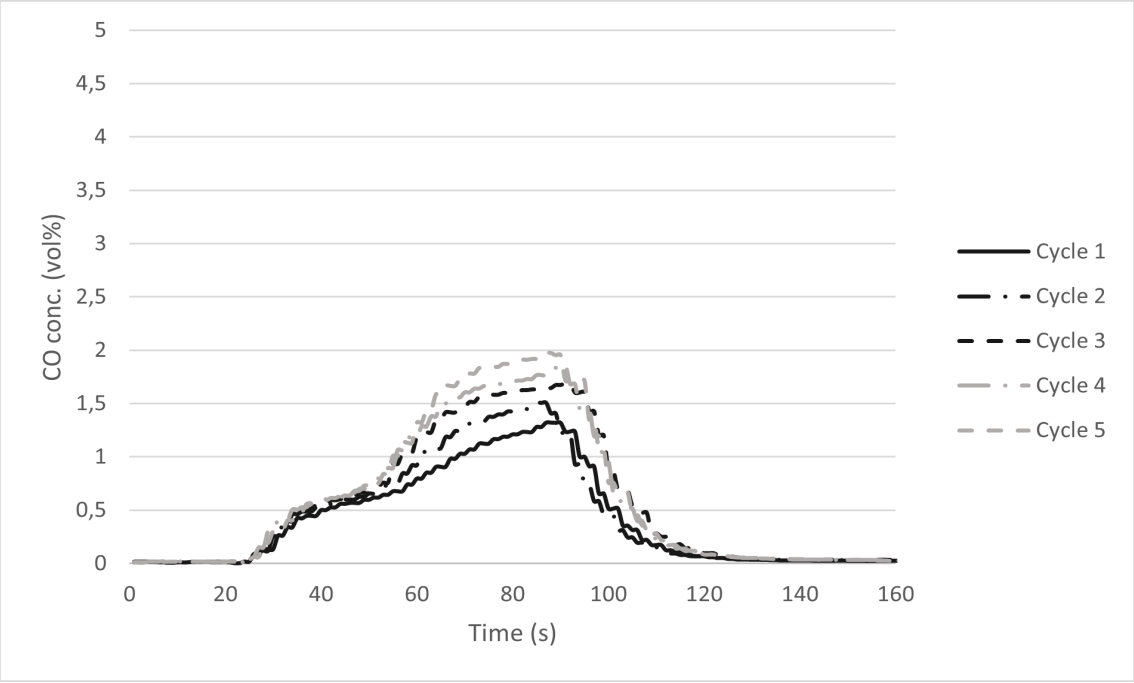

Figure A.30: *CO concentration over time during reduction with syngas in CLC cycle for copper smelter slag at 890°C*

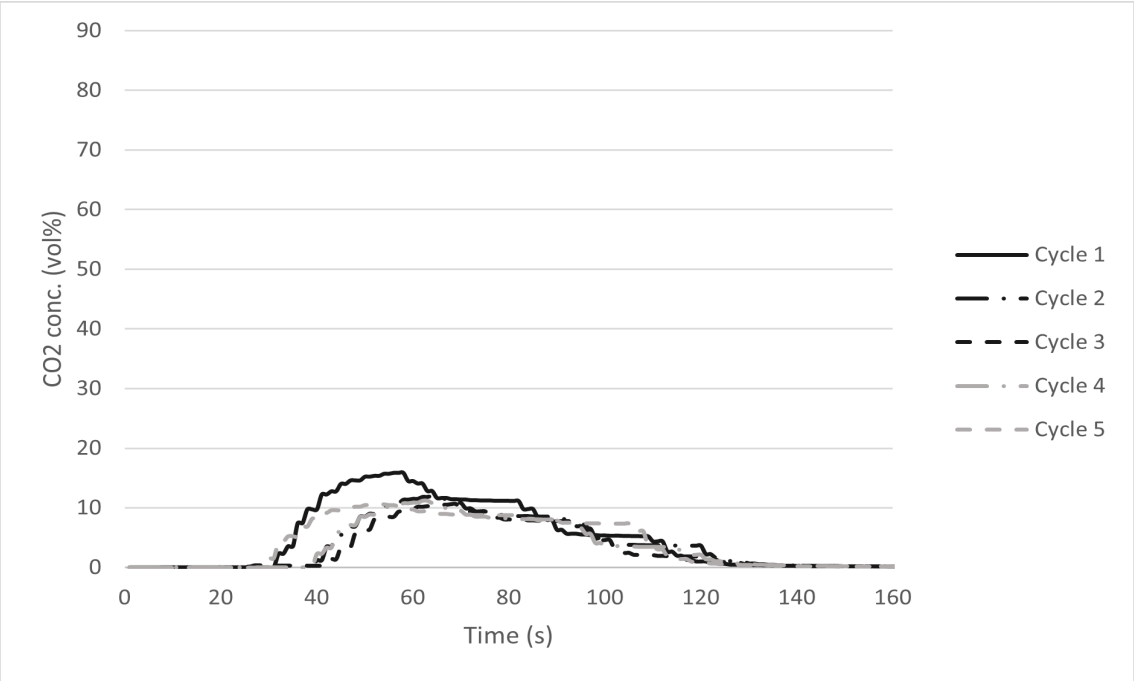

Figure A.31: *CO_2 concentration over time during reduction with syngas in CLC cycle for copper smelter slag at 940°C*

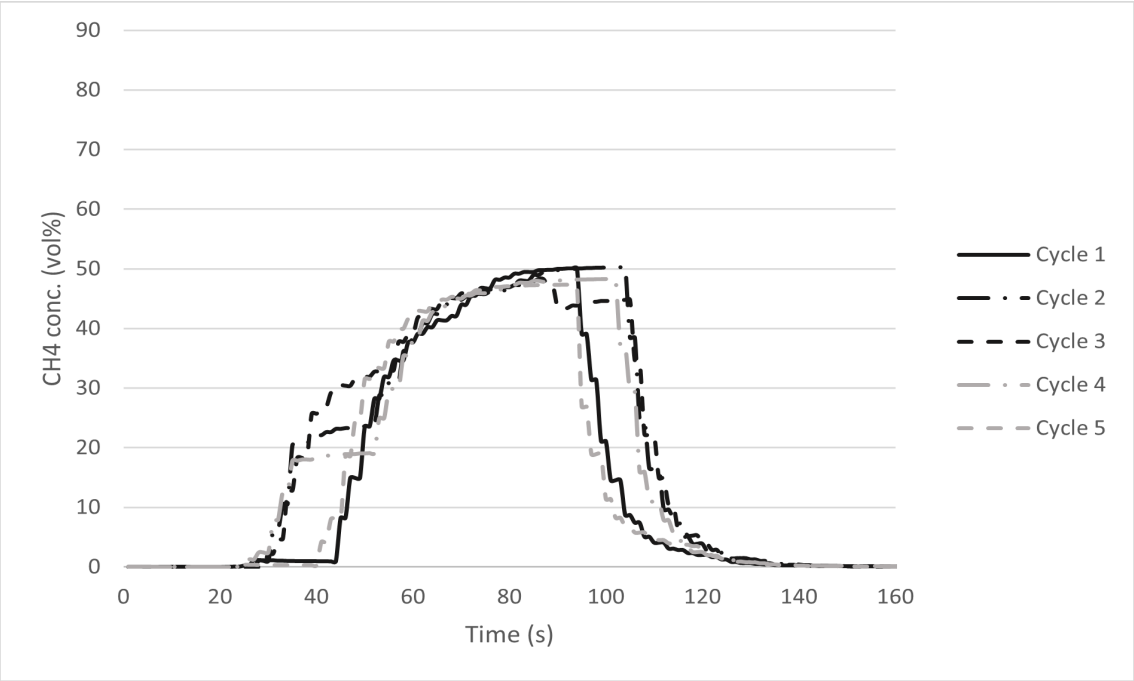

Figure A.32: *CH_4 concentration over time during reduction with syngas in CLC cycle for copper smelter slag at 890°C*

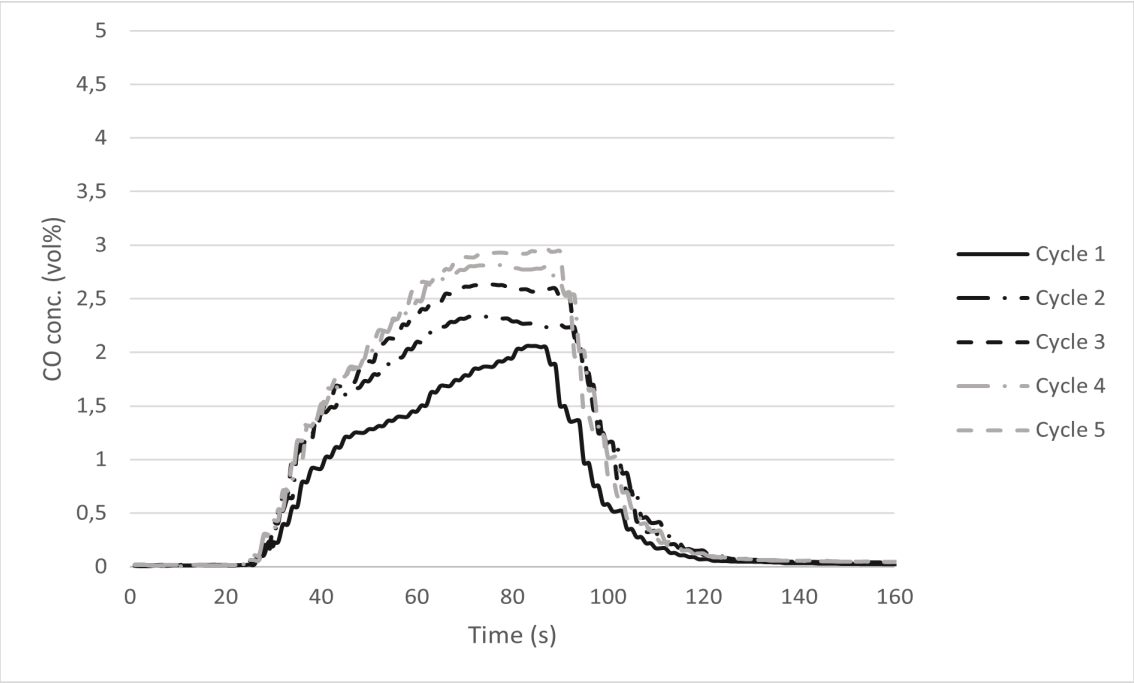

Figure A.33: *CO concentration over time during reduction with syngas in CLC cycle for copper smelter slag at 940°C*

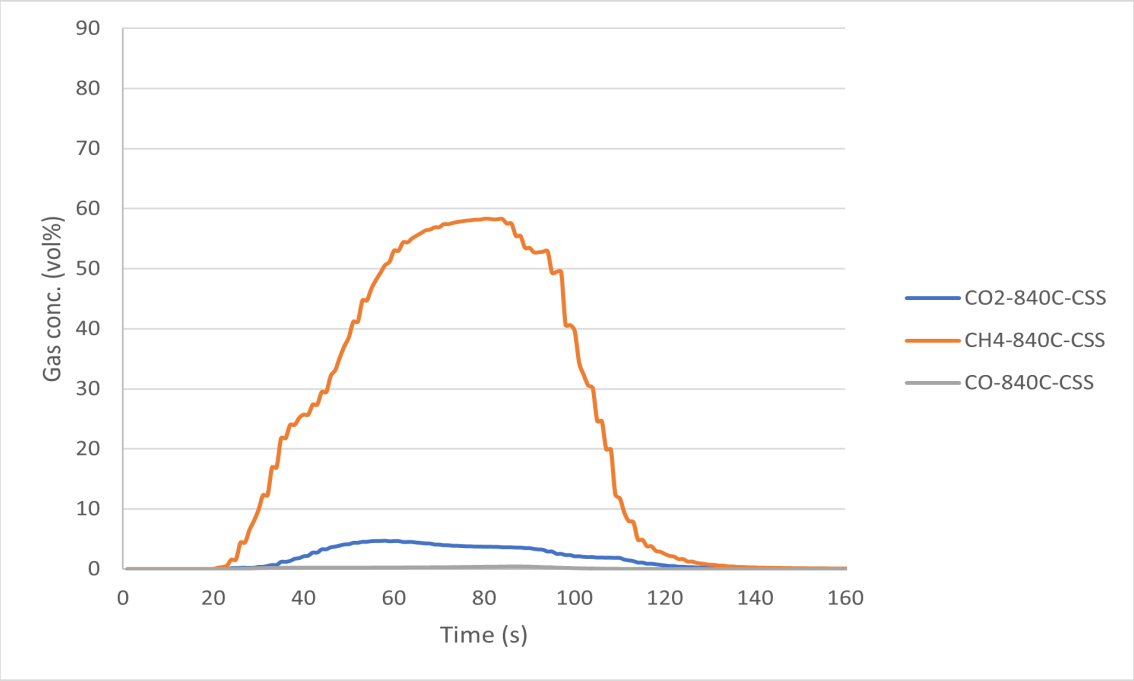

(a) *Bed temperature 840°C.*

Figure A.34: *Mean dry gas concentration for CLC cycles with copper smelter slag as bed material and syngas as fuel, for bed temperature s 840°C, 890°C and 940°C*

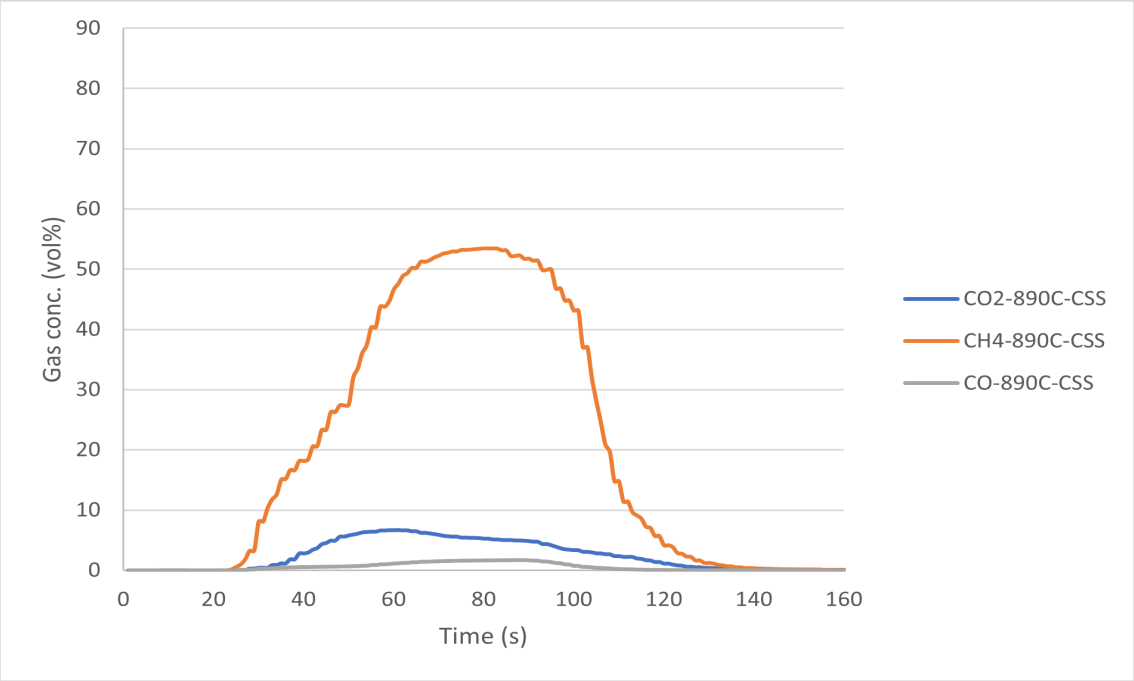

(b) Bed temperature 890°C

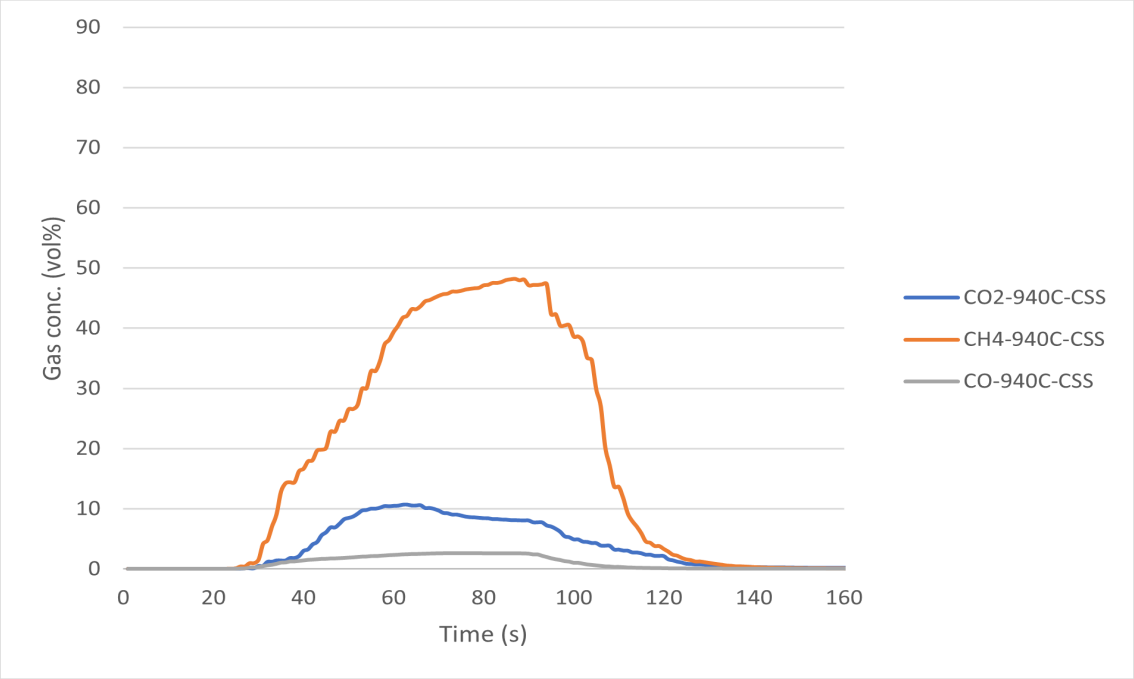

(c) Bed temperature 940°C

Figure A.34: *Mean dry gas concentration for CLC cycles with copper smelter slag as bed material and syngas as fuel, for bed temperature s 840°C, 890°C and 940°C*

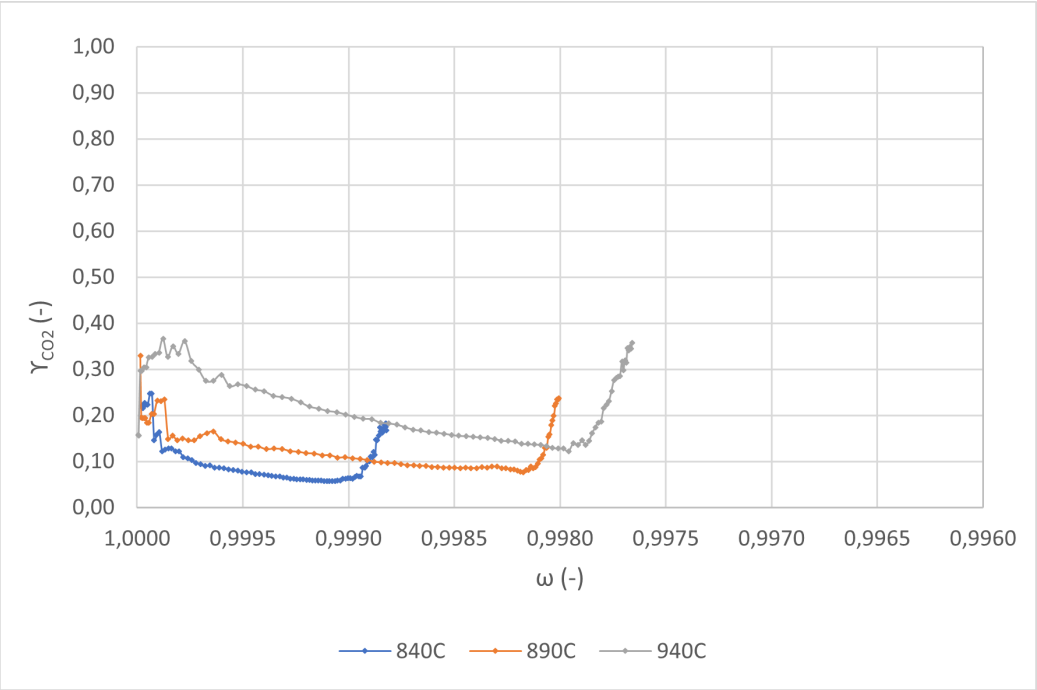

Figure A.35: *CO_2 yield as function of the mass based oxygen carrier conversion of copper smelter slag for combustion with methane, at different bed temperatures.*

A.2 Results for OCAC operation

A.2.1 Results for magnetite fines

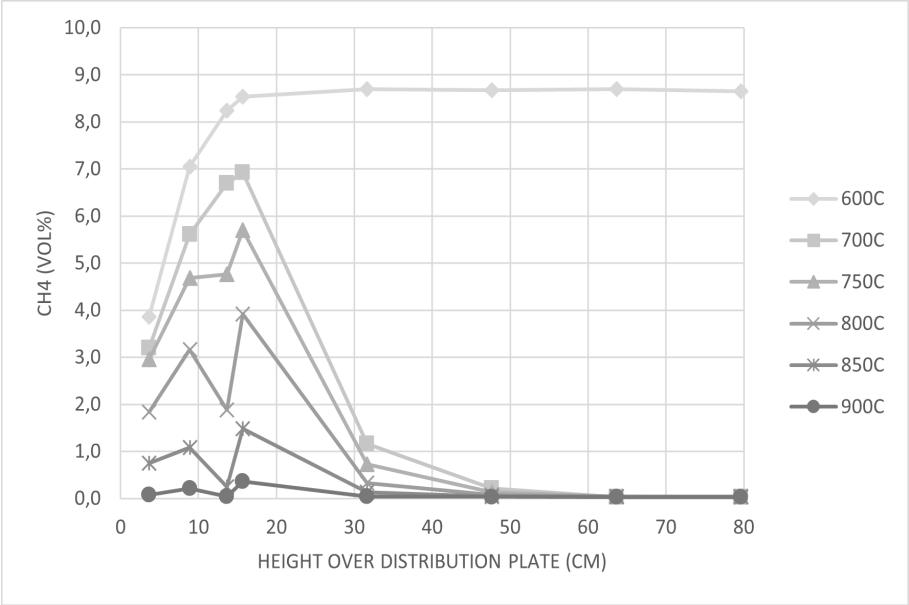

Figure A.36: *Dry gas concentration of CH_4 measured at different height over the distribution plate at bed temperatures 600°C, 700°C, 750°C, 800°C, 850°C and 900°C for magnetite fines in OCAC.*

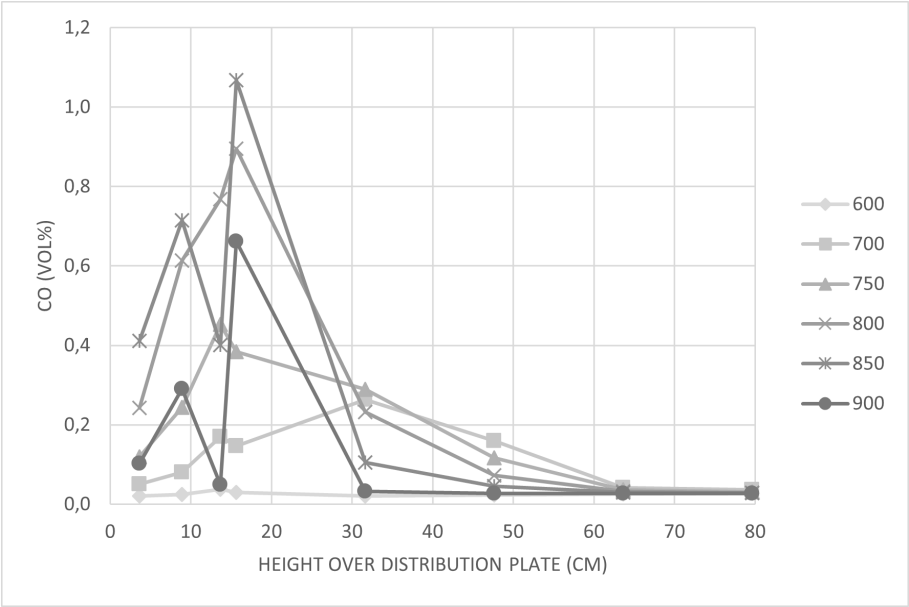

Figure A.37: *Dry gas concentration of CO measured at different height over the distribution plate at bed temperature 600°C, 750°C and 850°C for magnetite fines in OCAC.*

A.2.2 Results for copper smelter slag

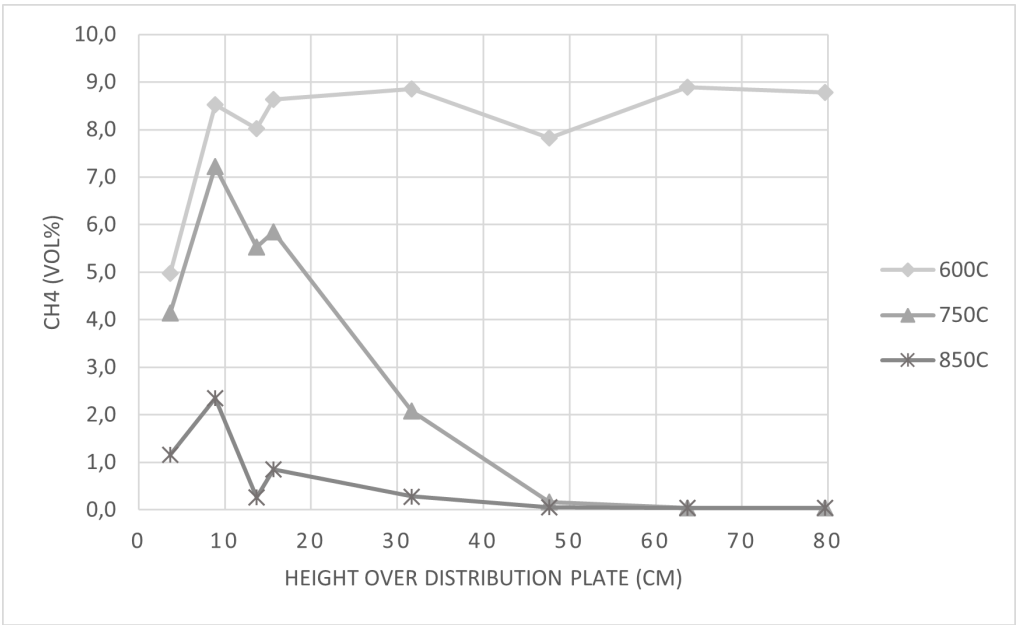

Figure A.38: *Dry gas concentration of CH_4 measured at different height over the distribution plate at bed temperatures 600°C, 700°C, 750°C, 800°C, 850°C and 900°C for copper smelter slag in OCAC.*

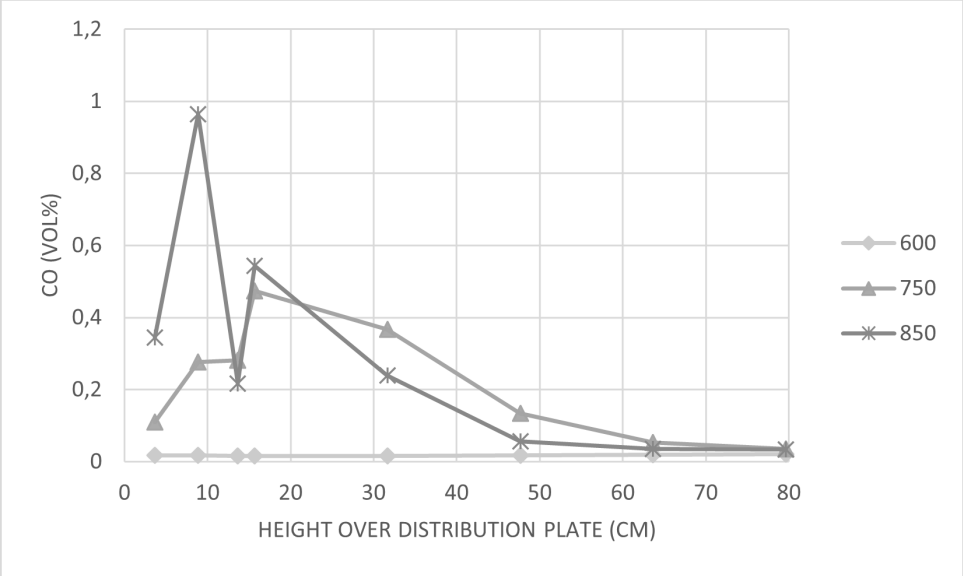

Figure A.39: *Dry gas concentration of CO measured at different height over the distribution plate at bed temperature 600°C, 750°C and 850°C for copper smelter slag in OCAC.*

DEPARTMENT OF SPACE, EARTH AND ENVIRONMENT, ENERGY TECHNOLOGY
CHALMERS UNIVERSITY OF TECHNOLOGY
Gothenburg, Sweden
www.chalmers.se

CHALMERS
UNIVERSITY OF TECHNOLOGY